Ana Luísa Grilo Pinho

Inside of the Creative Mind: Unravelling the Neurocognitive Mechanisms of Musical Creativity

Tese do Programa de Doutoramento em Ciências da Saúde, ramo de Ciências Biomédicas, orientada por Prof. Doutor Fredrik Ullén, Doutor Örjan de Manzano, Prof. Doutor Peter Fransson e Prof. Doutor Miguel Castelo-Branco e apresentada à Faculdade de Medicina da Universidade de Coimbra.

2014

· U C ·

UNIVERSIDADE DE COIMBRA

Inside of the Creative Mind:

Unravelling the Neurocognitive Mechanisms of Musical Creativity

Revised version

in collaboration with

Karolinska Institutet

Ana Luísa Grilo Pinho

2014

The studies presented in this thesis were carried out at Karolinska Institutet (KI), Stockholm, Sweden. They were supported by a PhD studentship (SFRH/BD/33895/2009) from the Foundation for Science and Technology of Portugal (FCT) and funding from the Swedish Research Council (521-2010-3195), the Sven and Dagmar Saléns Foundation as well as the Bank of Sweden Tercentenary Foundation.

Cover design: Francisca Ribeiro

Universidade de Coimbra

Faculdade de Medicina

Inside of the Creative Mind:

Unravelling the Neurocognitive Mechanisms of Musical Creativity

Dissertation presented to obtain a Ph.D. degree in Health Sciences (Biomedical Sciences) at the Faculty of Medicine of the University of Coimbra

Dissertação de Doutoramento apresentada à Faculdade de Medicina da Universidade de Coimbra para prestação de provas de Doutoramento em Ciências da Saúde no ramo de Ciências Biomédicas.

Ana Luísa Grilo Pinho

2014

Supervised by: Fredrik Ullén, Ph.D.

Co-Supervised by: Örjan de Manzano, Ph.D.

Peter Fransson, Ph.D.

Miguel Castelo-Branco, Ph.D.

To my parents:

João and Conceição

"I have found that all ugly things are made by those who strive to make something beautiful, and that all beautiful things are made by those who strive to make something useful."

Oscar Wilde (1854-1900), in the lecture on *The Value of Art in Modern Life* (1884)

Contents

Abstract

Creativity emerges from the individual or collective intellect in order to unfold the conundrum of life and give rise to meaningful deliberations for the attainment of a flourishing life. More specifically, creativity is commonly defined, within the framework of psychology, as a creative act or product that shall fulfill two main criteria: *(i)* it shall be novel (i.e. original and unexpected) and *(ii)* qualified judges shall agree upon its valuable contribution to the field. The cognitive science approach to creativity investigates the intellectual processes and representations concerned with the creative thinking. The methodologies of cognitive science, derived from the technological advancements of the past sixty years, have begun to adopt a more definitive and systemic perspective. Neuroscience has emerged, under this context, as the scientific study dedicated to explore the biological substrates of the nervous system, by utilizing a multitude of techniques such as neuroimaging. Cognitive neuroscience, in particular, studies the neural correlates of mental processes and it constitutes the central approach here adopted to study musical creativity. The primary goal of this thesis was thus to investigate the neurocognitive mechanisms underlying musical creativity. Functional magnetic resonance imaging was used to measure brain activity in thirty nine professional pianists and musical improvisation was employed as the ecologically valid behavioral model that could most accurately represent creative musical performance.

Study I sought to investigate the specific neurocognitive effects derived from expertise in musical improvisation. A natural question that arises is whether extensive improvisational musical training may induce neuroplasticity in the brain. Many of the observed correlates of general musical training reflect not only acquisition of highly specific sensorimotor skills but also cognitive abilities required for various aspects of musical expertise. However, no study has previously focused on the effects of training musical improvisation. The results revealed a significant negative association between improvisational training and activity in a number of cortical regions in the right hemisphere. Also, improvisational training was specifically associated with functional connectivity during musical improvisation, using the premotor and

prefrontal regions (previously reported to be involved during extemporization) as seed regions and controlling for age and conventional piano practice. More experienced improvisers showed higher functional connectivity during improvisation between prefrontal, premotor, and motor regions of the frontal lobe. Furthermore, the results were shown not be confounded by more experienced improvisers producing more complex improvisations.

Study II explored the contribution of the *dorsolateral prefrontal cortex* (DLPFC) in creative cognition. Different neuroimaging studies have shown so far seemingly paradoxical results regarding the implications of the DLPFC in creative functioning. On one hand, DLPFC has been argued to exert active control over free generative tasks by inhibiting habitual responses, thus enabling more original output; on the other hand, a deactivation and concomitant decrease in monitoring and focused attention has been suggested to facilitate more spontaneous associations and novel insights. Here, the study highlights that creative cognition can be implemented in different ways given different circumstances. Two categories of behavioral conditions were specified in the experimental design to convey constraints either on the musical structure (set of pitches) or on the emotional expression (happiness or fear) of the improvisations. The results confirmed higher activity in the right DLPFC, as well as in the parietal lobe and right dorsal premotor cortex, when contrasting structural conditions with emotional conditions. These results suggest higher attentional effort and cognitive control when the participants had to conform to the structural constraints. Conversely, deactivations were identified for the emotional constraints in the same regions, plus other regions explicitly contributing to emotion processing. In addition, DLPFC was found functionally connected with the frontoparietal network as well as the cerebellum during structural conditions and to various regions comprising the default network during emotional conditions.

Abstract in Portuguese

Resumo em Português

A criatividade emerge do universo intelectual, tanto individual como colectivo, com o objectivo de superar as limitações da existência e de promover decisões que conduzam a uma vida mais plena. No âmbito da psicologia, a criatividade é por norma definida como um acto ou produto criativo que deve cumprir com dois requisitos principais: *(i)* constituir algo novo (ou seja, ser original e inesperado) e *(ii)* reunir o consenso dos especialistas acerca da sua contribuição única na área. De acordo com a abordagem seguida em ciências da cognição, a criatividade é estudada a partir dos processos e representações intelectuais envolvidos no pensamento criativo. As respectivas metodologias, decorrentes dos avanços tecnológicos nos últimos sessenta anos, adoptaram uma perspectiva mais definitiva e sistémica. A neurociência surgiu, dentro deste contexto, como o estudo científico que se dedica a investigar os substratos neuronais, recorrendo para isso a uma diversidade de técnicas, entre as quais a neuro-imagem. Em particular, a neurociência da cognição estuda os substratos neuronais associados aos processos mentais, sendo esta a abordagem central adoptada no presente trabalho com vista ao estudo da criatividade musical. O principal objectivo desta tese foi, portanto, investigar os mecanismos neuro-cognitivos subjacentes à criatividade musical. A actividade cerebral de trinta e nove pianistas profissionais foi registada com recurso à ressonância magnética funcional, enquanto estes improvisavam pequenas peças musicais.

O estudo I teve o objectivo de investigar os efeitos neuro-cognitivos especificamente decorrentes da experiência em improvisação musical. A questão, aqui colocada, remete-se à identificação dos processos de neuroplasticidade que derivam da prática extensiva em improvisação musical. Muitos dos mecanismos observados e associados ao treino musical reflectem não só a aquisição de habilidades motoras e sensoriais de elevada especificidade, mas também o desenvolvimento de capacidades cognitivas essenciais em diversos aspectos relativos à experiência musical. No entanto, nenhum estudo, até ao momento, se focou nos efeitos relativos à prática improvisacional em música. Os resultados revelaram uma correlação negativa e significativa

entre a prática improvisacional e a actividade cerebral, num conjunto de regiões corticais do hemisfério direito. Os resultados evidenciaram, também, que a prática improvisacional está associada a uma maior conectividade funcional entre diversas áreas do córtex pré-frontal, pré-motor e motor do lobo frontal, durante a improvisação musical. A idade dos participantes e a prática musical convencional foram introduzidas no modelo de regressão linear como variáveis de controlo. Além disso, os resultados não apresentaram qualquer relação com a complexidade das peças produzidas por pianistas com maior experiência musical.

O estudo II examinou a contribuição do *córtex pré-frontal dorsolateral* (CPFDL) no processo cognitivo criativo. Até agora, diversos estudos em neuro-imagem têm revelado resultados aparentemente paradoxais no que respeita às implicações do CPFDL na actividade funcional responsável pelo pensamento criativo. Por um lado, foi comprovado que o CPFDL exerce um controlo activo sobre tarefas de produção livre, inibindo respostas habituais e promovendo consequentemente resoluções mais originais; por outro lado, a desactivação e concomitante diminuição do CPFDL, durante actividades cognitivas relacionadas com monitorização e concentração, sugere que esta região agiliza processos mentais de associação espontânea e de concretização de novas ideias. O presente estudo destaca que o mecanismo cognitivo associado à criatividade pode ser implementado de diversas formas, dependendo das circunstâncias externas. Duas categorias de restrições foram especificadas no paradigma experimental, de modo a condicionar o comportamento dos participantes. Essas restrições referiam-se à estrutura musical (conjunto de notas) ou à expressão emocional (alegria ou medo) das respectivas improvisações. Os resultados confirmaram uma maior actividade do CPFDL direito, do lobo parietal e do córtex pré-motor dorsal direito, durante a improvisação condicionada pela estrutura da música, quando comparada com a improvisação dependente da expressão emocional transmitida pela música. Os resultados sugeriram, portanto, um esforço maior na atenção prestada e um elevado controlo cognitivo, durante as improvisações condicionadas pela estrutura musical imposta. Em oposição, foram identificadas desactivações nas mesmas regiões, assim como em regiões tipicamente associadas ao processamento de emoções, durante as improvisações cujo desempenho remete para a expressão emocional da música. Além disso, os resultados comprovam que o CPFDL está funcionalmente conectado à rede de comunicação fronto-parietal e ao cerebelo, durante as improvisações condicionadas pela estrutura musical. Por sua vez, os resultados demonstram que o CPFDL está conectado a regiões associadas à rede neuronal em modo padrão, durante as improvisações musicais condicionadas pela expressão emocional.

Nota: Este texto não foi escrito ao abrigo do Acordo Ortográfico da Língua Portuguesa de 1990.

Glossary

FCT Foundation for Science and Technology (Fundação para a Ciência e a Tecnologia) (http://www.fct.pt/index.phtml.en) d, 141

FSL-BET FSL-Brain Extraction Tool (http://fsl.fmrib.ox.ac.uk/fsl/fslwiki/BET) 67

GE General Electric (http://www3.gehealthcare.com/en/Products/Categories/Magnetic_Resonance_Imaging/Discovery_MR750_3-0T) 57, 99, 125

KI Karolinska Institutet (http://ki.se/en/startpage) d, 33

SOI Structure of the Intellect - Guildford's divergent production tests 8

SPM8 Statistical Parametric Mapping (Wellcome Department of Imaging Neuroscience, London: http://www.fil.ion.ucl.ac.uk/spm/) 66, 67, 69, 74, 80, 82, 83, 85, 87, 102, 126

List of Abbreviations

ACC Anterior Cingulate Cortex 18, 19, 96, 118

ATP Adenosine Triphosphate 55

BOLD Blood-oxygenation-level dependent 41, 51, 54–58, 69, 74, 101, 103, 105, 107, 125, 128, 136, 137

cFWE cluster-level Family-Wise Error rate 86

CSF Cerebrospinal Fluid 67, 75

dHb Deoxygenated Hemoglobin 51, 54–57

DLPFC Dorsolateral Prefrontal Cortex 11, 16, 17, 19–21, 29, 79, 80, 96, 97, 103, 104, 118, 119, 121, 122, 127, 128, 130, 132–136, 138–141, 151, 156

DMPFC Dorsomedial Prefrontal Cortex 19, 132

EEG Electroencephalography 10, 12–14, 111

EPI Echo-Planar Imaging 52, 53, 58, 65–67, 101, 125

FFX Fixed-effects 17, 81

fMRI functional Magnetic Resonance Imaging 10, 12, 16, 17, 19–21, 33, 37, 38, 40, 41, 44, 48, 51, 54, 57, 58, 62, 63, 65, 69, 76, 79, 81, 82, 86, 96, 97, 99, 101, 102, 118, 121, 125–127, 139, 149, 157

FOV Field of View 67, 101, 125

FWE Family-Wise Error 86, 87, 128–131, 133–137

FWHM Full-Width at Half Maximum 69, 86, 103, 104, 127, 128

GLM General Linear Model 69, 70, 74, 76, 77, 79, 80, 102, 103, 127, 128

GRE Gradient-Echo Imaging Pulse Sequence 47, 49, 65

Hb Oxygenated Hemoglobin 54–56

HMAT Human Motor Area Template 103, 127

HRF Hemodynamic Response Function 69, 74, 77, 79, 80, 102, 103, 127, 128

IFG Inferior Frontal Gyrus 18, 19, 21, 96, 104, 118, 132, 138, 151

Lz Lempel-Ziv complexity 61, 62, 126–129

MFX Mixed-effects 81, 82, 84

MNI Montreal Neurological Institute 106, 108, 130, 131, 133–135

MR Magnetic Resonance 16, 19, 20, 33, 35–37, 41–46, 48, 49, 53–56, 98, 99, 123, 125

MRI Magnetic Resonance Imaging 37, 40, 41, 44, 48, 57, 67, 96, 102, 126, 157

Nkeys Number of keys played 62, 126–129

NMR Nuclear Magnetic Resonance 41

OLS Ordinary Least Squares 70, 76

PET Positron Emission Tomography 10, 11, 13

PMD Dorsal Premotor Cortex 16, 18, 20, 97, 103, 104, 107, 118, 121, 128, 130, 132, 136–138, 141, 151

PPI Psychophysiological Interaction(s) 20, 71–74, 77, 79, 80, 85, 103, 127, 128, 132–135

PreSMA pre-Supplementary Motor Area 16, 17, 19–21, 96, 97, 103, 118, 122, 141

RF Radiofrequency 42–47, 49, 52, 57

RFT Random Field Theory 86, 87

RFX Random-effects 81–84

rWLS robust Weighted Least Squares 75, 76

SE Spin-Echo Imaging Pulse Sequence 49

SMA Supplementary Motor Area 107, 132, 138, 141

SNR Signal-to-Noise Ratio 53, 57, 68

SS Summary-statistic 82, 83

STG Superior Temporal Gyrus 12, 16, 21, 132

TE Echo Time 49–52, 101, 125

TMS Transcranial Magnetic Stimulation 10, 11

TPJ Temporoparietal Junction 16, 18

TR Repetition Time 48–52, 75, 101, 125

WLS Weighted Least Squares 76, 82

List of Figures

List of Tables

Key Words

Creativity; dorsolateral prefrontal cortex; expertise; fMRI; functional connectivity; improvisation; music; plasticity;

Outline of the Thesis

While there is a rich psychological literature covering many aspects on creativity, little is still known about the brain mechanisms inherent to creative behaviors. Thus, the main purpose of this thesis was to attain a better understanding of the neurocognitive processes underlying the complex phenomena involved in musical creativity. The thesis comprises eight chapters described below.

Chapter 1 provides a comprehensive definition touching the concept of creativity and recounts its historical developments. It also describes how creativity has been addressed as a research topic not only within the field of psychology but also, and more recently, under the framework of cognitive neuroscience, which accounts for the main approach adopted on both studies featuring this thesis. In the end, it also includes a brief description of the latest advances on the research topic of musical creativity, specifically what relates to musical improvisation, with major contributions from the recent neuroimaging techniques.

Chapter 2 contains a brief description of the objectives guiding the research line of both studies (Study I and Study II) presented in this thesis.

Chapter 3 introduces an overview of the several experimental procedures employed for data acquisition, comprising both neuroimaging data and behavioral data. It also includes a general characterization of the principles governing functional magnetic resonance imaging.

Chapter 4 describes the data analysis pipeline, by presenting the algorithms used to retrieve information from music, the methods employed for preprocessing neuroimaging data, and the statistical approaches applied for inference.

Chapter 5 features the integral content of the peer-reviewed article on expertise in musical creativity published in *The Journal of Neuroscience*, by reporting the full technical description on research and findings of Study I.
(`http://dx.doi.org/10.1523/JNEUROSCI.4769-13.2014`)

Chapter 6 displays the first revised version of the manuscript describing Study II. The corresponding peer-reviewed article is currently published in the scientific journal *Cerebral Cortex*. (`http://dx.doi.org/10.1093/cercor/bhv130`)

Chapter 7 presents a detailed narrative concerning the final conclusions drawn upon both studies.

Chapter 8 refers to future lines of research that might follow the investigations herein formalized.

I am grateful to my supervisors and members of the dissertation committee for the comments, remarks and suggestions concerning the revision of this manuscript.

Part I

Introduction

Chapter 1

The Neuropsychological Aspects of Musical Creativity

1.1 Creativity

Nature evolves from transformation and adaptation based on fundamental processes that constitute the driving force towards creation. Evolution thus relies upon constructive mechanisms that progressively disrupt the current settings and conceive new possibilities. With regard to the anthropological perspective, the nourishment of the curiosity sustained by fostering imagination arises as an innate *modus vivendi* to surpass self-nature. These are the underpinnings that have enabled humankind to conceptualize about *creativity*.

1.1.1 Origins and Concept

Creativity emerges from the individual or collective intellect in order to unfold the conundrum of life and give rise to meaningful deliberations for the attainment of a flourishing life. Nonetheless, the concept of creativity has itself changed across time as an endeavor to grasp its meaning for humanity.

Ancient pre-Greek civilizations had developed the concept of genius, which came attached to the idea of mystical powers of protection and good fortune. However, Greeks gradually changed the concept when it started to be associated with the *Daemons*. The idea of genius became mundane and intrinsically linked to individual's abilities and appetites[1] Being a genius took thus a social value and, by the time of Aristotle, it was frequently associated with madness and frantic behaviors[2]. Romans additionally linked these ideas to exclusively male capacities

[1] These attributes were not necessarily pejorative. They might be constructive as well as destructive.

[2] This idea was recovered, during nineteenth and early twentieth centuries, to name eccentric and erratic behaviors.

(Sternberg, 1999, pp. 17-18).

The research community agrees that the earliest concept of creativity in the Western world came from the biblical story of the Creation, part of the *Genesis*, alluding to the idea of crafting on Earth under God's will. Some criticism was raised in the second century A.D. towards these interpretations but without marked success. In general, Western beliefs supported the idea that creativity could only happen by godlike intervention, while Eastern cultures emphasized the role played by the intervenients. Eastern philosophies defined creation as a process of discovery and mimicry, thus reflecting proneness to perceive natural cycles, harmony, regularity and balance[3] (Sternberg, 1999, pp. 18).

The assumptions about creativity linked to the divine were not challenged for a long period. During the Middle Ages, special talents or unusual abilities were usually interpreted as delegations of an outside spirit (Sternberg, 1999, pp. 18).

Only in the Renaissance, transformative ideas around this topic had clearly manifested as a consequence of the early modern cultural approach. At this period, the outstanding attributes of great artists had started to be recognized as their own. This rare chapter of the history of mankind brought out the power of discovery and the disruption of cultural and religious paradigms. Thence, when we examine the succeeding Age of Enlightenment's view in the eighteen century, we find two profoundly and intellectually new perspectives: reason and individualism. A new paradigm shift took place as a consequence of The Enlightenment's resistance towards religion's knowledgeability; Natural Science was thus taking shape as an institutionalized philosophy and methodology. Although not many changes related to ideas about creativity had occurred between the years of 1500 and 1700, a substantial amount of new contributions were of the utmost importance to foster the interest in research. It was around this period that science started to prevail as a role model of the Western thinking and, simultaneously, to develop instruments of discovery and models pertaining the physical world. This dramatic turn of events constituted for many scholars the beginning of a distinctive Western civilization embedded by Modernity (Sternberg, 1999, pp. 18-20).

According to what has been described, creativity arises as a universal concept crossing many different academic fields, such as philosophy, technology, economics, anthropology, psychology and, more recently, cognitive science. And while a multitude of approaches have been used to study the creative phenomenon, most of the conceptual and definitional work has been conducted in psychology, more specifically, using psychometric methods - *"the direct*

[3] As stated by Boorstin (1992), Eastern traditions were in favour that *"the idea of the creation of something ex nihilo ("from nothing") had no place in a universe of the yin and yang."* (Boorstin, 1992)

measurement of creativity and/or its perceived correlates in individuals" (Sternberg, 1999, pp. 35). Although psychology became a formal discipline already in the late nineteenth century, creativity have only attracted considerable attention for the latter half of the twentieth century. In 1950, J.P. Guilford pointed out in his *American Psychological Association* (APA) Presidential Address the scarce amount of entries focused on creativity (less than 0.2%) in *Psychological Abstracts* up that date and, thus, more attention should be paid to this research topic (Sternberg, 1999, pp. 3 and 35).

A common and generic definition of a creative act, widely accepted among scholars, is that *"Creativity is the ability to produce work that is both novel (i.e., original, unexpected) and appropriate (i.e., useful, adaptive concerning task constraints"* (Sternberg, 1999, pp. 3). Even so, creativity is not only about the individual, when one takes the enterprise of achieving a fine solution, but also about the way society addresses new scientific findings, new movements in art, new inventions as well as new social programs.

1.1.2 Confluence Theories of Creativity

Several explicit theories from the past thirty years have proposed different approaches, each of them emphasizing different factors that must converge for creativity to occur (Sternberg, 1999, pp. 10).

Amabile (1983) described creativity to be not solely associated with individual creative-relevant skills, but rather a confluence of creative proficiency, intrinsic motivation, domain-relevant knowledge and suitable abilities (Amabile, 1983). Grueber and his colleagues (1981, 1988) had proposed, in turn, an evolutionary system based on the interplay between individual's behavior and knowledge gradually acquired (Gruber, 1981, 1988; Gruber and Davis, 1988). On the other hand, Csíkszentmihályi (1988, 1996) described creativity as a synergy between the individual, the field and the cultural context, i.e., a subject transforms information on a specific topic, and potentially extends it, according to cognitive processes, personality traits and motivation (Csikszentmihályi, 1988, 1996). Gardner (1993) suggested that the development of creative projects may arise from singular and critical situations (e.g. tension promoted by two competing fronts) or mild asynchronies between the individual and the external context (e.g. uncommon individual talent for a particular domain) (Gardner, 1993).

Finally, Sternberg and Lubart (1991, 1992, 1995, 1996) presented the *investment theory of creativity* in which creativity springs up from the will and ability of "buy low and sell high" an idea; that stands for the ideas which are not usually well-accepted from the beginning,

yet they become of a great value due to the individual's transformative skills (Sternberg and Lubart, 1991, 1992, 1995, 1996).

1.1.2.1 Confluence Factors

There are six paramount confluence resources that partake of the model[4]: *(i)* intellectual abilities, *(ii)* knowledge, *(iii)* styles of thinking, *(iv)* personality, *(v)* motivation, and *(vi)* environment (Sternberg, 1999, pp. 11).

Three major categories of intellectual abilities can be distinguished: *(a)* the synthetic ability that conveys systematization for perceiving the whole-problem and thinking "out-of-the-box"; *(b)* the analytic ability that allows for pursuing what is useful from what is not; and *(c)* the practical-contextual ability that heightens the capacity to persuade others of the value of one's idea. Interestingly, the absence of factor(s) produces ineffectual results, such like: *(1)* if only synthetic ability exists, the whole-context will not be properly assessed, leading to pointless results; *(2)* if only analytical ability exists, the thinking will turn to be powerfully critical but not creative; and *(3)* if only practical-context ability exists, the idea will be transmitted not because it worth some thought, but rather because it was well and powerfully presented (Sternberg, 1999, pp. 11).

Knowledge also constitutes another important aspect to consider when we examine creativity and it is often called *crystalized intelligence* (Sternberg, 1999, pp. 256). It is a "double-edge sword" because one may find it necessary to advance beyond into the enterprise, yet knowledge can prevent creativity to occur by leading an individual to become entrenched.

With regard to styles of thought, a "legislative" style turns to be essential in the pursuit of creativity, i.e., the preference for thinking in new ways in respect to one's own choices. Yet, one may find appealing to think in novel ways, but such accomplishment requires analytical ability for the development of creative ideas (Sternberg, 1999, pp. 11).

Personality also plays a major role regarding creative achievement and their contributing factors include: *(I)* self-efficacy and willingness to overcome obstacles; *(II)* take sensible risks; and *(III)* tolerate ambiguity. Particularly, "buying low and selling high" implies self-determination in the enterprise of break conventions and act in creative ways (Sternberg, 1999, pp. 11).

Motivation is also recognized to be highly important for creativity, by influencing intrinsic task-focused disposition. Research in this topic (Amabile 1983, 1996), had revealed that truly

[4] In agreement with the Investment Theory of Creativity (Sternberg, 1999, pp. 11)

creative people are those who show inwardly involvement and commitment to work, because they do love what they are doing, rather than seek potential reward (Sternberg, 1999, pp. 11).

Finally, and in contrast to the aforementioned factors focused on individual differences, environment is crucial for creative functioning. Because it is very difficult to reproduce creative environments, where spontaneous and typically non-observed behavior takes place, the formal tests of creativity measuring the ability or tendency to be creative outside the test situation are scarce and, often, questionable (Sternberg, 1999, pp. 46 and 406). Simonton (1999) examined historiometric data[5], based on inquiries performed by creative individuals. The factors identified were: *(A)* birth order, i. e., whether the individual is the first-, middle-, last-born, or only child[6]; *(B)* childhood trauma (e.g. parental loss); *(C)* family background, e.g. creativity is frequently linked to disturbances in the familiar setting; *(D)* education, mostly related to less conventional environments; *(E)* role models and mentors, who become sources of inspiration, contributing as a major driving force on the creative achievement of the pupil; *(F)* cultural factors, by enforcing discipline or aesthetical suasion; *(G)* social factors, such like social structure or demographic phenomena, etc.; and *(H)* political factors, e.g. critical contexts, such as war, may promote uneasy psychological states (Simonton, 1999).

1.1.3 Creative Process

Several descriptions of the creative process were developed as an attempt to better explain the underlying psychological mechanism. The most widely accepted Western description involves four pivotal stages of progress: *(i)* preparation, *(ii)* incubation, *(iii)* illumination, and *(iv)* verification (Hadamard, 1945; Poincaré, 1921; Ribot, 1921; Rossman, 1931; Wallas, 1926). Preparation relates to the preliminary analysis of the problem as well as the first endeavors to execute the task. Incubation might be associated with active unconscious work on the problem, automatic spreading of activation in memory, associative play or disregard of issues potentially irrelevant and a subsequent mental rest. Illumination emerges afterwards when a sudden but promising idea consciously arises. Finally, the creative idea is evaluated, developed and refined during verification. Although the validity of this approach might be debatable, a certain consistency with introspective narratives by Western creators is still noticeable. Furthermore, an important and peculiar attribute that characterized undoubtedly the Western approach is its assertiveness towards cognitive problem-solving and subsequent product-oriented definition of creativity. In fact, evidence for an alternative approach congruent with Eastern philosophies has

[5] Historiometric methods are drawn upon quantitative data extracted mostly from historical documents.

[6] Interestingly, it was shown that notable scientists are more likely to be first borns than creative writers.

been reported by Maduro (1976) in a study conducted on Indian painters (Maduro, 1976). The outcomes seemed to indicate that the incubation process is rather implicated with "achievement of an internal identification with the subject matter of the painting" and illumination is, in turn, very much driven by personal-oriented motivations. Nevertheless, verification is still about social communication pursuing personal realizations, like in the Western model (Sternberg, 1999, pp. 341-342).

1.1.3.1 Divergent Thinking

As previously stated in the subsection 1.1.1, psychometric approaches are dominant with regard to the study of creativity. Specific areas of psychometric study applied to creativity research include investigations into creative process, personality and behavioral correlates, characteristics of creative products and attributes of creativity-fostering environment. On the quest for an operationalization of creativity, divergent thinking batteries will be briefly described hereafter.

Divergent-thinking tests are based on the extensive production of novel and meaningful responses by exploring many possible solutions. They contrast with standard tests of achievement and ability, which imply *convergent thinking*, since the latter essentially require only one correct answer. A peculiar characteristic ascribed to the test is the clear emphasis upon fluency, since it is seen as a key component while the creative process is still ongoing. Psychometric tests to measure individual abilities in divergent thinking were firstly introduced by Guilford, named the *Structure of the Intellect* (SOI) divergent production tests (Guilford, 1967). According to Guilford, creative people could be characterized by the capacity of quickly generate a multitude of novel and original ideas as well as to think in a flexible fashion (de Manzano, 2010, pp. 9).

Nevertheless, it is important to notice that divergent thinking does not stand for creativity. It conveys instead the ability to enable the creative thinking together with other confluence factors (see sub-subsection 1.1.2.1) (de Manzano, 2010, pp. 9).

1.1.4 Creative Cognition

The cognitive approach to creativity investigates the intellectual processes and representations concerned with the creative functioning. The corresponding methodologies adopt a more definitive perspective when compared to earlier approaches, such as psychometrics. Besides, the experiments quite often take place in a highly controlled environments. The human mind

is herein comprehended as *"a complex system that receives, stores, retrieves, transforms and transmits information"*, i.e., an information-processing system (Stillings et al., 1998). Thus, considering the systemic dimension of this approach, the capacity for creative thought is perceived as a rule rather than a combination of exceptional subject-specific features. Thence, the underpinnings of the creative cognition approach, undertaken to investigate human creativity, follow the next list of claims: *(i)* the *normative* human cognition property is the set of generative abilities that furthers everyday cognitive activities, surpassing discrete stored experiences usually linked to "creative geniuses"[7]; *(ii)* the identified generative abilities are open to rigorous experimental examination; and *(iii)* creative accomplishments, from the most ordinary to the most extraordinary, are based on common mental processes presumably observable (Sternberg, 1999, pp. 189-190).

A general framework which attempts to systematize creative functioning is the *Geneplore* model, grounded in the creative cognition approach. According to this heuristic model, creativity can be explained as a two step process: generative and exploratory. Generative processes reflect the variety of potentially creative ideas, named "the preinventive" structures (e.g. memory retrieval, formation and combination of the recalled memories, transfer of information from one domain to another, categorical reduction), whereas exploratory processes refers to the evaluation, interpretation and employment of the selected preinvented structures. The model also includes constraints on the (final) product, which can be accomplished by imposing them anytime during generative and/or exploratory phase. This allows the model to become flexible to a wide selection of possibilities. After the exploratory phase is finished, the processes can operate in cycle, up to the moment when preinventive structures result in a final creative idea (see Figure 1.1) (Sternberg, 1999, pp. 191-193).

Research encompassing studies both in human subjects and computer simulations have increased over the past thirty years, as an attempt to extricate the complex mechanisms implicated in creativity. Multiple methods have thus emerged primarily in the fields of: *(a)* psychology, mostly addressing experimental studies focused in human behaviour); *(b)* artificial intelligence, using computational models developed to simulate aspects of human performance; and *(c)* neuroscience, dedicated to study the biological substrates of the nervous system, addressing a multitude of techniques, such as neuroimaging (Thagard, 2014). *Cognitive Neuroscience* is drawn upon theories combining methodologies from the three aforementioned fields

[7] A corollary of this statement is that the few individuals, who demonstrate outstanding capacities, use cognitive processes very different from those employed by the majority of the people and, thus, methods of cognitive science are not suffice to characterize such processes (Hershman and Lieb, 1988).

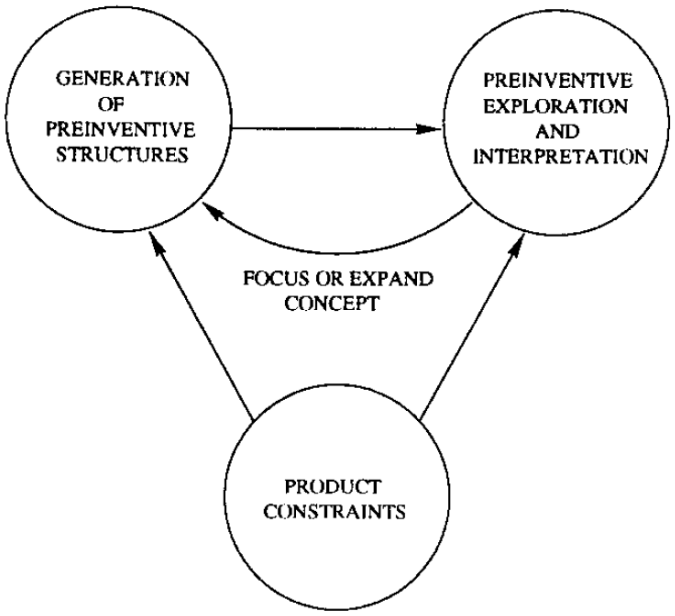

Figure 1.1: The basic structure of the Geneplore model. Preinventive structures are recovered and reconstructed during an initial stage, the generative phase. Afterwards, the emergent properties of these structures are exploited during exploration phase. The resulting creative products can be focused or expanded, according to task requirements or subject's intentions. Constraints on the final product can be imposed at any time during the generative or exploratory phases. Reproduced from (Finke et al., 1992), with permission from the publisher.

and it constitutes the central approach underlying the two studies anent creativity that feature this thesis. Henceforth, the present analysis will be focused on this approach.

1.1.4.1 The Neural Correlates of the Creative Thinking

Under the framework of cognitive neuroscience, many studies, focused on the neural correlates underlying creativity, have appeared with increasing frequently for the last fifteen years. The four predominant methodologies that have resulted in the most seminal, even though intriguing, findings are: *electroencephalography* (EEG), *positron emission tomography* (PET), *transcranial magnetic stimulation* (TMS), and *functional magnetic resonance imaging* (fMRI). According to Sawyer (2011), studies that yielded relevant contributions to the research of creativity, can be grouped into five main categories on experimental paradigms: *(i)* creative insight; *(ii)* mind wandering and incubation; *(iii)* creative brains *vs* non-creative brains; *(iv)* musical improvisation; and *(v)* differences with training (Sawyer, 2011).

1.1.4.1.1 Creative Insight

Insight (aka Illumination, see subsection 1.1.3) relates with the moment when a sudden but promising solution to a open-ended problem consciously arises. It may also involve the redevelopment of an ongoing situation in a new, more efficient as well as more productive manner. In both cases, it is still clear that creative insights occur in consciousness, which is, in turn, controlled by working memory processes sustained by the prefrontal cortex. Thus, when creativity is the result of the deliberate control, as opposed to spontaneous generation, the prefrontal cortex also instigates the creative process. Dietrich (2004) hypothesized that deliberate closed problem solving may show larger activation in the frontal areas, such as the *dorsolateral prefrontal cortex* (DLPFC), whereas solutions to open-ended problems may exhibit higher activity in the temporal, parietal and occipital areas. Because these latter areas are primarily devoted to perception[8] as well as long-term memory, it is argued that spontaneous insights may emerge from there. Contrariwise, the frontal lobe is generally implicated in highly processed information, enabling cognitive functions such as abstract thinking, planning, working memory and willed action (Sawyer, 2011).

Particularly, a systematic investigation of neural processes underlying free selection has been performed using PET and TMS by means of simpler model behaviors attempting to characterize willed action[9] (Jahanshahi and Frith, 1998). These model behaviors include: *(i)* finger and hand movements (Deiber et al., 1991; Frith, 2000; Lau et al., 2004; Playford et al., 1992); *(ii)* number generation (Jahanshahi et al., 2000). Further, contrasting pseudo-random generation of responses with stereotyped actions has also contributed for a better description of free selection. Several cortical regions were then identified, such as the DLPFC, medial and lateral premotor areas, as well as the anterior cingulate. This approach has thus allowed for an elegant analysis of the various aspects involved in free selection, such as attention to action, working memory, suppression of stereotype responses, and selection *per se* (Desmond et al., 1998; Lau et al., 2004; Nathaniel-James and Frith, 2002).

Given the aforementioned reasons, DLPFC is claimed to be involved in high-order executive functions, that is *"it further integrates already highly processed, formulates plans and strategies for appropriate behavior in a given situation and instructs the adjacent motor cortices to execute its computational product"*. Thus, it is expected that DLPFC together with motor cortical regions might be involved in conscious and deliberate creativity. Moreover, the

[8] The whole-set of areas aggregate sensory information decoded firstly in the primary cortex

[9] *Willed actions* can be described as self-generated behaviors. It involves: *(i)* attention and conscious awareness; *(ii)* choice and control and *(iii)* intentionality (Jahanshahi and Frith, 1998).

superimposition of these highly complex structures allows for a dramatic increase of cognitive flexibility, furthering sophisticated cognitive processes required for the creative thinking (Dietrich, 2004).

Many studies using either EEG or fMRI have contributed to clarify specificities associated with the mechanisms involved during insight, in order to fully characterize its neural correlates (Sawyer, 2011). For instance, a general important question is whether insightful solutions recruit different cognitive machinery than ordinary problem solving or they are just a result of a purely subjective feeling of emotional intensity at the time of discovery. Jung-Beeman et. al (2004) conducted experiments by solving verbal problems that could lead to insight versus non-insight solutions. Although both cases shared a largely cortical network, the results showed distinct cognitive processes associated with "Eureka!" experiences, such as significant activity in the anterior *superior temporal gyrus* (STG) of the right hemisphere previously reported to be implicated in remote association tasks (Jung-Beeman et al., 2004).

1.1.4.1.2 Mind Wandering and Incubation

As mentioned above, a creative idea often succeeds a stage of incubation. Previous studies have suggested possible descriptions for this phenomenon, such like random subconscious recombination, spreading of activation or mental relaxation and subsequent selective forgetting (see subsection 1.1.3). Nevertheless, the exact nature of this process remains quite unclear. Brain imaging studies have recently sought for further explanations, by drawing analogies with *mind wandering*. The unintentional shift from a primary task to another in which no personal goal lies within such behavior, is often described as mind wandering. It is thus argued that mind wandering may potentiate creative thoughts[10]. Indeed, the *default network*[11] was already found to be active in tasks involved in passive sensoring processing, but, conversely, it showed less activity on tasks associated with high central executive demand. Accordingly, results from an fMRI investigation performed by Mason et. al (2007) support the idea that the same areas involved in a default network are also implicated on high-incidence mind-wandering periods, introduced (in the context of this particular experiment) by extensive training of visuospatial working-memory tasks (Manson et al., 2007). In conclusion, the latest findings have suggested that these momentary episodes of mind wandering may reflect ongoing processes of "mini-

[10] *"We often assume that if we don't notice our thoughts they don't exist,(...) When we don't notice them is when we may be thinking most creatively."* - Dr. Kalina Christoff, University of British Columbia, Vancouver (Hotz, 2009)

[11] Brain system active in resting state but typically reduced during active conditions (Buckner et al., 2008). Interestingly, it also exhibits less activity during unconscious states (Andrews-Hanna et al., 2010).

incubation" that can further an insight and, thus, contribute for the awake of the creative mind (Sawyer, 2011).

1.1.4.1.3 Creative brains *vs* Non-creative brains

Differences in neural activity between people who gets greater scores on tests of creativity and people who scores lower, have also been explored. An early study, using EEG, Martindale and Hines (1975) found that high creative people showed higher levels of alpha wave activity[12], while performing a test[13]. In contrast, people with lower scores had lower alpha wave activity (Martindale and Hines, 1975). Another study, using PET, employed three different tasks with expected three different levels of cognitive recruitment in the frontal lobe. The tasks, listed next by ascending order of cognitive load, are: *(i)* automatic speech task (count aloud, starting with 1); *(ii)* word fluency task (i.e. say all words that come to mind, starting with the three specific letters); and *(iii)* a divergent thinking task[14]. The results revealed that high creatives exhibited greater levels of *regional Cerebral Blood Flow* (rCBF) on both hemispheres during both word fluency task and divergent thinking task in the anterior prefrontal cortex, whereas low creative showed a decrease of activity frontotemporal and anterior prefrontal areas in the left hemisphere when performing the same tasks. On the other hand, high creatives had more increased activity in the aforementioned regions during the execution of the divergent thinking task, when compared with the corresponding activity while performing the word fluency task. No differences in the activity level of both tasks were identified for low creatives (Carlsson et al., 2000). In general, several studies have provided evidence that less creative people activate slightly less the right hemisphere, whereas high creative people exhibit patterns of bilateral activation. Results from a PET study undertaken by Chávez-Eakle (2007), also indicated bilaterally distributed patterns of activity, displaying greater prevalence in the right hemisphere for higher scorers on verbal creative tasks (Chávez-Eakle, 2007). Despite many studies, including the aforementioned as well as meta-analysis (Mihov et al., 2010), have reported right dominance of hemispheric specialization for creative thinking, one must not conclude that creativity "is placed in" the right hemisphere (Sawyer, 2011). Indeed, Dietrich and Kanso (2010) reviewed the research findings about creativity and the main conclusion was that no other specific centers but frontal lobe at both hemispheres is always involved during creative process (Dietrich and Kanso, 2010) (Carlsson, 2014, pp. 59).

[12] Alpha waves (8-13HZ) - occurs while awake, under relaxation and with eyes closed

[13] The tests of creativity used in this study were the *Alternate Uses Test* and the *Remote Associates Test*.

[14] Brick Test

1.1.4.1.4 Differences with Training

Brain imaging studies have also explored differences due to extensive training. Regarding art training, EEG studies have indicated that well-mastered tasks typically correspond to greater coherence or synchronization across several cortical regions. For instance, Bhattacharya and Petsche (2005) found that MFA[15] students generally exhibited enhanced delta[16] band synchronization in the frontal regions upon performance of a mentally composing drawing, while non-artists exhibited short-range beta[17] and gamma[18] band synchronization. In addition, the study also revealed that artists had greater delta and alpha band synchronization with stronger effects in the right hemisphere, when compared with non-artists. Other studies involving chess players also demonstrated that professional players showed higher delta band coherence than amateurs, when trying to anticipate the next moves (Bhattacharya and Petsche, 2005). The findings overall suggest amelioration of long-term visual memory efficacy due to task-specific training. With regard to dance training, Fink et al. (2009) concluded, in a research study using EEG, that professional dancers had enhanced alpha synchronization in post parietal regions when executing a creative test[19]. When professional dancers were directly compared with novices, greater alpha synchronization at the right hemisphere became visible while performing an improvisation imagery task (Fink et al., 2009). These studies assessing for expertise generally support the idea that neuroplasticity mechanisms may evolve across lifetime due to extensive practising of the technique. Besides, there's considerable evidence that expertise is closely related to domain-specific creative performance and it may allow for retrieval of relevant information as well as recognition when a new idea is worthwhile. However, some researchers have pointed out the broad and comprehensive features of certain creative skills that can be acquired and applied in various and distinct problems and situations (Sternberg, 1999, pp. 207-208). According to Finke (1999), *"expert knowledge may be most useful when applied in conjunction with general principles for generating and exploring preinventive structures"* (Sternberg, 1999, pp. 208).

The neural correlates of musical improvisation and corresponding effects of expertise constitute the groundwork of this thesis. They are explored in greater detail over the next sections.

[15] Master of Fine Arts

[16] Delta waves (0.5-5Hz) - occurs during sleep

[17] Beta waves (13-30Hz) - occurs due to increased alertness and focused attention

[18] Gamma waves (>30Hz) - presumably implications in creating the unity of conscious perception

[19] Alternative Uses Test

1.2 Musical Creativity

Creativity is typically perceived and acknowledged in terms of its final outcome, i.e., the creative product. Although no clear objective criteria has been established, novelty is usually taken as a distinctive characteristic that must be fulfilled in order to produce a valuable creative product. Given the utilitarian perspective, a widely accepted normative to reach general consensus, one can claim that a creative product shall also contain some level of usefulness and appropriateness according to the social context. The social value of a creative product can thus be reflected in the visual arts, literature, scientific theories, technologic advancements as well as music (Sternberg, 1999, pp. 393). Musical creativity thus arises as a social practise that embodies and mediates the inner need of communication among individuals.

Investigating the neuropsychological mechanisms that underlie musical creativity involves the identification of suitable behavioral models. Possible aspects of these models include performing, listening, writing and analysing. Composition and improvisation can be described in terms of such aspects and they have been generally considered to play a central role in research. They both account for the fundamental activity which is the "creation of new music". Yet, their practice are naturally very different. Composition draws upon revision, i.e. the chance to go back and forth over the process, whereas improvisation relates directly to performance in which the inwardly associated extemporaneous process is marked by irreversibility (Tafuri, 2006, pp. 138).

Musical performance provides a suitable model behavior because it can be easily recognized and it enhances the ongoing progress of the task. It constitutes a platform for self-expression, since it is linked to the intrinsic and immediate interchangeability of different ideas. Particularly, musical improvisation involves a permanent exchange of ideas that are original, unpredictable, and emergent. As a consequence, it became one of the most accepted behavioral models for experimental paradigms in research.

Musical improvisation was the model behavior adopted to study musical creativity in the context of the investigation featuring this thesis. The next section is thus dedicated to a general overview of its neural correlates.

1.2.1 Musical Improvisation

As stated above, musical improvisation has been widely used as a valid model behavior in many research topics and it has been particularly acquainted in neuroimaging studies dedicated to investigate the neural correlates of musical creativity. Yet to the date, very little work was

undertaken in this specific topic and the literature accounts only seven studies (excluding the two studies presented in this thesis) that have directly examined creative musical improvisation in terms of musical performance. They are discussed next in further detail, following the chronological order.

The first of these studies refers to an fMRI experiment conducted by Bengtsson et. al (2007). Brain activity of eleven professional pianists was measured while the participants were improvising on the basis of a visually displayed melody and using a one octave MR-compatible piano keyboard (see Figure 3.1), as well as when the participants had to reproduce thereupon the previously improvised melody. In addition, the participants were also asked during neuroimaging data acquisition to perform free improvisation without memorizing the performance. The main findings were the result of a conjunction analysis between the contrasts *Improvise-Reproduce* and *FreeImp-Rest*. The brain regions found to be predominantly involved were the right DLPFC, the bilateral rostral area of the *dorsal premotor cortex* (PMD), *pre-supplementary motor area* (PreSMA), left posterior STG[20], the right fusiform gyrus and the bilateral middle occipital gyrus. Further, the PreSMA was positively correlated with the degree of complexity of the improvisations. According to the authors, the key finding of the study was the significant activity found in the DLPFC, since this region was previously reported to be involved in free selection, attention to action, working memory and suppression of stereotype responses (see sub-subsection 1.1.4.1) (Bengtsson et al., 2007).

In Limb and Braun (2008), six professional jazz pianists were asked to perform a improvisation musical task in a *magnetic resonance* MR - compatible piano keyboard with thirty five full-size piano keyboard, while fMRI data of brain activity were collected. The tasks consisted of two types of conditions: an *over-learned* condition and an *improvise* condition. During over-learned conditions, the participants were asked either *(i)* to repeatedly play a one octave ascending or descending C major scale in quarter notes, or *(ii)* to improvise in quarter notes using a single octave C major scale. During improvise conditions, they were instructed either *(i)* to play a novel melody, which was previously memorized before the scanning, or *(ii)* improvised based on a given composition's chord structure. When contrasting improvisation to over-learned sequences, the results displayed a broad pattern of deactivation in the medial prefrontal cortex, medial portions of the DLPFC, lateral orbital regions, the limbic and paralimbic regions, the basal ganglia, insula and the temporoparietal junction (Limb and Braun, 2008). The results are interesting and raise intriguing issues concerning improvisation. Yet,

[20] Close to the *temporoparietal junction* (TPJ)

they shall be interpreted under the context of a case study due to the small sample size used and the fixed effects analysis (FFX) employed for the statistical inference (see section 4.7). So, they represent possible implications rather than provide definite conclusions. In fact, the results regarding DLPFC involvement lead to opposite interpretations when compared to the ones referring the earlier Bengtsson's study. One can speculate that effects due to improvisational skills might have determined the results on both studies. Improvisation constitutes an essential feature in jazz performance, whereas classical pianists might improvise less frequently. Further, one can also hypothesize about differences in complexity between the two experimental paradigms. Improvisation is less demanding when it is based on a scale or chord structure than a musical template provided with ornamentations[21] (Berkowitz, 2010, pp. 6, 28 and 29). Besides that, activity elicited in the frontal lobe for classical pianists, namely in DLPFC and PreSMA explains explicit processing of novel motor sequences, whereas jazz pianists seem to depend on regions for implicit routine and automated behavior relying on interactions among cortical regions and limbic structures (Doyon and Benali, 2005). It shall also be noticed that the experimental design employed on Limb's study relates to over-learned tasks which generally constitutes a simple endeavor. This can probably explain the widespread patterns of deactivation during improvisation, resembling the *default network* associated with resting state activity, which become usually less active upon engagement on cognitive tasks (de Manzano, 2010). In fact, Mason (2007) suggested that extensive training could lead to mind wandering, allowing people to daydream. It is thus a task characterized by passive sensory processing, typically described by activation of the default network ((Manson et al., 2007); see section 1.1.4.1.2 for further details concerning "mind wandering"). One could thus speculate that control conditions were triggering mind wandering as a preparatory process for the next improvisation conditions.

Berkowitz and Ansari (2008) studied twelve trained undergraduate pianists in an fMRI

[21] Heinrich Schenker theorized on the model of the two level of musical formulas (or musical schemata, i.e. the archetypal patterns which define a musical style (Gjerdingen, 1988, 2007)). Such model attempts to describe the structural basis of tonal improvisation. The first level relates to bass lines and their harmonic progressions (harmonic progressions can be defined as musical treatises presented in a systematic, simplified and stylistic neutral fashion, such as a block of chords), whereas the second consists on perceiving such harmonic progressions idiomatically, i.e. through the use of melodic figures (Rink, 1993). Pressing denominates the first level as referent (Pressing, 1984). The referent is thus a structure of events in which improvisation can be crafted. Also, and according to Pressing's terminology, the second level represents the knowledge used to build the "musical surface" of the underlying referent. From the cognitive perspective, the referent allows for the internalization of certain features in musical language, so that they can be conceived with some degree of automaticity. On the other hand, conscious attention mechanisms regulate decision-making cognition on higher-level musical processes (e.g. relationships between events, form and feel).

experiment using a five-key piano-like response device from C to G, only with white keys. The experimental paradigm consisted on a 2×2 factorial design where rhythmic and melodic motor sequence creation were examined both separately and together. Specifically, the tasks were classified in four kinds of conditions varying in melodic and rhythmic freedom. The main effect of melodic improvisation showed significant activity in rostral and anterior cingulate cortices, ventral and dorsal premotor cortices, supramarginal gyrus and cerebellum. Deactivated regions relative to rest, displaying an increase deactivation with and increase of melodic freedom, were the superior and medial frontal gyry, posterior cingulate cortex and angular gyrus. The main effect of rhythmic improvisation was identified on the *anterior cingulate cortex* (ACC), *inferior frontal gyrus* IFG, PMD, sensorimotor and parietal cortices (Berkowitz and Ansari, 2008). The pattern of deactivation in e.g. medial frontal areas, comes into line with results from Limb and Braun (2008), suggesting deactivation of the default network during improvisation (Limb and Braun, 2008). There are, however, some issues that shall be addressed: *(i)* $\sim 33\%$ of the data, from the twelve subjects accounting for the analysis, were removed; *(ii)* conditions with melody constraint, where the participants were asked to play patterns, contained a free-choice element (free choice is cognitively implicated in improvisation) because they could play any of the pre-demonstrated patterns allowed for the experiment; *(iii)* metronome was only used during conditions with rhythm constraint and not for those related to improvisation, constituting a possible auditory confound (since it is not clear whether there might be interactions between regions involved in explicit auditory processing and regions involved in the creative process *per se*); and *(iv)* behavioural results show a main effect of melodic freedom on the variability assigned to the interval between two consecutive keystrokes as well as interaction between melodic freedom and rhythmic freedom on the variety of note combination, suggesting that the neurocognitive components controlling different aspects of rhythm and melody might have not been entirely isolated (de Manzano, 2010).

Berkowitz and Ansari (2010) examined functional expertise-related differences between musicians and non-musicians during improvisation. The experimental paradigm was the same as the one employed in studies from the same authors described above (Berkowitz and Ansari, 2008). The main finding was a deactivation during melodic improvisation in the right temporoparietal junction TPJ, whereas non-musicians exhibited no change in activity in this region (Berkowitz and Ansari, 2010). Nevertheless, there are few considerations that shall be pointed out. Behavioral results showed a three-way interaction of melodic freedom, rhythmic freedom and group on the variability of note combination. This is a direct consequence from the

interaction between melodic freedom and rhythmic freedom within musicians group already identified in the previous study. The variability of note combination was slightly greater during melodic improvisation with rhythmic constraint than in melodic improvisation with rhythmic improvisation. One can speculate that this interaction is a consequence of the auditory stimulation from the metronome present during conditions with rhythmic constraint, to which the musicians are more sensible. Given this, one can argue whether there was a true behaviorally matched performance as claimed by the authors. On the other hand, similar levels of musical performance between musicians and non-musicians is most likely related with the dimension of the musical keyboard. Thus, the question about the ecological validity of the task may arise. Even if the results reflect cognitive mechanisms underlying behavior with improvisatory content, that does not necessarily represent musical improvisation to the full extent and, thus, creative decision making *per se*. Very little is known about expertise-related neurocognitive processes involved in musical improvisation among trained musicians. It is, thus, necessary to isolate first and properly their specific components, in order to perform further endeavors on the investigation of functional differences between musicians and non-musicians during musical improvisation. Study I featuring this thesis gives a first step towards a better comprehension of the specific effects of training musical creativity.

The neural correlates of musical improvisation and pseudo-random generation was also tackled by de Manzano and Ullén (2012). Brain activity was measured in a group of professional classical pianists using fMRI, who performed musical improvisation of melodies in two generative tasks - pseudo-random sequence generation and musical improvisation - on a twelve-key/one octave MR-compatible piano keyboard (see Figure 3.1). Three main findings are notable from this study. First, there was a considerable overlap between brain regions involved in the two generative tasks. These regions included the DLPFC, *dorsomedial prefrontal cortex* (DMPFC), IFG, ACC and PreSMA. Secondly, the DLPFC as well as other association areas in the dorsomedial prefrontal cortex and parietal cortex were more active during pseudo-random response generation than during musical improvisation; no areas were more active during musical improvisation than during pseudo-random generation. Thirdly, the size of the response space was parametrically manipulated, i.e. the number of allowed notes (pitches) in the generative tasks. For the reasons given above, DLPFC activity was expected to be related to the size of the response space. However, this hypothesis could not be confirmed; no regions showed activity related to response space size (de Manzano and Ullén, 2012b). These findings can be interpreted as follows. First, it appears clear that there is a common core of regions,

including the DLPFC, that are involved in both pseudo-random generation and musical improvisation, and thus are likely to play domain-general functions in generative tasks. Secondly, the higher DLPFC activity in pseudo-random generation may have several reasons: that musical improvisation is an innately more natural behavior than pseudo-random generation; that musical improvisation was more trained than pseudo-random generation; that spontaneous musical responses need to be suppressed during pseudo-random generation. Thirdly, the lack of a relation between DLPFC activity and response space size may reflect that the three different response sets used in this study all represented different musical modes. The smallest set consisted of 2 notes only; the middle set (6 notes) were notes from an F major scale; and largest set (12 notes) consisted of the complete chromatic scale. Accordingly, there may have been a possibility for the subject to use strategies, i.e. improvise in a certain mode or style, to shortcut the need to maintain a particular response set online during the improvisation.

The PreSMA and lateral premotor regions have been proposed to be involved in sequential control and learning of spatial sequences, respectively. Thence, de Manzano and Ullén (2012) proposed these regions could also be implicated in controlling rhythmic and melodic aspects of the improvisation (de Manzano and Ullén, 2012a). Earlier studies of temporal and ordinal control of sequence performance sustained this hypothesis (Bengtsson et al., 2004; Schubotz and von Cramon, 2001). The idea was thus tested in an fMRI experiment using a 2×2 factorial design where the rhythmic and melodic structures of musical samples were either unspecified or determined (i.e. notated) with need for improvisation[22]. The results confirmed the hypothesis. Main effect analyses reinforced the idea of the PreSMA to be predominantly involved in rhythmic improvisation. The results also showed more activity in the PMD during melodic improvisation[23]. Nevertheless, a substantial overlap between brain regions involved in rhythmic and melodic improvisation was identified, i.e. both PreSMA and PMD displayed an increased activity throughout all improvisation conditions. These results come into line with the findings of Berkowitz and Ansari (2008) (Berkowitz and Ansari, 2008). In addition, a psychophysiological interaction analysis (PPI, consult 4.3.1) demonstrated that the correlation in activity between the PreSMA and cerebellum was higher during rhythmic improvisation than during other conditions. The authors concluded that functional connectivity between premotor areas and other regions depends on the spatiotemporal demands of movement sequencing control.

[22]The MR-compatible piano keyboard was the same as the one used in the previous investigation (de Manzano and Ullén, 2012b).

[23]The PreSMA was also significant activity in the main effect of melodic improvisation.

Lastly, Donnay et al. (2014) have recently reported a study which describes the neural correlates underlying interactive generative musical improvisation between two expert jazz musicians. A two block designed paradigm was used to assess such interaction between subjects. The two paradigms differed in level of complexity; "Scale" was a highly constrained task of minimal complexity, whereas "Jazz" represented a task with greater complexity and ecological validity. In Scale, there were two tasks: *(1)* both subjects play alternately a D Dorian scale in quarter notes or *(2)* they took turns improvising four measure phrases. The Jazz paradigm was also constituted by two different tasks: *(3)* both subjects played alternately four-measure segments of a novel jazz composition, which was memorized prior to scanning and *(4)* they improvised monophonically with no melodic and rhythmic restriction. For all experiments, one of the two participants was laid in the scanner, while the second one was in the control room. Brain activity using fMRI was measured in eleven male musicians. The interactive tasks were based on alternate responses between both participants. The subject inside of the scanner was always the first one who started the task. Contrasting the improvise tasks with the memorized tasks, the results showed an intense bilateral activation in IFG (corresponding left hemisphere area was placed in Broca's area), posterior STG (corresponding left hemisphere area was placed in Wernicke's area), as well as in the PreSMA. Deactivations during improvisation accounted for bilateral angular gyrus. General spontaneous musical exchange was associated with bilateral activation of the DLPFC. The authors concluded that regions involved in syntax processing, usually assigned to linguistic semantic processing, are not domain-specific for language but rather domain-general for communication (Donnay et al., 2014). Previous investigation from Limb and Braun (2008) revealed an extended deactivation over many areas, including the DLPFC, when musicians were performing improvisational musical tasks (Limb and Braun, 2008). The present study, in line with other studies, showed completely opposite results. The authors of this study thus claimed that such deactivation described in Limb and Braun's findings was due to a presumably state of "flow", often reported by musicians while playing. The authors also concluded that the activation exhibited in the DLPFC, on the latest results, is associated with conscious self-monitoring of behavior, due to the social context implied in the musical exchange paradigm. Indeed, DLPFC was previously identified to be involved on selection of suitable response's set given the task on demand (Nathaniel-James and Frith, 2002), suggesting a correlation between its activation and increased working memory demands while musical exchange. Study II featuring this thesis tackles the importance of providing a clear explanation about the specific contributions of the DLPFC in creative

cognition, by introducing a broader description based on the findings presented.

In conclusion, the differences in results suggest that musical improvisation is not restricted to a fixed set of regions but rather a network of interchangeably functional regions dependent of task- and context-specific domain. Nevertheless, further investigation is essential to identify the neurocognitive components, which may control the different aspects of the behavior.

References

Amabile, T. M. (1983). *The Social Psychology of Creativity*. Springer-Verlag, New York, USA.

Andrews-Hanna, J. R., Reidler, J. S., Huang, C., and Buckner, R. L. (2010). Evidence for the Default Network's Role in Spontaneous Cognition. *Journal of Neurophysiology*, 104(1):322–335.

Bengtsson, S. L., Csíkszentmihályi, M., and Ullén, F. (2007). Cortical Regions Involved in the Generation of Musical Structures during Improvisation in Pianists. *Journal of Cognitive Neuroscience*, 19(5):830–842.

Bengtsson, S. L., Ehrsson, H. H., Forssberg, H., and Ullén, F. (2004). Dissociating brain regions controlling the temporal and ordinal structure of learned movement sequences. *European Journal of Neuroscience*, 19(9):2591–2602.

Berkowitz, A. L. (2010). *The Improvising Mind: Cognition and Creativity in the Musical Moment*. Oxford University Press, New York.

Berkowitz, A. L. and Ansari, D. (2008). Generation of novel motor sequences: The neural correlates of musical improvisation. *Neuroimage*, 41(2):535–543.

Berkowitz, A. L. and Ansari, D. (2010). Expertise-related deactivation of the right temporoparietal junction during musical improvisation. *Neuroimage*, 49(1):712–719.

Bhattacharya, J. and Petsche, H. (2005). Drawing on Mind's Canvas: Differences in Cortical Integration Patterns Between Artists and Non-Artists. *Human Brain Mapping*, 26(1):1–14.

Boorstin, D. J. (1992). *The Creators: A History of Heroes of The Imagination*. Random House, New York.

Buckner, R. L., Andrews-Hanna, J. R., and Schacter, D. L. (2008). The Brain's Default Network: Anatomy, Function, and Relevance to Disease. *Annals of the New York Academy of Sciences*, 1124:1–38.

Carlsson, I. (2014). Biological and neuropsychological aspects of creativity. In Shiu, E., editor, *Creativity Research: An Inter-Disciplinary and Multi-Disciplinary Research Handbook*, number 34 in Routledge Studies in Innovation, Organizations and Technology. Routledge.

Carlsson, I., Wendt, P. E., and Risberg, J. (2000). On the neurobiology of creativity. Differences in frontal activity between high and low creative subjects. *Neuropsychologia*, 38(6):873–885.

Chávez-Eakle, R. A. (2007). Creativity, DNA, and cerebral blood flow. In Martindale, C., Locher, P., and Petrov, V. M., editors, *Evolutionary and Neurocognitive Approaches to Aesthetics, Creativity and the Arts*, Foundations and Frontiers in Aesthetics Series. Baywood Publishing Company, Inc., Amityville, New York.

Csikszentmihályi, M. (1988). Society, culture and person: a systems view of creativity. In Sternberg, R. J., editor, *The nature of Creativity: Contemporary psychological perspectives*, Part III The role of the individual-environment interaction in creativity The study of creative systems, pages 325–339. Cambridge University Press.

Csikszentmihályi, M. (1996). *Creativity*. HarperCollins, New York.

de Manzano, Ö. (2010). *Biological Mechanisms in Creativity and Flow*. PhD thesis, Karolinska Institutet.

de Manzano, Ö. and Ullén, F. (2012a). Activation and connectivity patterns of the presupplementary and dorsal premotor areas during free improvisation of melodies and rhythms. *Neuroimage*, 63(1):272–280.

de Manzano, Ö. and Ullén, F. (2012b). Goal-independent mechanisms for free response generation: Creative and pseudo-random performance share neural substrates. *Neuroimage*, 59(1):772–780.

Deiber, M.-P., Passingham, R. E., Colebatch, J. G., Friston, K. J., Nixon, P. D., and Frackowiak, R. S. J. (1991). Cortical areas and the selection of movement: a study with positron emission tomography. *Experimental Brain Research*, 84(2):393–402.

Desmond, J. E., Gabrieli, J. D. E., and Glover, G. H. (1998). Dissociation of Frontal and Cerebellar Activity in a Cognitive Task: Evidence for a Distinction between Selection and Search. *Neuroimage*, 7(4 Pt 1):368–376.

Dietrich, A. (2004). The cognitive neuroscience of creativity. *Psychonomic Bulletin & Review*, 11(6):1011–1026.

Dietrich, A. and Kanso, R. (2010). A Review of EEG, ERP, and Neuroimaging Studies of Creativity and Insight. *Psychological Bulletin*, 136(5):822–848.

Donnay, G. F., Rankin, S. K., Lopez-Gonzalez, M., Jiradejvong, P., and Limb, C. J. (2014). Neural Substrates of Interactive Musical Improvisation: an fMRI Study of 'Trading Fours' in Jazz. *PLoS One*, 9(2):e88665.

Doyon, J. and Benali, H. (2005). Reorganization and plasticity in the adult brain during learning of motor skills. *Current Opinion in Neurobiology*, 15(2):161–167.

Fink, A., Graif, B., and Neubauer, A. C. (2009). Brain correlates underlying creative thinking: EEG alpha activity in professional vs. novice dancers. *Neuroimage*, 46(3):854–862.

Finke, R. A., Ward, T. B., and Smith, S. M. (1992). *Creative Cognition: Theory, Research and Applications*. MIT Press, Cambridge, MA.

Frith, C. (2000). The Role of Dorsolateral Prefrontal Cortex in the Selection of Action as Revealed by Functional Imaging. In Monsell, S. and Driver, J., editors, *Control of Cognitive Processes*, Attention and Performance XVIII, pages 549–566. MIT Press, Cambridge, MA.

Gardner, H. (1993). *Creating Minds: An Anatomy of Creativity Seen Through the Lives of Freud, Einstein, Picasso, Stravinsky, Eliot, Graham, and Gandhi*. BasicBooks, New York.

Gjerdingen, R. (1988). *A Classic Turn of Phrase: Music and the Psychology of Convention*. University of Pennsylvania Press, Philadelphia, PA.

Gjerdingen, R. (2007). *Music in the Galant Style*. Oxford University Press, New York.

Gruber, H. E. (1981). *Darwin on man: A Psychological Study of Scientific Creativity*. University of Chicago Press, Chicago, USA, 2nd edition. Original work published 1974.

Gruber, H. E. (1988). The evolving systems approach to creative work. *Creativity Research Journal*, 1:27–51.

Gruber, H. E. and Davis, S. N. (1988). Inching our way up Mount Olympus: the evolving-systems approach to creative thinking. In Sternberg, R. J., editor, *The nature of Creativity: Contemporary psychological perspectives*, Part III The role of the individual-environment interaction in creativity The study of creative lives, pages 243–270. Cambridge University Press.

Guilford, J. P. (1967). *The Nature of Human Intelligence*. McGraw-Hill, New York.

Hadamard, J. (1945). *An Essay on the Psychology of Invention in the Mathematical Field*. Princeton University Press, Princeton, NJ.

Hershman, D. J. and Lieb, J. (1988). *The Key to Genius*. Prometheus Books, Buffalo, NY.

Hotz, R. L. (2009). A Wandering Mind Heads Straight Toward Insight. *The Wall Street Journal*, page A11. Friday, June 19.

Jahanshahi, M., Dirnberger, G., Fuller, R., and Frith, C. D. (2000). The Role of the Dorsolateral Prefrontal Cortex in Random Number Generation: A Study with Positron Emission Tomography. *Neuroimage*, 12(6):713–725.

Jahanshahi, M. and Frith, C. D. (1998). Willed Actions and Its Impairments. *Cognitive Neuropsychology*, 15(6-8):483–533.

Jung-Beeman, M., Bowden, E. M., Haberman, J., Frymiare, J. L., Arambel-Liu, S., Greenblatt, R., Reber, P. J., and Kounios, J. (2004). Neural activity when people solve verbal problems with insight. *PLoS Biology*, 2(4):0500–0510.

Lau, H. C., Rogers, R. D., Ramnani, N., and Passingham, R. E. (2004). Willed action and attention to the selection of action. *Neuroimage*, 21(4):1407–1415.

Limb, C. J. and Braun, A. R. (2008). Neural Substrates of Spontaneous Musical Performance: and fMRI Study of Jazz Improvisation. *PLoS One*, 3(2):e1679.

Maduro, R. (1976). *Artistic Creativity in a Brahmin Painter Community*, volume 14 of *Research Monographs Series*. Center for South and Southeast Asia Studies, University of California, Berkeley.

Manson, M. F., Norton, M. I., Horn, J. D. V., Wegner, D. M., Grafton, S. T., and Macrae, C. N. (2007). Wandering Minds: The Default Network and Stimulus-Independent Thought. *Science*, 315(5810):393–395.

Martindale, C. and Hines, D. (1975). Creativity and cortical activation during creative, intellectual and EEG feedback tasks. *Biological Psychology*, 3(2):91–100.

Mihov, K. M., Denzler, M., and Förster, J. (2010). Hemispheric specialization and creative thinking: A meta-analytic review of lateralization of creativity. *Brain and Cognition*, 72(3):442–448.

Nathaniel-James, D. A. and Frith, C. D. (2002). The Role of the Dorsolateral Prefrontal Cortex: Evidence from the Effects of Contextual Constraint in a Sentence Completion Task. *Neuroimage*, 16(4):1094–1102.

Playford, E. D., Jenkins, I. H., Passingham, R. E., Nutt, J., Frackowiak, R. S. J., and Brooks, D. J. (1992). Impaired Mesial Frontal and Putamen Activation in Parkinson's Disease: A Positron Emisssion Tomography Study. *Annals of Neurology*, 32(2):151–161.

Poincaré, H. (1921). *The Foundations of Science*. Science Press, New York.

Pressing, J. (1984). Cognitive Processes in Improvisation. In Crozier, W. R. and Chapman, A. J., editors, *Cognitive Processes in the Perception of Art*, pages 346–347. Elsevier, Amsterdam.

Ribot, T. A. (1921). *Essay on the Creative Imagination*. Open Court, Chicago.

Rink, J. (1993). Schenker and Improvisation. *Journal of Music Theory*, 37(1):1–54. Summary of Heinrich Schenker's ideas about improvisation.

Rossman, J. (1931). *The Psychology of the Inventor*. Inventors Publishing, Washington, DC.

Sawyer, K. (2011). The Cognitive Neuroscience of Creativity: a Critical Review. *Creativity Research Journal*, 23(2):137–154.

Schubotz, R. I. and von Cramon, D. Y. (2001). Interval and Ordinal Properties of Sequences Are Associated with Distinct Premotor Areas. *Cerebral Cortex*, 11(3):210–222.

Simonton, D. D. K. (1999). *Origins of Genius : Darwinian Perspectives on Creativity*. Oxford University Press, New York.

Sternberg, R. J., editor (1999). *Handbook of Creativity*. Cambridge University Press, Cambridge, United Kingdom.

Sternberg, R. J. and Lubart, T. I. (1991). An investment theory of creativity and its development. *Human Development*, 34:1–32.

Sternberg, R. J. and Lubart, T. I. (1992). Buy Low and Sell High: An Investment Approach to Creativity. *Current Directions in Psychological Science*, 1(1):1–5.

Sternberg, R. J. and Lubart, T. I. (1995). *Defying the crowd: cultivating creativity in a culture of conformity*. The Free Press, New York.

Sternberg, R. J. and Lubart, T. I. (1996). Investing in creativity. *American Psychologist*, 51(7):677–688.

Stillings, N. A., Weisler, S. E., Chase, C. H., Feinstein, M. H., Garfield, J. L., and Rissland, E. L., editors (1998). *Cognitive Science: An Introduction*. MIT Press, Cambridge, MA, 2nd edition.

Tafuri, J. (2006). Processes and teaching strategies in musical improvisation with children. In Deliège, I. and Wiggins, G. A., editors, *Musical Creativity: Multidisciplinary Research in Theory and Practice*. Psychology Press.

Thagard, P. (2014). Cognitive Science. In Zalta, E. N., editor, *The Stanford Encyclopedia of Philosophy*. forthcoming `http://plato.stanford.edu/archives/fall2014/entries/cognitive-science/`.

Wallas, G. (1926). *The Art of Thought*. Harcourt, Brace and Company, New York.

Chapter 2

Aims of the Thesis

The aim of this thesis was to carry out two studies to investigate the neurocognitive mechanisms underlying musical creativity. Musical improvisation is taken here as the ecologically valid behavioral model that can most accurately represent creative musical performance.

2.1 Study I: Expertise in Musical Creativity

Study I sought to investigate the neural networks which evolve from systematic and long-term practice of creative musical performance. Particularly, the aim was to study the specific neurocognitive effects derived from expertise in musical improvisation. Both functional specialization and functional connectivity associated with hours of improvisational musical training were explored in order to understand the influence of creative musical practice to the fullest extent.

2.2 Study II: Dual Neural Pathways to Creativity

Study II was dedicated to explore the neural correlates of creative musical performance under particular constraints. Real life improvisation typically involves both expressive goals, e.g. to convey a particular mood or emotion, and constraints on the musical structure of the improvisation. The neurocognitive effects of musical improvisation were explored using either an emotional constraint (happy or fearful) or a structure constraint (set of pitches). Further, the involvement of the DLPFC was specifically examined in the analysis. Many neuroimaging studies have reported contradictory results with regard to its contribution to creative cognition. The present study is thus an attempt to clarify this matter more definitely.

Part II

Methods

The aim of this part is to provide a general outline of the experimental procedures and data analysis employed in the studies featuring in this thesis. The techniques include the acquisition and the statistical analysis of functional neuroimaging data using fMRI and methods of retrieving information from music. Additionally, this section contains a brief description regarding participants, recruitment processes, procedures during data collection and questionnaires administered. For a complete description and technical details of each study, the reader is referred to the original version of the corresponding article in part 4.9.

All studies share the same data set collected from a magnetic resonance imaging experiment conducted at the Karolinska Institutet (KI) MR-Research center located at the Karolinska Hospital (Stockholm, Sweden).

Chapter 3

Materials and Experimental Procedures

3.1 Participants and Ethical Considerations

All participants recruited for the experiment were active and highly proficient in piano playing. They confirmed to have a daily routine of piano practice from their childhood up to date. They also stated to have always had piano as their first musical instrument. This profile is especially important since there is clear evidence that creative performance is associated to expertise in a particular field, i.e., domain-specific skills allows for retrieval of relevant information and recognition when a novel and original idea is likely to be valid or significant (Sternberg, 1999, pp. 207-208).

The set of participants recruited for the experiment comprised two different types of experience in piano playing: classical and jazz. Since one study was dedicated to investigate specificities in expertise across different levels of musical professionalism, it was argued during the design of the experiment that it would be important to have different kinds of expertise in piano playing.

All participants were healthy human volunteers with no history of neurological or psychiatric illness in order to avoid any possible clinical confounds. They were right-handed and handedness was accessed through the Swedish version of the Edinburgh Handedness Inventory (Oldfield, 1971).

The Regional Ethical Review Board in Stockholm approved the experiments. Upon recruitment, all subjects were screened according to MR safety protocols. The participants were informed in advance about the purpose of the study, the techniques employed and safety

procedures. They also provided their informed written consent prior to taking part in the experiment and according to The Code of Ethics of the World Medical Association (Declaration of Helsinki).

Thirty nine participants out of fifty participants took part of the final sample. The remaining eleven subjects had to be excluded from the analyses due to several reasons: technical failure of the MR-scanner, problems with recording the musical samples played by the participants over the experiment and health issues.

Descriptive statistics for the sample are presented in the tables 3.1 and 3.2.

Table 3.1: Age range (years) of the final sample of participants

	Classical	Jazz	Total Range
Male	19-49	19-67	19-67
Female	24-42	20-56	20-56
Total Range	19-49	19-67	19-67

Table 3.2: Mean Age and the corresponding Standard Deviation (SD) of the final sample of participants

	Mean (years)	SD (years)
Male	32.71	12.17
Female	32.00	9.15
Classical	31.95	8.38
Jazz	32.95	13.42
Total	32.44	10.98

3.2 Behavioral Data Acquisition and Audio Feedback

A custom designed MR-compatible fiber-optic piano keyboard (LUMItouch, Inc.) was used to record the musical samples performed by the participants (see Figure 3.1). This keyboard of one octave was constituted by twelve authentic keys ranging from F2 to E3. The keyboard was connected to an optical-electrical converter placed outside the scanner in the control room. The converter was in turn connected to a MIDI-keyboard (Midistart-2 Pro Keys; Miditech)

specifically customized for this setup, thus generating a signal in a standardized protocol, such as MIDI. The MIDI signal was subsequently sent to a MIDI patchbay/processor (MX-8; Digital Music Corp.) which in turn produced two different MIDI outputs. The first output was relayed to a sound module (Roland SD-50) which synthesized the piano sound (GM2, European Pf). This device was connected to the audio system of the *magnetic resonance imaging* (MRI) scanner in order to provide music feedback to the participants. In this way, it was guaranteed that a more ecological sound feedback of the musical performance would be provided to the participant. The second output was relayed to an external sound card which was in turn connected to a PC recording the musical samples through a music production software (Cubase Studio 5; Steinberg). A sound sampler (Kontakt 4, Concert Grand Piano; Native Instruments) was used in addition with Cubase allowing for a more ecological sound record.

Figure 3.1: MR-compatible fiber-optic piano keyboard (LUMItouch, Inc.)

3.3 Experimental Design

The paradigm of the fMRI experiment was a *block-design*. This category consists on the maintenance of cognitive task engagement during and/or after presentation of the stimulus within a 'block period' (or *condition*). A sequential set of conditions, which repeats over time, is known as a *trial*. A pre-determined number of trials constitutes one *session*. Finally, a set of sessions composes an entire experiment performed by the participant (see Figure 3.2).

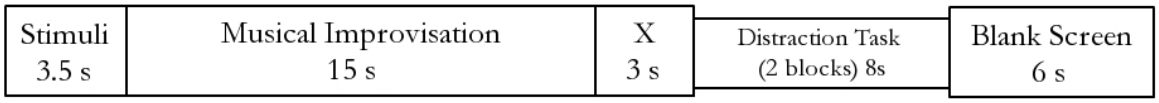

Figure 3.2: Schematic representation of a trial of the experimental paradigm. The trial began with the presentation of the musical stimulus for three and a half seconds, containing a cue for the next musical improvisation block period with a respective duration of fifteen seconds. Afterwards, a cross was shown for three seconds, indicating the compulsory stoppage of the musical performance, followed by a distractor task (constituted by two block periods) with a respective duration of eight seconds. At last, a blank screen was displayed for six seconds, marking the resting state period.

3.3.1 Visual Stimuli

During the fMRI experiment, a visual instruction slide was presented right before the improvisational moment. The slide contained a cue for the upcoming improvisational performance. These cues consisted on four active conditions differing in executive constraints that the participants should engage when improvising. The conditions were grouped in two different categories: *Structural* and *Emotional* (see Figure 3.3).

In *Structural*, the participants were instructed to improvise using only six different pitches. These were displayed as 6 whole notes, notated on a single G-clef staff. There were two different types of conditions in this category: *Tonal* and *Atonal*. In *Tonal*, a subset of pitches from the same Western musical scale (major and minor) was represented, thus naturally suggesting a tonality for the improvisation. In contrast, a random generated subset of pitches was represented during *Atonal*. Two different criteria were employed for the randomization: *(i)* the pitches were not all part of the same scale; *(ii)* there would be at least one interval equal to or larger than a minor third, in order to avoid chromatic sequences. Hence, the pitch set for *Atonal* did not suggest any particular tonality. The pitch sets were unique in every trial of *Tonal* and *Atonal* across the whole experiment.

In *Emotional*, the participants were instructed to produce an improvisation corresponding to the emotional character previously presented. There were two different types of conditions in this category: *Happy* and *Fearful*. Hence, the instruction slide for these conditions showed a happy or fearful clip art face. The fact that these particular emotional descriptors both have different affective valences (i.e. happiness and fear refer to attraction/pleasant and aversion/unpleasant states, respectively) and share approximate levels of arousal accounted

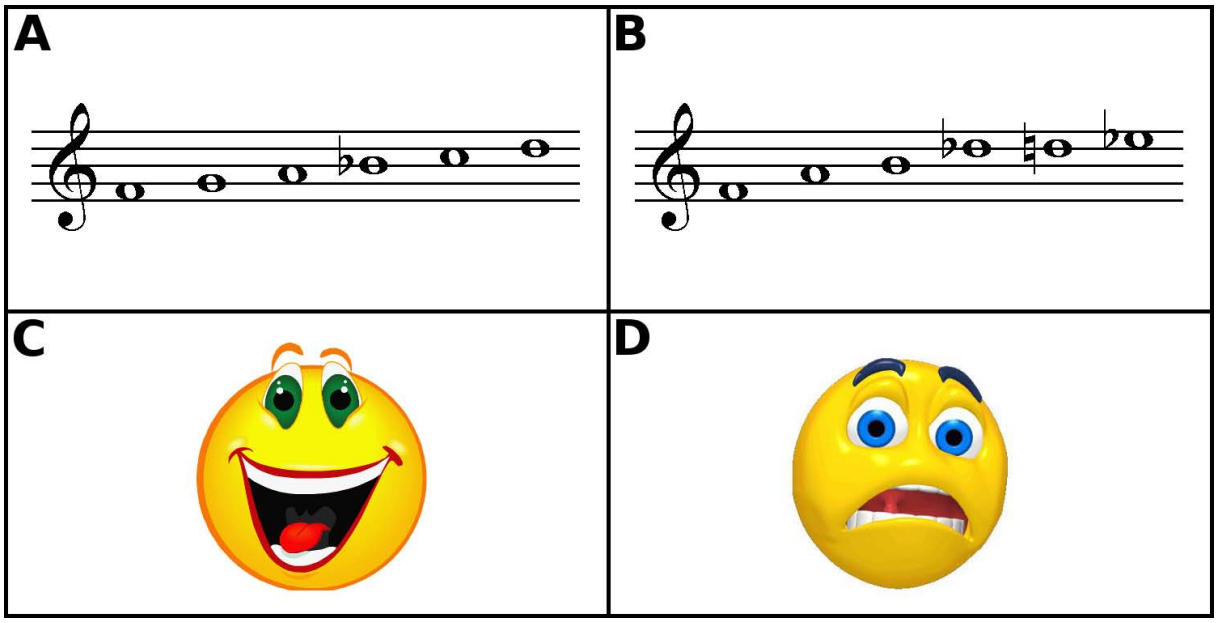

Figure 3.3: Examples of visual stimuli presented during experimental conditions. Four active conditions were used in the experimental block design arranged according to two different categories of conditions: (**A** and **B**) *Structural*, where improvisations were performed given a specific set of six different pitches and (**C** and **D**) *Emotional*, where improvisations were performed given a specific emotional descriptor. The conditions were: (**A**) *Tonal* - improvisations were performed according to a subset of pitches from the same Western musical scale; (**B**) *Atonal* - improvisations were performed according to a random generated set of pitches; (**C**) *Happy* - improvisations were performed so that the music expressed happiness; (**D**) *Fearful* - improvisations were performed so that the music expressed fear.

for the reason of their choice (Lang, 1995). While differences in emotional processing between positive and negative emotions were investigated, one could thus expect that the amount of notes played throughout these conditions would be similar between them, ensuring as well the non-occurrence of major discrepancies in the motor outcome.

There were never more than two consecutive trials presenting the same condition nor more than three consecutive trials displaying conditions from the same category. The restrictions employed in all conditions promote the same level of complexity on the musical performances.

3.4 Piano Experience Questionnaire

In study I, piano experience was evaluated using a customized questionnaire. The questionnaire was administrated right before the neuroimaging experiment. It contained separate estimates of the mean intensity for total number of hours dedicated per week to piano playing, as well as the number of hours per week spent on improvisation training. These estimates were assessed in three age periods: *(i)* six to eleven years old, *(ii)* twelve to seventeen years old and *(iii)* eighteen up to present. From these data, the total number of hours spent improvising (*Imphours*), total experience (*Totalhours*) and experience in classical (non-improvisatory) piano playing (*Classhours* = *Totalhours* - *Imphours*) was calculated.

The test-retest reliability of the practicing data was performed with data collected from thirty out of the original set of participants using an online questionnaire. This questionnaire was developed in our research group for an independent study (Ullén et al., 2014) and it had also included the same estimates of the previous one.

3.5 Functional Magnetic Resonance Imaging

Functional magnetic resonance imaging (fMRI) is a class of imaging techniques devoted to measure regional, time-varying changes in the brain metabolism. These metabolic changes can come as a consequence of task-induced cognitive state changes (Bandettini et al., 1992; Kwong et al., 1992; Ogawa et al., 1990; Glover, 2011).

Since the early nineties, fMRI has been extensively used in studies encompassing cognitive neurosciences as well as clinical psychiatry/psychology. It is a non-invasive technique because it requires no administration of pharmacological agents. As its name implies, fMRI uses a strong magnetic field to create images depicting neural activity and static magnetic fields, even extremely strong ones, have no known long-term deleterious effects on biological tissues, unlike other techniques using ionizing radiation. It has also very good spatial resolution, allowing for the registration of fluctuations in activity across different spatial locations in the brain (Glover, 2011; Huettel et al., 2009). Thus, the possibility to capture time variations of the neural signal with high spatial specificity and relate those changes to ongoing behavior offers a unique tool to investigate the functional organization of the human brain. It is therefore the technique par excellence to unravel the neurophysiological pathways underlying high cognitive behaviors, such as creativity.

fMRI is a procedure based on magnetic resonance imaging (MRI). The underpinnings of

image formation in MRI uses *nuclear magnetic resonance imaging* (NMR), where uniform magnetic fields are used, together with a superimposed gradient in the magnetic field to create the images. The difference in signal intensity between two distinct tissues depicted on an image is known as a contrast. Different types of contrast can be employed depending on the properties of the tissues being measured. *Blood-oxygenation-level dependent* (BOLD) contrast is the one typically used in fMRI to describe metabolic changes in the brain.

The following subsections provide an overview of fMRI methodology from the generation of the MR signal in a standard MRI scanner to the measurement of the BOLD signal intensity from the acquired images.

3.5.1 Principles of MR Signal Generation

MRI relies upon the interaction between an applied magnetic field and a nucleus that possesses NMR property. Since human body is mostly constituted by water and fat, the far most abundant atoms in the tissues are the hydrogen uniquely composed by single-protons. The hydrogen nuclei are thus the most common nuclei imaged using MRI and the upcoming description regarding the underlying physical phenomena in both MRI and fMRI will be focused on single-proton properties.

Under normal conditions, thermal energy promote the protons to spin around their own axis, so that each will possess an angular momentum (spin). The protons also carry positive charge and their spins generate an electric current on their surfaces, thus creating an individual magnetic moment. In the absence of a strong external magnetic field, the spin axes of the protons are randomly oriented and as a consequence the sum of the magnetic moments of all spins (net magnetization) will be approximately zero.

In the presence of an external magnetic field, the spins will start precessing around an axis which is either parallel to the magnetic field (low-energy state) or antiparallel to the magnetic field (high energy state). The frequency of the precession (a gyroscopic motion) is determined by the type of the nucleus and it is proportional to the magnitude of the external magnetic field. It is named *Larmor frequency* and it can be determined as follows:

$$\omega = \gamma B \tag{3.1}$$

where ω is the Larmor frequency of the precession, B is the magnitude of the applied magnetic field and γ is the gyromagnetic ratio specific to each nucleus. Considering the principle of energy minimization, the majority of these spins will assume the low-energy state, creating a

net magnetization parallel to the magnetic field. If the spins in the low-energy state receive energy equivalent to the difference between the two states, they will transit to high-energy state, turning the longitudinal magnetization into transverse magnetization. This phenomenon is known as *excitation* and the energy absorbed corresponds to the resonance frequency, i.e., the Larmor frequency. When the energy source ceases, the spins will release the same energy, falling back to the original state of low-energy and restoring the longitudinal magnetization. The electromagnetic energy emitted provides the MR signal, which is in turn recorded by a *radiofrequency* (RF) coil tuned to the resonance frequency.

Both excitation of the spins and reception of the energy emitted by them are accomplished by the same RF coil, since the corresponding frequencies are at the Larmor frequency. When the net magnetization is aligned along the external magnetic field, its precession cannot be detected by the coils in the scanner. But when the net magnetization is flipped onto the transverse plane, the precession generates an oscillating electric current in these coils. This current constitutes the MR signal.

The detected MR signal depends on the change of the net magnetization over time across different tissues. When the net magnetization is flipped onto the transverse plane due to the emission of an excitation pulse by the radiofrequency coils in the scanner, all the spins are precessing at the same phase and with the same resonance frequency. However, the spin-spin interaction during their excitation leads to differences in precession frequencies and, in consequence, a dispersion in the relative phases occurs over time. The *spin-spin relaxation time*, or T_2, is a time constant which describes the decay of the transverse component of the net

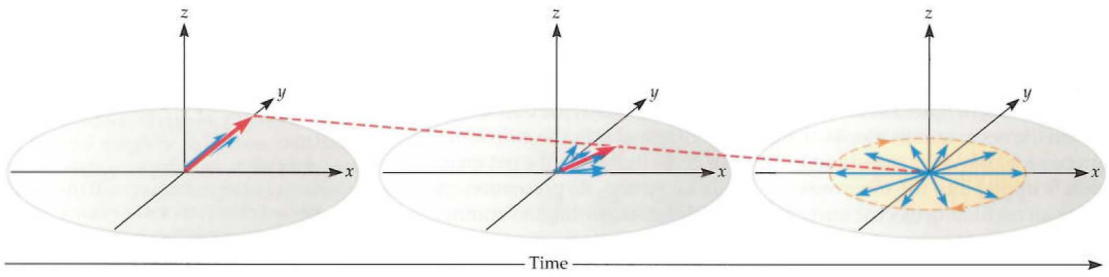

Figure 3.4: A conceptual depiction of T_2 decay. After the net magnetization has been flipped onto the transverse plane, it decays straight off because the spins start precessing out of phase. For most type of tissues, the net magnetization decays almost to zero within a few hundred miliseconds (red dashed line). Reproduced from (Huettel et al., 2009, pp. 66), with permission from the publisher.

magnetization. Besides, the combined effects of spin-spin interactions with inhomogeneities in the magnetic field is described by the time constant T_2*. The decay of the transverse component of the net magnetization is followed by a recovery of its longitudinal component along the orientation of the main magnetic field (see Figure 3.4). The *spin-lattice relaxation time*, or T_1, is a time constant characterizing the transfer of energy from the precessing spins to the surrounding atoms (the lattice), resulting in the recovery of the longitudinal component of the net magnetization (see Figure 3.5). T_1 is significantly longer than T_2, i.e., approximately one order of magnitude larger. Depending on when the acquisition of the image starts, these parameters will determine the amplitude of the MR signal and thus the intensity of the acquired image. Since they are inherent properties of the tissues, they assume different fixed values according to the type of tissue and the magnitude of the magnetic field. Hence, presetting the values of T_1 and T_2 will establish different intensities for different tissues, providing a specific contrast on the image. The contrasts thus enhance tissue-specific properties, allowing for their investigation concerned with research or clinical purposes. In addition, T_1 also influences the acquisition rate of the images, since it is by definition the exact time required for the total recovery of the longitudinal magnetization. Consequently, it also represents the necessary time for the application of the next excitation pulse into the spin system (Huettel et al., 2009).

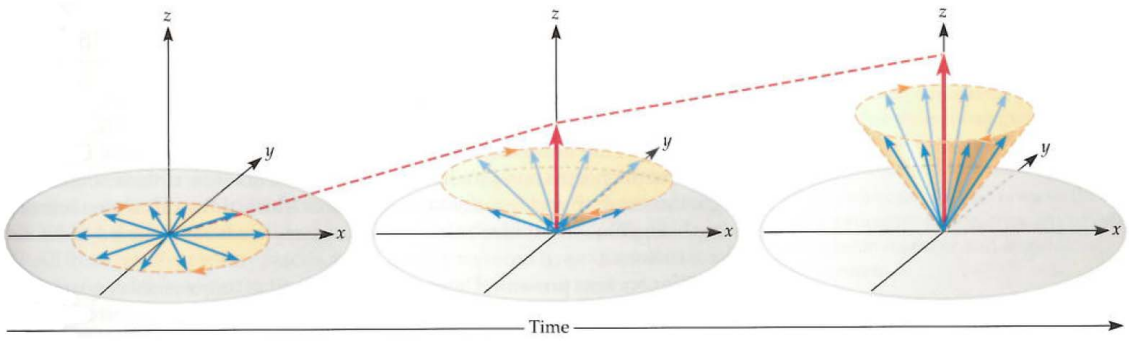

Figure 3.5: A conceptual depiction of T_1 recovery. The net magnetization flips onto the transverse plane due to the absorption of energy that allows the spins to transit from low-energy state to high-energy state. When the energy source (RF coil) stops emitting the excitation pulse, the spins liberate the absorbed energy to the lattice. The net magnetization will therefore return to the initial longitudinal orientation along the main magnetic field, recovering usually its original amplitude within a few seconds (red dashed line). Reproduced from (Huettel et al., 2009, pp. 67), with permission from the publisher.

3.5.2 Principles of MR Image Formation

An MRI (or fMRI) image is a representation of the spatial distribution of one or more properties of the spins. These properties reflect tissue-specific features related with the spins' density, their mobility or their respective T_1 and T_2 values. Therefore, a critical concept in reference to MRI images' formation is how to encode and decode spatial information due to the spatial variability of the measurements across different tissues. In 2003, Paul Lauterbur and Peter Mansfield were awarded the Nobel Prize in Physiology or Medicine for their discoveries regarding this topic. They demonstrated that spatial encoding relies on the superimposition of additional magnetic fields, whose magnitude vary linearly across space. As a result, all spins from the sample will precess at slightly different frequencies from each other (Mansfield and Maudsley, 1976; Mansfield, 1977).

In order to access correctly the relative location of the spins that contribute for the generation of the MR signal in a three-dimensional space, three spatial gradient magnetic fields must be superimposed to the static magnetic field. The gradient magnetic fields indicate how the magnitude of the static magnetic field varies along the three directions. In this way, the MR signal will allow of three different components that will characterize the signal at a specific position in space from which the signal originated. It is important to emphasize that the direction of the static magnetic field always remains the same; only its magnitude (i.e., its *strength*) changes at a given spatial location.

Because the gradient fields along any of the three directions solely modulate the frequency of the precessing spins, only one spatial dimension can be encoded at the time. Thus, a sequential set of changes on the gradient fields combined with the RF pulses emitted by the coils in the scanner is employed in order to create an MR image. There are three main conventional steps involved in the formation of a three-dimensional MR image: *(i)* slice selection, *(ii)* frequency encoding, and *(iii)* phase encoding (Huettel et al., 2009; Goebel, 2007).

3.5.2.1 Slice Selection

The most common technique used to acquire three-dimensional MR images is the collection of two-dimensional slices of the entire brain volume per unit of time. Since spins precess at different frequencies along the applied spatial gradient, they can be excited in a selective fashion using a RF pulse within a specific range. As a result, spins precessing at frequencies outside from this range will not resonate. It is important to emphasize that the selected spins are located in a slice oriented perpendicularly in reference to the direction of the gradient and,

consequently, the acquisition of the slices is performed along the axis of the gradient.

Slice location and thickness depend on three factors: *(i)* the central value in frequency of the RF excitation pulse; *(ii)* the bandwidth of the respective pulse; and *(iii)* the magnitude of the gradient field (see Figure 3.6). The central value in frequency of the RF pulse combined with the gradient field determine the slice location, whereas the bandwidth and the gradient field determine the slice thickness. Therefore, a successive variation of the central value in the frequency of the pulse will enable a selective acquisition of the MR signal in consecutive slices along the axis of the gradient. Likewise, the thickness of the respective slices will be determined by the bandwidth, since the range of frequencies presented in the excitation pulse will influence how many spins will be in resonance. Note that a stronger gradient will result in greater differences between spins at nearby location, allowing for more spatial specificity in excitation at a given RF pulse. Consequently, stronger gradients increase spatial resolution across slices, i.e., the same RF pulse can be applied to collect a slice with a different location and thickness (Huettel et al., 2009; Goebel, 2007).

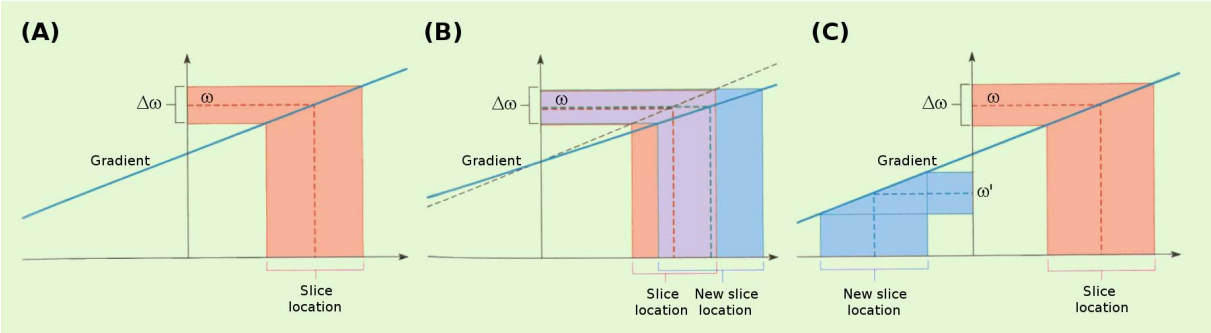

Figure 3.6: Setting slice thickness and location. **(A)** The specification of the linear gradient (solid line) and the RF pulse, i.e. the bandwidth $\Delta\omega$ and its center value ω, is required for selecting the slice location (horizontal axis). **(B)** By adjusting the slope of the gradient, the same RF pulse can determine a different slice location and thickness. **(C)** By choosing different values for the frequency of the pulse (e.g. ω'), the same gradient can be employed to select a different slice location. Adapted from (Huettel et al., 2009, pp. 109), with permission from the publisher.

3.5.2.2 Frequency Encoding

After slice selection, a second gradient aligned along one dimension of the selected slice is applied. Since the spins' frequency is proportional do the applied magnetic field, slower oscillations are now superimposed to the faster ones resultant from the RF excitation pulse. The corresponding MR signal will thus reflect the constructive and destructive interference between signals with small differences in frequency. Hence, this technique allows for spatial differentiation according to the position of the spins within that specific slice, since the spins start precessing at slight different frequencies along the respective dimension. Due to this effect, this second gradient is usually called the *frequency-encoding gradient* (Huettel et al., 2009; Goebel, 2007).

3.5.2.3 Phase Encoding

A third gradient must be added in order to differentiate signal components originated from different positions along the second dimension within the same slice. Nonetheless, this gradient shall be applied in a sequential fashion in relation to the second gradient. By doing otherwise, it would result in an ambiguous spatial encoding because it would only introduce one linear change.

This gradient is usually referred as the *phase-encoding gradient* and it is in fact applied before the frequency-encoding gradient and along an axis orthogonal to the latter. The spins will thus start precessing at slightly different rates, depending on their positions along the axis of the applied gradient field. When the gradient is interrupted, the precession frequency of the spins will return to the original value (i.e. Larmor frequency) but the spins will also be precessing out of phase. As a result, the spins of a particular slice which are located on the same orthogonal row to the gradient direction will have the same phase.

The application of phase encoding must be repeated successively (i.e. row-by-row) for one single slice. At each time the phase-encoding gradient is applied, its magnitude is slightly changed in order to obtain a complete frequency phase encoding of the entire slice. The phase differences remain until the signal is recorded.

It is important to emphasize that the phase-encoding gradient is very weak when compared to the frequency-encoding gradient. In this way, it is assured that no big changes will occur at the precessing frequency along the phase-encoding gradient field. If a strong positive gradient was applied during phase encoding, the combination of both phase and frequency encoding gradients would generate a diagonal change (i.e. only one linear change) of the precession

frequency across the slice and it would be no longer possible to resolve the two-dimensional spatial information (Huettel et al., 2009; Goebel, 2007).

3.5.2.4 Two-Dimensional κ-Space

The data collected from the superimposition of the gradient fields can be arranged in a two-dimensional space usually referred as the κ space. In a typical acquisition sequence of anatomical images, like the *gradient-echo imaging pulse sequence* (GRE, see Figure 3.7 **A**), the κ-space is filled one line (row) at a time (cycle), as a consequence of successive excitation pulses. During each cycle of excitation, the combination of the RF pulse with the gradient along the main magnetic field selects the slice. Afterwards, the phase-encoding gradient is applied right

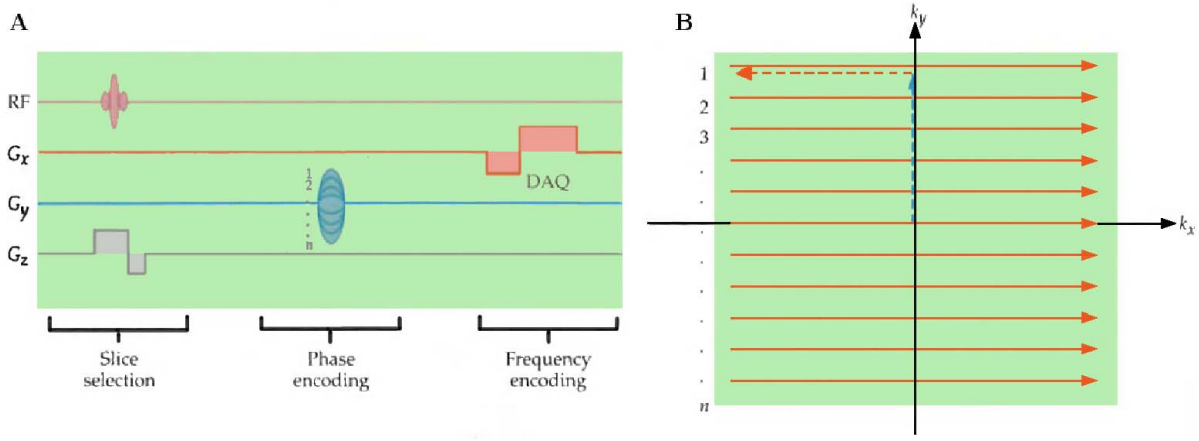

Figure 3.7: 2D gradient-echo pulse sequence. On **A**, it is represented the timeline of a typical two-dimensional gradient-echo imaging pulse sequence (GRE); the RF excitation pulse begins at the same time as the slice selection gradient field (G_z); afterwards, the phase-encoding gradient field (G_y) is applied in order to select one line of the κ-space; then, the frequency-encoding gradient field (G_x) is turned on for the data acquisition (DAQ). The sequence is repeated with slight changes in the magnitude of G_y. On **B**, it is represented the scheme of the pulse sequence on the κ-space. The lines (shown as $1...n$) are acquired within a particular slice selection. After one excitation pulse, G_y is applied with a particular magnitude at a specific line, followed by the application of G_x with a constant magnitude and duration. The process repeats for the acquisition of the n lines, always assured by the successive application of G_y and G_x, respectively, with increasing changes in their respective magnitudes. The acquisition will thus follow an upward and downward pathway between lines and a rightward pathway within lines in the κ-space, due to the respective directions of G_y and G_x. After n excitations, all of the frequencies in the κ-space are collected and image acquisition is complete. Adapted from (Huettel et al., 2009, pp. 112), with permission from the publisher.

before the data acquisition period. This gradient yields a phase offset before the application of the frequency-encoding gradient. Since the phase-encoding gradient changes magnitude by a constant value across cycles and, thus, from line to line in the κ space, the data acquisition will be performed cycle-by-cycle along the direction of the phase-encoding gradient (as shown by the blue narrow in Figure 3.7 **B**). Nevertheless, the data acquisition only starts when the frequency-encoding gradient is turned on. In other words, the signal readout occurs upon the spins' frequency changing within each slice.

The set of phase encoding steps is implemented in a discrete fashion. Each line depicts a separate amplitude of the phase-encoding gradient along its direction (see Figure 3.7 **B**). The MR signal is thus sampled with a specific interval, so that each row consists of a number of discrete data points. On the other hand, the acquisition along the axis of the frequency-encoding gradient is continuous.

The κ space contains two-dimensional frequency encoded information of a particular slice. This can be transformed into two-dimensional image space using the two-dimensional *Fourier transform* (2D FT). The image reconstruction thus relies on the inverse Fourier transform which allows the conversion of κ-space data in spatial frequency domain into data reflecting magnetization of the spins at each spatial location (Huettel et al., 2009; Goebel, 2007).

3.5.3 MR Pulse Sequences and Contrast Mechanisms

MRI allows for a multiplicity of contrasts, depending on the type of tissues' properties under consideration. There are two main kinds of contrast for MRI: *static contrasts* and *motion contrasts*. Static contrasts give information concerning number or content of atomic nuclei, whereas motion contrasts describe dynamic characteristics of the protons in the brain. Each type may also be classified according to the intrinsic properties of the biological tissues (aka *endogenous contrast*) or the presence of an external agent that have been introduced into the body (aka *exogenous contrasts*). Since brain anatomy imaging as well as fMRI rely on static contrasts based on the relaxation times of the different tissues with no intervention from MRI contrast agents, the upcoming discussion will be focused on T_1, T_2 and T_2* dependent contrasts and related pulse sequences.

3.5.3.1 MRI Pulse Sequences

There are two important factors that determine the time at which MR images are collected. The first one is the *repetition time* (TR), which describes the time interval between successive

RF excitation pulses. The second one is the *echo time* (TE), which refers to the time between excitation and data acquisition from the center of the κ-space[1] (see section 3.5.2.4). By controlling TR and TE plus considering the relaxation times of the tissues, the MR signal can be manipulated. As it is stated in the beginning of this section, the differences in the signal intensity between multiple tissues represent the contrast. A pulse sequence is thus a predefined set of several components, such as: *(i)* the primary RF excitation pulse; *(ii)* the gradient fields used for spatial encoding; *(iii)* the relaxation times of the biological tissues; *(iv)* the applied TR and TE and; *(v)* type of echo signal recorded (i.e. whether or not it uses a refocusing pulse for generating the echo signal). It is, usually, repeated many times during a scan and its settings reflects the characteristics (e.g. properties of the tissues, space resolution, etc.) of the MR images. It also determines the speed of the acquisition and it restricts the amount of artifacts without changing the signal-to-noise ratio of the MR signal. Hence, it becomes essential to set the proper pulse sequence in order to get the intended contrast.

There are two main families of pulse sequences, depending on which type of echo signal is recorded: the *gradient-echo imaging* (GRE) and *spin-echo imaging* (SE). The GRE makes only use of the gradients to generate the signal echo (see Figure 3.7), whereas the SE also uses a second 180° rephasing RF pulse.

GRE has been widely used due mostly to faster acquisitions. In this imaging technique, the applied flip angle is usually lower than 90° which promotes a faster recovery of the longitudinal magnetization, allowing for shorter TR/TE and thus decreasing the scanning time (Huettel et al., 2009).

3.5.3.2 T_1 contrast

The formation of T_1 - weighted images is based on the difference of signal intensity between voxels that depends on the T_1 values of the corresponding tissues. In order to maximize these differences in the signal among different tissues, the TR and TE values must be set accordingly. For very short TR values, there's no time for longitudinal magnetization recovery and thus no MR signal is registered for either tissues. On the other hand, the longitudinal magnetization will totally recover for both tissues if the TR is very long and, consequently, no MR signal will be recorded either. Therefore, intermediate TR values must be set to allow for registration of the differences in T_1 recovery amidst different tissues. In this way, the tissues that have a shorter T_1 value recover faster and hence have greater MR signal. There is an optimal TR

[1]The MR signal received at the center of the κ-space has maximum amplitude, such that it resembles an echo of the initial transmission.

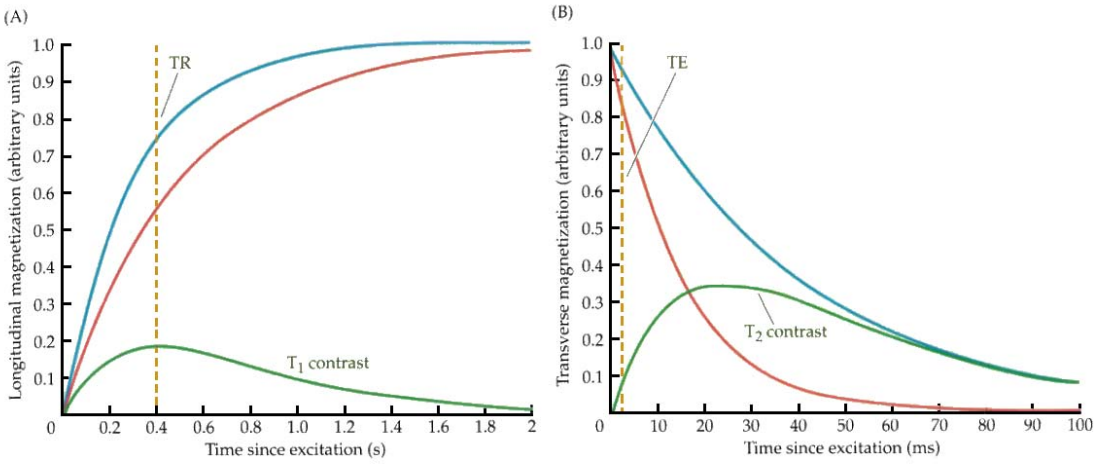

Figure 3.8: Optimal TR and TE values for T_1 contrast. The graphs exhibit **(A)** TR and **(B)** TE values (vertical, dashed orange lines) that maximize the T_1 contrast and minimize the T_2 contrast, providing images with exclusive T_1 contrast. The green lines represent the contrast related to different **(A)** TR and **(B)** TE values. Adapted from (Huettel et al., 2009, pp. 127), with permission from the publisher.

value such that the difference between the T_1 recovery of two distinct tissues is maximum (see Figure 3.8). Additionally, in order to get T_1 contrasts solely, the TE value must take very short values, to minimize T_2 contrast (see section 3.5.3.3).

T_1 - weighted contrast is frequently used for structural contrast of anatomical images of the brain (Huettel et al., 2009).

3.5.3.3 T_2 contrast

T_2 - weighted images depend on differences of the signal intensity across voxels which vary according to the T_2 values of the respective tissues. These differences relate to the amount of signal loss between excitation and data acquisition, i.e. the TE. Similarly to T_1 contrasts, the values for TR and TE must be optimized in order to maximize the T_2 contrast. If TE is very short, there will be no decay of the transverse magnetization and thus differences in the signal between different tissues will be minimal. Conversely, if TE is too long, the transverse magnetization will totally disappear and no differences between tissues will also be registered. Therefore, an intermediate TE value is required to allow for greater differences of the signal among the tissues and thus enhancement of the T_2 contrast (see Figure 3.9).

Unlike T_1 - weighted images, T_2 - weighted images can only be generated using spin-echo pulse sequences. Since this sequence uses a 180° refocusing pulse at time TE/2, all the spins

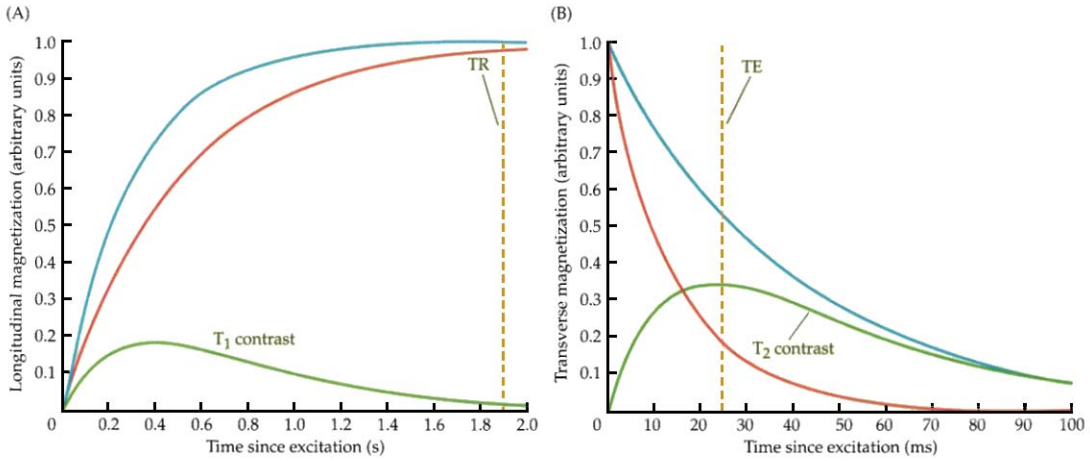

Figure 3.9: Optimal TR and TE values for T_2 contrast. The graphs exhibit **(A)** TR and **(B)** TE values (vertical, dashed orange lines) that will maximize the T_2 contrast and minimize the T_1 contrast, providing images with exclusive T_2 contrast. The green lines represent the contrast related to different **(A)** TR and **(B)** TE values. Adapted from (Huettel et al., 2009, pp. 129), with permission from the publisher.

will restore the same original phase at the precise time TE. In this way, we assure that the signal obtained is totally independent from magnetic field inhomogeneities and only due to spin-spin interaction. Thus, the T_2 contrast is consistent with the relative T_2 values of the different tissues, reflecting their intrinsic properties (Huettel et al., 2009).

3.5.3.4 T_2* contrast

As it was mentioned previously, there are two main factors for the relaxation of the transverse component of the net magnetization: spin-spin interaction and inhomogeneities in the magnetic field. T_2* is the time constant which describes the decay of the transverse magnetization due to both factors. T_2 is always longer than T_2* because $1/T_2{}^* = (1/T_2) + (1/T_2{}')$, where $T_2{}'$ represents the dephasing effect caused by inhomogeneities in the magnetic field. Therefore, T_2 decay is always slower that T_2* decay.

Like T_2 contrasts, T_2* also requires long TR and medium TE values. They use gradient-echo pulses instead of spin-echo because refocusing pulses are employed to eliminate magnetic field inhomogeneities effects (see Figure 3.10).

T_2* contrast constitutes the basis for BOLD-contrast fMRI, since it is sensitive to changes on the levels of dHb, which vary according to the metabolic activity of the neurons (Huettel et al., 2009).

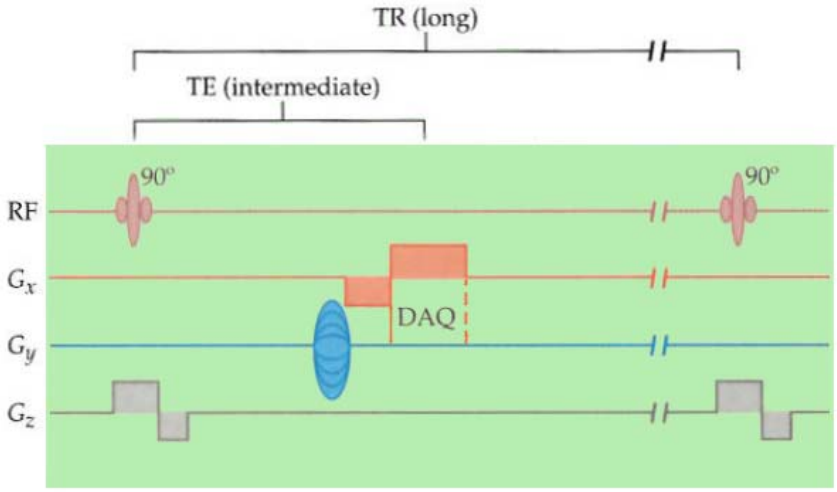

Figure 3.10: Pulse sequence of T_2* - weighted images. T_2* contrast requires a long TR and intermediate TE. Gradient-echo pulses are the most frequently used, since the refocusing pulses commonly employed during spin-echo pulses are in this context applied to supress magnetic field inhomogeneities. Adapted from (Huettel et al., 2009, pp. 132), with permission from the publisher.

3.5.3.5 Echo-Planar Imaging

Speed data acquisition is not a critical issue for the formation of anatomical images of the brain. Contrast is, in this particular case, of the utmost importance because different features of the biological tissues will show up according to what is used. Hence, structural parameters, such as size and shape, highly depend on contrast but not in speed, since they change little over the time of a scanning session. However, collecting meaningful functional data requires high speed acquisition at rates approximately similar as the physiological changes of interest. In 1977, Mansfield proposed a novel technique in response to this need: the *echo-planar imaging* (EPI). EPI consists in the application of a rapid gradient switching direction after the RF excitation, in order to execute the whole κ - space filling before significant T_2* decay (Mansfield, 1977). More precisely, the frequency-encoding gradient is continuously applied along one direction within the slice, with positive and negative alternations and, thus, κ - space will be scanned consecutively back-and-forth along this direction at each echo[2]. Immediately before, discrete pulses of the phase-encoded gradient, i.e. the *blips* (Howseman et al., 1988), are applied

[2]Since EPI implies the acquisition of a series of gradient echoes after a single excitation pulse, each echo has a different echo time. Nevertheless, as explained in section 3.5.3.1, these echoes have different amplitudes with greater signal strength for the echo that covers the center of the κ-space. Therefore, the TE of an EPI sequence is defined as the echo time of the central echo (Deichmann, 2009, pp. 28).

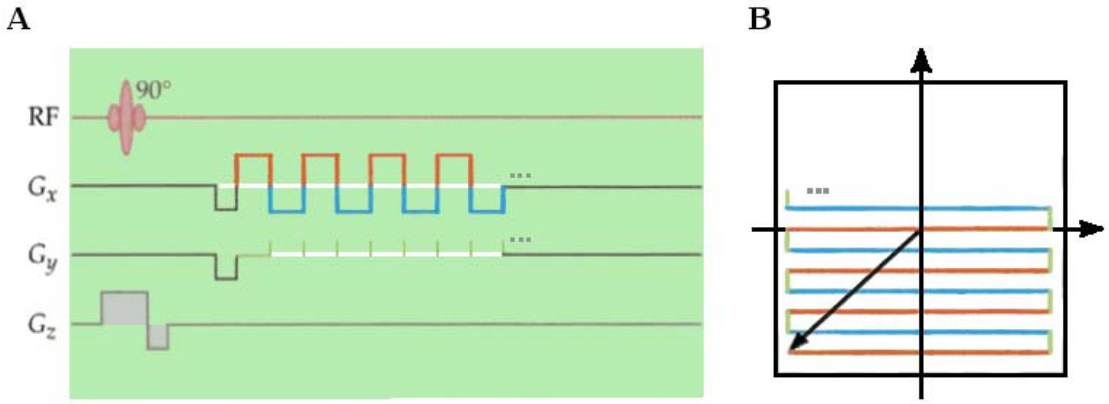

Figure 3.11: (**A**) EPI Pulse Sequence and **B** its κ - space rectilinear pathway. The black arrow represents the initial applied frequency-encoding (G_x) and phase-encoding gradients (G_y). The following changes of the gradients are depicted in different colors for easy comparison between the pulse sequence and the respective κ - space representation. The back-and-forth pathway through the κ - space becomes possible due to the rapid alternation of gradients' direction. Adapted from (Huettel et al., 2009, pp. 147), with permission from the publisher.

towards the orthogonal direction (see sections 3.5.2.2 and 3.5.2.3), producing a rectilinear path on κ - space sampling (see Figure 3.11). EPI sequences thus require a high performative gradient system that enables very rapid gradient switching (Huettel et al., 2009; Goebel, 2007).

Another important method deployed in EPI is parallel imaging, which also reduces substantially the scanning time. It allows for the partial encoding of the κ - space lines and the subsequent reconstruction of the remaining lines. The reconstruction is based on the acquisition of extra spatial information linked to the sensitivity profiles of the receiver coils, which determines the *signal-to-noise ratio* SNR. Higher magnetic fields improve parallel imaging performance combined with more complex sensitivity profiles of the coil and increased SNR (Uğurbil et al., 2006, pp. 321). In addition, parallel reconstruction techniques are also used to achieve better image quality, as a consequence of a higher SNR.

EPI is a fast MR imaging techniques much preferred because of its speed and the fact that only requires a single excitation per image acquisition. Nevertheless, it still remains somewhat troublesome because it can be influenced by a number of factors that may lead to loss of resolution signal, sensitivity or geometric fidelity. Even though these problems can be corrected by proper slice selection and image reconstruction, many of them are related with the

higher field strength, such as: *(i)* local magnetic field inhomogeneities increase linearly with the magnitude of the field, causing undesirable geometric distortions; *(ii)* T_2* decreases at high field, promoting signal amplitude reduction and, thus, image blurring on the phase-encoding direction that compromises spatial resolution in this dimension; *(iii)* dephasing of magnetization becomes more pronounced with increased magnetic field inhomogeneities, leading to signal loss. Another big inconvenience is the high acoustic noise produced during acquisition, due to the fast switching of the gradients. This issue is particularly important in the experiment featuring this thesis, regarding its inherent musical nature. Yet, a relatively high magnetic field is very important concerning fMRI data acquisition, since higher magnetic fields improve dramatically BOLD signal sensitivity (see section 3.5.4) (Speck et al., 2011).

3.5.4 BOLD fMRI

As it is stated previously, the BOLD-contrast fMRI is a static and endogenous contrast. It is by definition the difference in signal intensity on T_2* - weighted images that depends on the amount of deoxygenated hemoglobin present in the blood (Ogawa et al., 1990).

Neural activity demands consumption of oxygen, which is continuously supplied by the cardiovascular system through the hemoglobin molecule. The *hemoglobin* is a metalloprotein in the red blood cells that carries oxygen. Since it is an iron-containing molecule, it has magnetic properties, which in turn depend on whether or not the oxygen is bound to it. *Oxygenated hemoglobin* (Hb) is diamagnetic (i.e. it has no unpaired electrons and null magnetic moment), whereas *deoxygenated hemoglobin* (dHb) is paramagnetic (i.e. it has unpaired electrons and a significant magnetic moment). Therefore, deoxygenated blood has a magnetic susceptibility approximately 20% greater than completely oxygenated blood.

The paramagnetic effects of a substance induce fluctuations on the magnetic field in the surroundings, causing the nearby spins to precess at different frequencies. They thus start to experience a faster decay of the respective transverse magnetization, i.e., a shorter T_2*. It is hence straightforward to infer that the transverse relaxation values of the tissues vary according to the proportion of the deoxygenated blood. Besides, this variation increases with the square of the magnitude of the magnetic field. So, strong magnetic fields are of the utmost importance for MR imaging of T_2* - weighted images contrast in blood, i.e., for fMRI.

When neural activity increases, oxygen consumption also increases, leading to more quantity of dHb present in the blood. The quantity of dHb thus depends on the balance between consumption and supply of oxygen. Because T_2* is greater for fully oxygenated blood than for

deoxygenated blood, one can expect that the MR signal shall become stronger for highly oxygenated blood and, conversely, it will become weaker when the blood is highly deoxygenated. Increased neural activity would then be expected to correspond to darker MR images. However, higher neural activity reflects higher signal intensity on T_2* - weighted images. The answer relies on the intricate relationships between cerebral blood flow, blood oxygenation level and metabolism (Huettel et al., 2009).

3.5.4.1 Neurovascular Coupling

Neural activity can be construed as a chain of metabolic pathways. They assure the permanent supply of energy to the neurons, which is required for the maintenance and restoration of their membrane potentials. Glucose is the major source of energy for most organisms and its aerobic degradation is the most efficient process for generating *adenosine triphosphate* (ATP, a coenzyme that transports chemical energy within the cells).

The enduring process of oxygen delivery in order to ensure the production of ATP inside the neurons triggers an increase of cerebral blood flow through active regions. Consequently, a surplus of oxygenated blood occurs in these regions some seconds after their activation, draining at the same time the existing deoxygenated blood (see Figure 3.12). The BOLD contrast is thus the result of the signal loss due to T_2* effects that reflect the decrease in the amount of dHb. In other words, the BOLD contrast constitutes an indirect measure of neural activity because it relies on differences in the local ratio Hb/dHb and the respective change in the transverse magnetization. This ratio is thus an endogenous marker of neural activity (Huettel et al., 2009; Goebel, 2007).

It is important to notice that different ratios between rates of cerebral metabolism and blood flow may have functional consequences across regions. It was found that some brain regions exhibit greater flow than glucose metabolism, such as amygdala, basal ganglia, thalamus and cingulate cortex. On the other hand, cortical regions related to high cognition show reduced flow compared with glucose metabolism, namely lateral frontal and parietal lobes. This seems to indicate that vascular properties of each region are influenced by its function. Many inner regions of the brain are involved in modulation of emotional behaviour that implies rapid reaction, whereas cortical regions are more devoted to high cognition that, conversely, requires greater preparedness for deployment. So, one can speculate that an adaptive anticipatory metabolic state associated with increased blood flow may have benefits upon quick responses to external stimuli (Gur et al., 2009). It was also demonstrated that differential coupling across

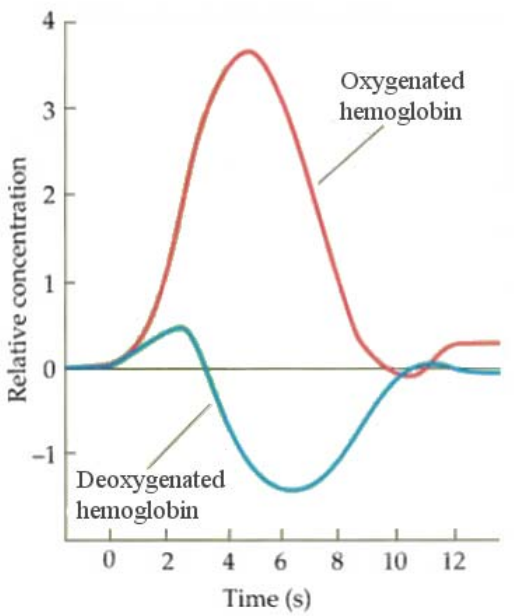

Figure 3.12: Hb and dHb concentration profiles after neural stimulation. The concentration of dHb rapidly increases right after the onset of the stimulus, reaching the peak at 2 seconds, approximately. This is a direct consequence of the immediate consumption of the oxygen already present in the blood cells by the active neurons, in order to support their initial activity. Afterwards, the concentration of dHb decreases to a minimum value at about 6 seconds after the onset and returns to the baseline level at 10 seconds, approximately. On the other hand, the concentration of Hb shows an increase shortly after the stimulus onset, reaching the peak at about 5-6 seconds after the beginning of the process; it slowly declines to levels close to baseline at about 10 seconds. Adapted from (Huettel et al., 2009, pp. 199), with permission from the publisher.

regions may reflect differences in the BOLD signal sensitivity, i.e., BOLD signal response relative to changes in the metabolic rate of oxygen is rather weaker in subcortical than in cortical regions (Ances et al., 2008). Hence, whole-brain analyses shall be carefully regarded due to differences in the BOLD response amplitude across brain regions.

3.5.4.2 The BOLD Hemodynamic Response

The change in the MR signal on T_2* - weighted images caused by local neural activity is known as the *hemodynamic response*. It measures the changes in the total amount of dHb in a voxel over time. Nevertheless, it is important to stress that the quantity of dHb depends not only on oxygen consumption by active neurons but also on changes in blood flow and blood volume (Kwong et al., 1992). These factors shape the BOLD hemodynamic response and it

can be divided in three distinct phases (see Figure 3.13): *(i)* **the initial dip**, which represents a short-term decrease in the signal immediately after the neural activity onset and it may result from initial consumption of oxygen already existing in the blood; *(ii)* **the positive BOLD response**, which represents an increase of the signal due to the increased inflow of oxygenated blood and the consequent decrease in the amount of dHb, reaching the maximal amplitude at about 4-6 seconds after the neural activity onset; *(iii)* **the undershoot**, which represents the signal decrease below baseline level immediately after neural activity has ceased and for a certain period of time, followed by its slow reestablishment up to baseline (de Sousa Bernardino, 2013; Huettel et al., 2009; Goebel, 2007).

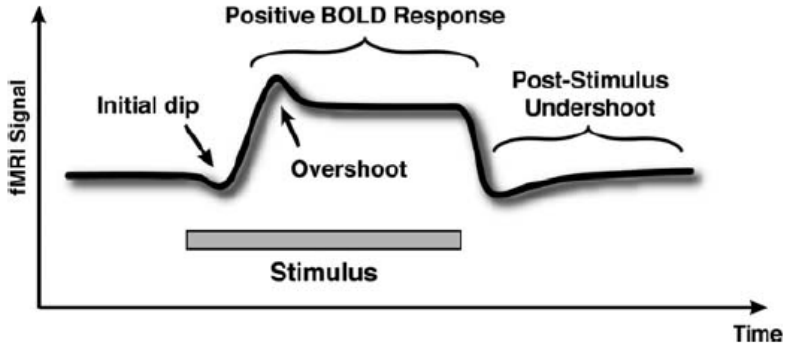

Figure 3.13: Schematic representation of the hemodynamic BOLD response. The plot depicts a representative waveform for the hemodynamic response during a block of multiple consecutive events. A short and negative **initial dip** is followed by a **positive BOLD response** that reaches a plateau at approximately 5-6 seconds after the onset. For long stimulation events, the signal may rise up to a level slightly above the plateau, named as **overshoot**. Afterwards, the signal starts decreasing upon the cease of the stimulus below baseline, followed by a gradual return to baseline (**post-stimuli undershoot**). Reproduced from (Goebel, 2007, pp. 19), with permission from the publisher.

3.6 fMRI Data Acquisition

fMRI data were collected from a 3 Tesla MRI system (Discovery MR750, GE Healthcare) with a standard RF thirty-two element head coil array (MR Instruments). Several studies generally indicate that thirty-two channel coils show higher performance than coils possessing less elements (Lattanzi et al., 2010). In particular, it has been suggested that thirty-two channel coil may provide greater SNR in cortical regions when compared with coils displaying

only eight or twelve channels. Since the studies featuring this thesis were conceived in order to cover aspects related to neurocognitive mechanisms at cortical regions, a thirty-two channel coil was thus chosen.

Functional image data were collected using a gradient echo-pulse, EPI T_2* - weighted sequence with BOLD contrast (Ogawa et al., 1990; Kwong et al., 1992). Image volumes were constructed from 48 contiguous axial slices. (for more details, consult subsection 5.3.5). After the fMRI sessions, a 3D T_1 - weighted anatomical image volume of the whole brain was collected.

References

Ances, B. M., Leontiev, O., Perthen, J. E., Liang, C., Lansing, A. E., and Buxton, R. (2008). Regional differences in the coupling of cerebral blood flow and oxygen metabolism changes in response to activation: Implications for BOLD-fMRI. *Neuroimage*, 39(4):1510–1521.

Bandettini, P. A., Wong, E. C., Hinks, R. S., Tikofsky, R. S., and Hyde, J. S. (1992). Time course EPI of human brain function during task activation. *Magnetic Resonance in Medicine*, 25(2):390–397.

de Sousa Bernardino, I. (2013). *Investigation of the dorsal stream hypothesis in Williams syndrome*. PhD thesis, Universidade de Coimbra, Faculdade de Medicina, Coimbra, Portugal.

Deichmann, R. (2009). Principles of MRI and Functional MRI. In Filippi, M., editor, *fMRI Techniques and Protocols*, Neuromethods, pages 3–31. Humana Press.

Glover, G. H. (2011). Overview of Functional Magnetic Resonance Imaging. *Neurosurgery Clinics of North America*, 22(2):133–139.

Goebel, R. (2007). Localization of Brain Activity using Functional Magnetic Resonance Imaging. In Stippich, C., editor, *Clinical Functional MRI: Presurgical Functional NeuroImaging*, Medical Radiology, pages 9–51. Springer.

Gur, R. C., Ragland, J. D., Reivich, M., Greenberg, J. H., Alavi, A., and Gur, R. E. (2009). Regional Differences in the Coupling between Resting Cerebral Blood Flow and Metabolism may Indicate Action Preparedness as a Default State. *Cerebral Cortex*, 19(2):375–382.

Howseman, A. M., Stehling, M. K., Chapman, B., Coxon, R., Turner, R., Ordidge, R. J., Cawley, M. G., Glover, P., Mansfield, P., and Coupland, R. E. (1988). Improvements in snap-shot nuclear magnetic resonance imaging. *The British Journal of Radiology*, 61(729):822–828.

Huettel, S. A., Song, A. W., and McCarthy, G. (2009). *Functional Magnetic Resonance Imaging*. Sinauer Associates, Inc., Sunderland, MA, 2nd edition.

Kwong, K. K., Belliveau, J. W., Chesler, D. A., Goldberg, I. E., Weisskoff, R. M., Poncelet, B. P., Kennedy, D. N., Hoppel, B. E., Cohen, M. S., Turner, R., Cheng, H.-M., Brady, T. J., and Rosen, B. R. (1992). Dynamic magnetic resonance imaging of human brain activity during primary sensory stimulation. *Proceedings of the National Academy of Sciences of the United States of America*, 89(12):5675–5679.

Lang, P. J. (1995). The emotion probe - studies of motivation and attention. *American Psychologist*, 50(5):372–385.

Lattanzi, R., Grant, A. K., Polimeni, J. R., Ohliger, M. A., Wiggins, G. C., Wald, L. L., and Sodickson, D. K. (2010). Performance evaluation of a 32-element head array with respect to the ultimate intrinsic SNR. *NMR in Biomedicine*, 23(2):142–151.

Mansfield, P. (1977). Multi-planar image formation using NMR spin echoes. *Journal of Physics C: Solid State Physics*, 10. Letter to the Editor.

Mansfield, P. and Maudsley, A. A. (1976). Line Scan Proton Spin Imaging in Biological Structures by NMR. *Physics in Medicine and Biology*, 21(5):847–852. Scientific Note.

Ogawa, S., Lee, T. M., Kay, A. R., and Tank, D. W. (1990). Brain magnetic resonance imaging with contrast dependent on blood oxygenation. *Proceedings of the National Academy of Sciences of the United States of America*, 87(24):9868–9872.

Oldfield, R. C. (1971). The assessment and analysis of handedness: the Edinburgh inventory. *Neuropsychologia*, 9(1):97–113.

Speck, O., Weigel, M., and Scheffler, K. (2011). Contrasts, Mechanisms and Sequences. In Hennig, J. and Speck, O., editors, *High-Field MR Imaging*, Medical Radiology, chapter EPI, pages 109–116. Springer.

Sternberg, R. J., editor (1999). *Handbook of Creativity*. Cambridge University Press, Cambridge, United Kingdom.

Ullén, F., Mosing, M. A., Holm, L., Eriksson, H., and Madinson, G. (2014). Psychometric properties and heritability of a new online test for musicality, the Swedish Musical Discrimination Test. *Personality and Individual Differences*, 63:87–93.

Uğurbil, K., Adriany, G., Akgün, C., Andersen, P., Chen, W., Garwood, M., Gruetter, R., Henry, P.-G., Marjanska, M., Moeller, S., de Moortele, P.-F. V., Prüssman, K., Tkac, I., Vaughan, J. T., Wiesinger, F., Yacoub, E., and Zhu, X.-H. (2006). High Magnetic Fields for Imaging Cerebral Morphology, Function, and Biochemistry. In Robitaille, P.-M. and Berliner, L. J., editors, *Ultra High Field Magnetic Resonance Imaging*, volume 26, chapter Parallel Imaging, pages 321–322. Springer.

Chapter 4

Data Analysis

4.1 Analysis of Behavioral Data

In order to account for neural activity associated with motor cognition, number of notes were extracted from the musical samples played by the participants. Also, brain activity related to cognitive mechanisms potentially involved during improvisation, were explored by estimating measures of musical complexity. Measures of *melodic entropy* and *Lempel-Ziv complexity* (Lz) were thus assessed in the present studies.

Entropy measurements for music can be estimated under the framework of information theory. According to the field, entropy quantifies the *information*[1] of a specific outcome in a data stream. Thus, it characterizes the level of *uncertainty* as well as *unpredictability* underlying that outcome, such that less likely outcomes convey more information than more likely ones. Outcomes can be translated by *bits* of information. In a system with n equally likely outcomes, the entropy can be characterized by the $\log_2 n$. For instance, if an outcome represents a note, the maximum entropy of a system containing 12 notes uniformly distributed (i.e. all equally likely) will be $\log_2 12 = 3.585$ bits. If all notes happen with the same probability p, it means that there are $1/p$ outcomes. Thus, the maximum entropy can be redefined as $\log_2(1/p) = -\log_2(p)$. However, real life's contexts always account for non-uniform distributions of the outcomes, where the outcome x_i is assigned to a probability $p(x_i)$. Thus, the entropy becomes the expected value of the outcomes weighted by their corresponding probabilities. The concept was developed and formally described for the first time by Shannon (Shannon, 1948) as it follows:

[1] In this context, information doesn't stand for *meaning*. It represents instead the statistical character of the whole ensemble. It is *"a measure of one's freedom of choice when one selects a message"*. (Weaver, 1949)

$$H(p) = -\sum_{i=1}^{n} p(x_i) \log_2 p(x_i) \tag{4.1}$$

where $p(x_i)$ is the empirical probability of the i-*th* outcome, i.e., the ratio between the number of times the i-*th* melodic element appears and the total number of melodic elements present in the sample; n represents all possible existing melodic elements. In the present context, if one assumes $n = 12$ and given the size of the piano (see section 3.2), melodic element will then correspond to a single note[2]. Equation 4.1 considers all melodic elements independent from each other; it is often referred as the 0 - order entropy. By contrast, 1 - order entropy considers the transitions between melodic elements, i.e., the probability of selecting one melodic element that precedes another specific melodic element:

$$H(p) = -\sum_{i=1}^{n} p(x_i) \sum_{j=1}^{n} p(x_j \mid x_i) \log_2 p(x_j \mid x_i) \tag{4.2}$$

where $p(x_i)$ is the empirical probability of the i-*th* melodic element and $p(x_j \mid x_i)$ is the empirical probability of the j-*th* melodic element given the previous i-*th* melodic element.

The Lempel-Ziv complexity measure denotes the number of different patterns in a sequence, starting from short patterns up to the longer ones. The measure essentially captures repetitions of patterns referring to different structural levels. In the present case, Lz was employed to compute different melodic combinations (Doğanaksoy and Göloğlu, 2006).

In Study I, to investigate whether the observed effects of improvisation experience could be confounded with the complexity of motor output during performance, correlations between number of hours of improvisation training and each of the complexity measures aforementioned were computed.

In Study II, differences in number of keystrokes and complexity between structural and emotional conditions were evaluated. A two-sample t - test was performed to assess whether there were differences in the mean number of notes played (Nkeys) and the Lz between the two conditions.

4.2 fMRI Data Preprocessing

In order to prepare the fMRI data for statistical analysis, a series of preprocessing steps must be executed. The central goals of these operations are: *(i)* identification and correction of

[2]In Study I, melodic elements were considered single notes. In Study II, melodic elements were considered chunks of notes with an interval <75ms between two consecutive notes.

physiological artifacts, *(ii)* transform the data to meet further statistical assumptions and *(iii)* standardize the data across subjects in order to achieve validity and sensitivity in the statistical analysis at the group level.

In the present project, the procedures performed in order to properly preprocess the data according to the context of our research, were: *(i)* realignment and unwarp of the fMRI image volumes; *(ii)* co-registration of each individual's T_1-weighted image; *(iii)* subsequent segmentation of the T_1-weighted (see section 3.5.3.2) image; *(iv)* normalization of the data into the standard space; and, lastly, *(v)* smoothing (or convolving) image volumes with an isotropic Gaussian filter of a pre-specified halfwidth.

All the aforementioned operations were executed before the statistical analyses of the fMRI data, except the smoothing. The reason is the algorithm applied during within-subject model estimation that accounts for the noise's variance contained in each image of the time series (for a full explanation, consult section 4.4). It is thus recommendable to use the method on unsmoothed data, so the data points remain independent to properly estimate the variance of the images (Diedrichsen and Shadmehr, 2005).

At this point, it is useful to introduce a flow chart that better represents the squence of procedures employed for the whole analysis. It gives special emphasis to the steps concerned with the preprocessing, though (see Figure 4.1).

Next, a brief description of the preprocessing procedures undertaken for the imaging data is presented.

4.2.1 Realignment and Unwarp

Head movements constitute an inevitable issue on neuroimaging, since its prevention is unattainable. Retrospective motion correction (aka *Realignment*) is thus the most common procedure undertaken during image preprocessing. The main purpose is to reduce the misalignment between images in a set of fMRI time series that occurs due to head motion (Poldrack et al., 2011, pp. 44).

Realignment is essential to ensure sensitivity on the statistical tests. Movement artifacts are often explained by the error of the linear model (if they are not explicitly introduced as a regressor of no interest) and t-tests results are influenced by signal changes relative to the variance of the error. So, increasing the error of the model by adding movement artifacts will reduce the sensitivity of the test on detecting true activations. Furthermore, Realignment becomes important for experiments where the task correlates with the movements. Hemodynamic re-

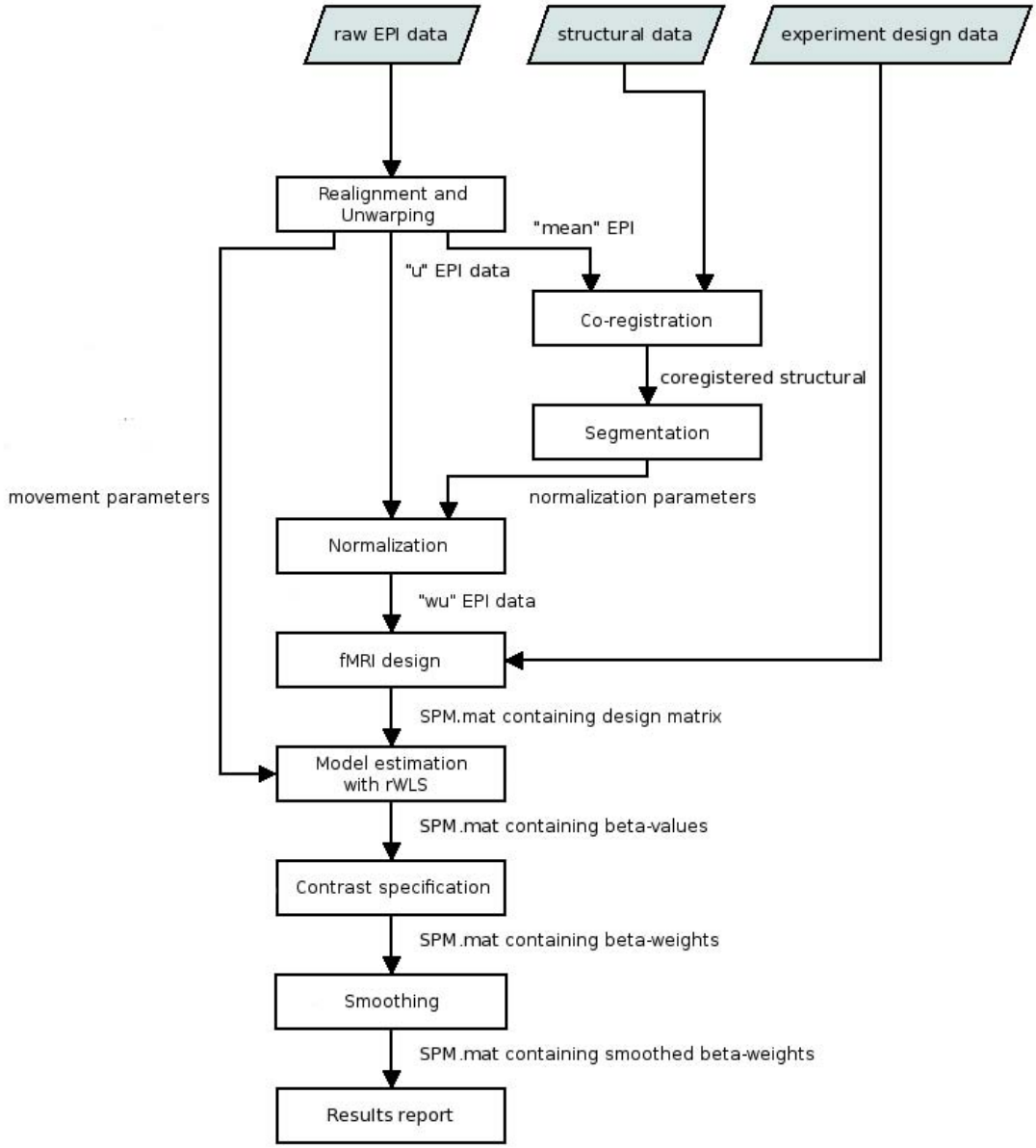

Figure 4.1: Flow chart of the analysis pipeline. The scheme depicts the overall sequence of procedures employed for the analysis of the neuroimaging data. The representation focuses on the aspects referring to the preprocessing. The analysis pipeline is valid for both studies. Adapted from (Ashburner et al., 2010, pp. 453).

sponse changes are considerably smaller than signal variations resulting from movements. So, it is worthwhile to assure the elimination of signal variance not strictly related to neural activity of the cognitive task (Friston et al., 2007, pp. 49). However, it shall not be dismissed the trade-off underlying this process, since the full extent of both effects in the signal is unknown

in any situation. In addition, a correct realignment is of the utmost importance to assure a good co-registration and, consequently, a successful normalization, which is, in turn, crucial for achieving validity in the statistical analysis.

Briefly, each image in the fMRI time series is aligned to a common reference image using the registration method. Afterwards, the images are resliced in order to create the new realigned set.

Realignment usually assumes that the head motion can be registered using a *rigid body transformation*, whereby the position of the head can change by translation or rotation along each of the three axes. The shape of the head must be kept unchanged, though. The registration normally involves an interactive process, testing different parameters, where different orientations of the image are evaluated. The process stops when a particular transformation meets the matching criterion (Friston et al., 2007, pp. 50). Nevertheless, this method can only correct whole-head movements. Disruption of the image intensities due to intra-scan movements are not accounted for this approach (Poldrack et al., 2011, pp. 45). This issue will be further addressed in section 4.4.

The rigid body model is used for registering images of the same subject. During registration, the sessions of a particular subject are firstly realigned to each other, by aligning the first scan from each session to the first scan of the first session. After that, the images within each session are aligned to the first image of the session. The operation is set in this fashion because it is assumed that there are systematic differences in the images between sessions (Ashburner et al., 2010, pp. 34).

Once the coordinates of the rigid body transformation are computed for every image, is is necessary to resample it in order to apply the spatial transform. This involves to estimate for every voxel on the new frame of the transformed image, the corresponding intensity in the raw image. This process implies sampling between the center of the voxels from the old frame and the ones belonging to the new frame. It thus requires the usage of an interpolation method (Ashburner and Friston, 1997). Higher-degree interpolation methods, such as high-order B-spline interpolation, are recommendable for fMRI data resampling because it gives better results (Unser et al., 1993). B-splines are a family of functions with different degrees. When resampling with a n-*th* degree B-spline, a linear combination of $n + 1$ basis functions are necessary to compute the interpolated value (Friston et al., 2007, pp. 51).

One big drawback of GRE-EPI is the increased sensitivity to susceptibility artifacts. This type of artifacts are characterized by local distortions in the magnetic field due to transitions

between tissues with different magnetic susceptibilities. They are responsible for signal loss as well as image distortion. Effects of motion placed in regions affected by susceptibility artifacts may enhance the problem and they can not be explained using the rigid-body transformation. One way to compensate for magnetic field inhomogeneities is to introduce a field map that describes the deformation of the external magnetic field. This deformation field contains descriptions about directions and magnitudes of the deflections throughout the magnetic field with respect to the real object (Poldrack et al., 2011, pp. 38-41).

The *Unwarp*, implemented on SPM8, is built upon the assumption that the susceptibility-by-movement interaction contributes for a substantial amount of the error's variance in the model. The method corrects the time-series distortion using a previously formulated field map template included in SPM8. This template already contains an average contribution for distortion according to the characteristics of the movement. Therefore, this technical procedure adjusts the signal intensity in the time series by correcting spatial variations on the magnetic field attributed to movement effects (Ashburner et al., 2010, pp. 31-33).

The unwarping procedure is thus an asset on the pipeline analysis of the present studies, because it handles with predicted patterns of deformations change when the subject changes position (i.e it deals with the derivatives of the deformation according to the subjects' movements) (Ashburner et al., 2010, pp. 32). Due to the naturalistic features of the experimental paradigm described in this thesis, movements are intrinsically associated with the cognitive tasks under assessment. Thence, controlling for movements within subject-level analysis, by assigning covariates-of-no-interest in the model, would result on the exclusion of variance that could be explained by the dependent variables. It is thus an ineligible option. The Unwarp appears to be the alternative solution to cope with this limitation.

4.2.2 Co-registration

The realignment process, described in the previous subsection (i.e. subsection 4.2.1), is based on the *within-modality rigid transformation*. Unlike Realignment, *Co-registration* implies a *between-modality rigid transformation*. That consists on the superimposition of a high resolution structural image of the individual (usually a T_1-weighted image; see section 3.5.3.2) onto the mean of the functional images (aka the mean EPI image) for that individual. Nonetheless, this method is computationally more challenging, because there is no linear relationship between both types of images in this case. Therefore, a rigid body model transformation is not applicable anymore (Friston et al., 2007, pp. 58). The method employed in SPM8 relies

on a voxel similarity based registration algorithm, which optimizes a function measuring the similarity of all possible pairs of voxel grey-values (Collignon et al., 1995).

The main purpose of this step is to further achieve a more precise spatial normalization. Instead of using the mean EPI image, it can thus be computed based on a detailed structural image (Friston et al., 2007, pp. 58).

4.2.3 Segmentation

Another operation on the individual's structural images is still required before submitting all images to normalization. It is named *Segmentation*. This function ensures the correct partitioning of brain tissue by identifying different categories of tissue: grey matter, white matter, *cerebrospinal fluid* CSF, bone, soft tissue and air/background. The Segmentation is thus based on the overall difference of the intensity in the different tissues. However, this operation often raises issues, constituting the most troublesome step of the entire preprocessing stream and requiring frequent control. There are several factors that contribute for problems in segmentation: *(i)* noise in the MRI data may introduce variation in the signal intensity assigned to different tissues and, consequently, promote their misclassification; *(ii)* voxels containing different tissues in varying proportion may exhibit a broad range of signal intensity depending on their position; and *(iii)* non-uniformities across image's *field of view* (FOV) may misattribute the signal intensity featuring different tissues in different regions of the brain (Poldrack et al., 2011, pp. 57-58).

The *unified segmentation* approach, developed by (Ashburner and Friston, 2005) and implemented in SPM8, combines spatial normalization (described in the next subsection 4.2.4) and bias field correction (technique which aims to adjust for smooth, spatially varying artifacts on structural images that modulate signal intensities) with tissue segmentation. The method employs a probabilistic atlas for specification of tissue types. So, for instance, two voxels displaying identical signal intensities can be identified as different tissue types if the probability atlas assigns their corresponding locations to different categories of brain tissue (Poldrack et al., 2011, pp. 58).

In addition, it follows a brief mention about brain extraction. Scalp and skull are potential sources of artifacts on structural images because they display brighter signal intensity when contrasted with the remaining tissues. That was the case in the present data set. Therefore, the "FSL-Brain Extraction Tool" (FSL-BET) was utilized to remove correctly non-brain tissue before segmentation (Smith, 2002).

The unified segmentation also produces *deformation fields*, which are essential for spatial normalization (see next subsection 4.2.4).

4.2.4 Normalization

The main purpose of *spatial normalization* is to match images from different individuals into a common spatial framework, so that they can be integrated in a group analysis.

We chose an approach from the *computational anatomy* category that uses deformation field maps to normalize the images. These maps typically contain information about the transformation to be employed at every voxel. They are represented as a vector field, where the vector at every point describes how the data in that specific voxel shall be transformed from the original image to the final image (Poldrack et al., 2011, pp. 61).

The family of computational anatomy methods have thus proved to be highly effective on the alignment of structures across subjects, due to its flexibility of manipulation in a way that respects anatomical constraints. They contrast with standard models based on volume-based registration, which typically apply *affine transformations* involving combination of linear transforms (Poldrack et al., 2011, pp. 60-61). This family of methods show, in turn, a very limited performance handling with data severely corrupted by non-uniformities (Ashburner et al., 2010, pp. 48). Broad intensity of spatial variations often appear on 3 Tesla scanners and, thus, our data set displayed some inhomogeneities in the structural images for the majority of the participants. Thence, the function *New Segment* combined with the function *Deformations* provided the best solution in our particular case.

4.2.5 Smoothing

Spatial smoothing (aka *Smoothing*) consists in applying a filter to the image in order to remove high-frequency signals, since they mostly relate to noise. Nevertheless, there are a number of other reasons that turns it into common practise. First, remove high-frequency signal improves SNR for signals with a large spatial extent profile (the benefits of getting better signal that extends across many voxels, may prevail over the costs of eliminating smaller features). Furthermore, decreasing the voxel size may reduce signal dropout due to susceptibility artifacts but it increases the amount of noise. Smoothing helps to compensate for this issue, too. Second, some variability still remains on the images even after the spatial normalization. Smoothing the signal across space mitigates this effect. However, it markedly worsen the spatial resolution. Third, multiple comparison procedures, applied during between-subject

analysis and implemented within the framework of Gaussian random fields (for further details, consult section 4.9), require some level of spatial smoothness.

The Smoothing means essentially the convolution of a three-dimensional image with a three-dimensional Gaussian filter (or kernel). The extent of the smoothing applied by the kernel is determined by the *full-width at half maximum* (FWHM) of the distribution. It thus measures the width of the distribution given by the difference of the independent variable at the point where the dependent variable is equal to the half of its maximum value. FWHM relates to the standard deviation of the distribution by the expression $FWHM = 2\sqrt{2\ln 2}\sigma \approx 2.355\sigma$ (Poldrack et al., 2011, pp. 50-51).

We can conclude that the larger FWHM, the greater is the effect of the smoothing on the images. Gaussian smoothing is in fact equivalent to a low-pass filter, attenuating the range of higher frequency signals according to the value assigned to FWHM.

4.3 Fundaments of General Linear Models for Analysis of fMRI Data

The fMRI data from both studies presented in this thesis were analyzed by building a univariate *General Linear Model* (GLM) using the SPM8 software package (Wellcome Department of Imaging Neuroscience, London, United Kingdom). The GLM is a statistical model that predicts a *dependent variable* from a set of *independent variables*. In this case, the GLM explains the variability of the time series of neural activity (the *dependent variable*) as a linear combination of explanatory regressors ascertained from the experimental conditions (the independent variables) plus an error term. Nuisance regressors can also be added when appropriate. They may include motion correction parameters or covariates estimated from the behavioral data that must be controlled. The explanatory regressors were defined according to the onset time and duration of each condition. The correct synchronization of both the different conditions displayed during the experiment (using the adequate software tools) and the data acquisition devices assured the collection of an accurate timing information. Because time series reflect the temporal variation of the BOLD signal which is, in turn, shaped by the hemodynamic response (see section 3.5.4.2), the predictors were also convolved in time with the standard *hemodynamic response function* HRF implemented in SPM8 (Friston et al., 2007, pp. 178-192). Because SPM is a mass-univariate approach, the GLM is applied at each voxel in the brain volume. Thus, the corresponding univariate statistical model in agreement to the sequence of conditions for each session of each experiment was employed at the voxel

level, as defined by the following equation:

$$\boldsymbol{Y} = \boldsymbol{X}\boldsymbol{\beta} + \boldsymbol{\epsilon} \tag{4.3}$$

where $\boldsymbol{Y}$ is a random variable, represented as a column vector containing the time series at each voxel, $\boldsymbol{X}$ is the *design matrix* including all explanatory regressors (columns) per voxel (rows), $\boldsymbol{\beta}$ is the column vector of unknown parameters (per explanatory regressor) to be estimated, and $\boldsymbol{\epsilon}$ contains the error terms assumed to be independent and identically distributed normal random variables with zero mean and variance σ^2, i.e., $\boldsymbol{\epsilon} \overset{iid}{\sim} \mathcal{N}(0, \sigma^2)$.

The *ordinary least squares* (OLS) estimates the β-values which minimize the residual sum-of-squares, that is, the ones that have the minimum variance. Considering that $\boldsymbol{X}$ is of full rank, then the ordinary least squares estimates are:

$$\hat{\boldsymbol{\beta}}_{OLS} = (\boldsymbol{X}^T\boldsymbol{X})^{-1}\boldsymbol{X}^T\boldsymbol{Y} \tag{4.4}$$

for each voxel in the brain volume. The estimated β-values were combined linearly to produce contrasts of interest:

$$[c_1\ c_2\ ...\ c_p]\hat{\boldsymbol{\beta}} = \boldsymbol{c}^T\hat{\boldsymbol{\beta}} \tag{4.5}$$

where c_p represents the contrast weight for the p-*th* regressor included in the linear contrast. The statistics were estimated for each voxel from the the variance related to a specific contrast and the corresponding *p*-values were considered for significance testing (consult section 4.8) (Friston et al., 2007, pp. 101-125).

4.3.1 Psychophysiological Interactions

Standard GLM analyses of functional imaging data usually attempt towards the understanding of specific functional effects featuring distinct brain regions (often named *functional specialization*), whereas approaches aiming to study *connectivity* are based on descriptions about behavior of neural systems due to interactions of different elements (often named *functional integration*). Thus, models depicting dynamics of neural systems are tightly linked to brain connectivity (Stephan et al., 2008).

Functional connectivity encompasses non-mechanistic approaches describing statistically valid correlates between different areas in the brain. It typically refers to the temporal correlation of time series between brain regions relatively distant from each other. In general,

functional connectivity refers to model-free methods since it essentially captures statistical dependencies based on whole-brain analysis. It is thus an exploratory and data-driven approach. Lastly, it shall be stressed that functional connectivity does not convey inferences based on directional effects, i.e. it does not imply causation (Friston, 1994).

In contrast, *effective connectivity* involves causality. It is described as 'the influence that one neuronal system exerts over another' (Friston, 1994). It addresses directionally oriented networks of interactions between specific brain regions, where the causal effects can be usually determined due to systematic perturbations of the system. In addition, it often arises to confirm previously formulated hypotheses.

One approach of effective connectivity analysis is to estimate parameters that reflect how regions' dependencies change over time under the influence of experimental tasks. Simplified methods can be drawn by modelling the data under the assumption of no influences within and between regions. They are classified as *static models*, since they are intended to describe immediate interactions across regions under the assumption that no previous state have led to the current response. In static linear models, the time series of a particular region i is described as the linear combinations of the time series in all regions plus an error factor (Friston et al., 1997) (Friston et al., 2007, pp. 512-513). The linear model is defined as follows:

$$\boldsymbol{y}_i = [\boldsymbol{y}_1 \dots \boldsymbol{y}_k \dots \boldsymbol{y}_K][\beta_{i1} \dots \beta_{ik} \dots \beta_{iK}]^T + \boldsymbol{\epsilon}_i \tag{4.6}$$

where $\boldsymbol{y}_k$ is a column vector and denotes the time series of region k, constituting one of the K explanatory variables included in the model; β_{ik} is the parameter estimate of $\boldsymbol{y}_k$ and it can be interpreted as the 'strength' in connectivity from k to i (note: unlike correlations, effective connectivity is not symmetric, i.e., $\beta_{ik} \neq \beta_{ki}$) and $\boldsymbol{\epsilon}_i$ is the associated error term.

The model expressed in equation 4.6 does not account for possible interactions between different regional responses, preventing any inferences about connectivity *per se*. In order to compensate for this problem, *bilinear models* must be considered. The interaction is thus represented by the bilinear term of such kind of models (Friston et al., 2007, pp. 513).

In both studies featuring this thesis, we were interested to examine regionally specific neural responses due to the interaction between distal brain regions (aka seed regions) and an experimental factor. This approach, known as *psychophysiological interactions* (PPI), typically investigates the contribution of a selected seed region on the significant response's changes of another region under a predetermined psychological context. Therefore, equation 4.6 simply becomes:

$$\boldsymbol{y}_i = \boldsymbol{y}_k \beta_{ik} + \boldsymbol{\epsilon}_i \tag{4.7}$$

A closer look to 4.7 allows to conclude that β_{ik} does not describe exactly effective connectivity from k to i because all the remaining regions were ignored. Actually, a test of significance of the regression ($H_0 : \beta_{ik} = 0$) corresponds to a test for the significance of the correlation between $\boldsymbol{y}_i$ and $\boldsymbol{y}_k$, i.e., a test of functional connectivity. As many more areas are included in the model, the parameter estimates change (progressively following the estimate of effective connectivity), whereas the correlation does not change. It shall be stressed that conceptually PPI analysis is built upon effective connectivity framework and, it is thus based on a mechanistic approach. Subsequently, a test for a change in regression slope shall not be compared to a test for a change in correlation, even in the particular case of a single explanatory region (Friston et al., 1997). In addition, it must be stressed that PPI analysis indicates no directionality in the modulation of the connectivity. Upon interchangeability between seed and target regions, the linear regression equations are approximately reversible[3]. Thence, directionality shall be assessed through other methods based on effective connectivity *per se*, such as Structural Equation modelling, *Granger* causality or *Dynamic Causal Modelling* (DCM).

PPI analysis is equivalent to a factor analysis, involving a classic 2×2 factorial design (Friston et al., 1997). Identically, the covariance-based method, where experimental effects on both regional activity and interregional covariance are assessed, can also be adopted (McIntosh and Gonzalez-Lima, 1994, pp. 5). Therefore, the statistical model for PPI can be written as follows:

$$\boldsymbol{y}_i = \boldsymbol{y}_k \beta_{ik} + \boldsymbol{u} \beta_{iu} + (\boldsymbol{u} \circ \boldsymbol{y}_k) \beta_i + \boldsymbol{G} \beta_G + \boldsymbol{\epsilon}_i, \tag{4.8}$$

where the interaction term contains the Hadamard product $\boldsymbol{u} \circ \boldsymbol{y}_k$ (i.e. the element-by-element multiplication) between the physiological activity in region k and the psychological parameters of the experimental design $\boldsymbol{u}$, whereas the first and second terms represent respectively the *main effects* of the seed region and the experimental factor. It is also considered in equation 4.8 a term for the confounds $\boldsymbol{G}\beta_G$, such as movement parameters, session effects, etc., and the error term $\boldsymbol{\epsilon}_i$.

Importantly, two distinct interpretations on PPI point out different perspectives upon the source and mediation of the interaction. The interaction might be a result from either *(i)* the modulation of the effect of the seed region due to the influence of the psychological factor

[3] They are not exactly reciprocal because of the measurement error.

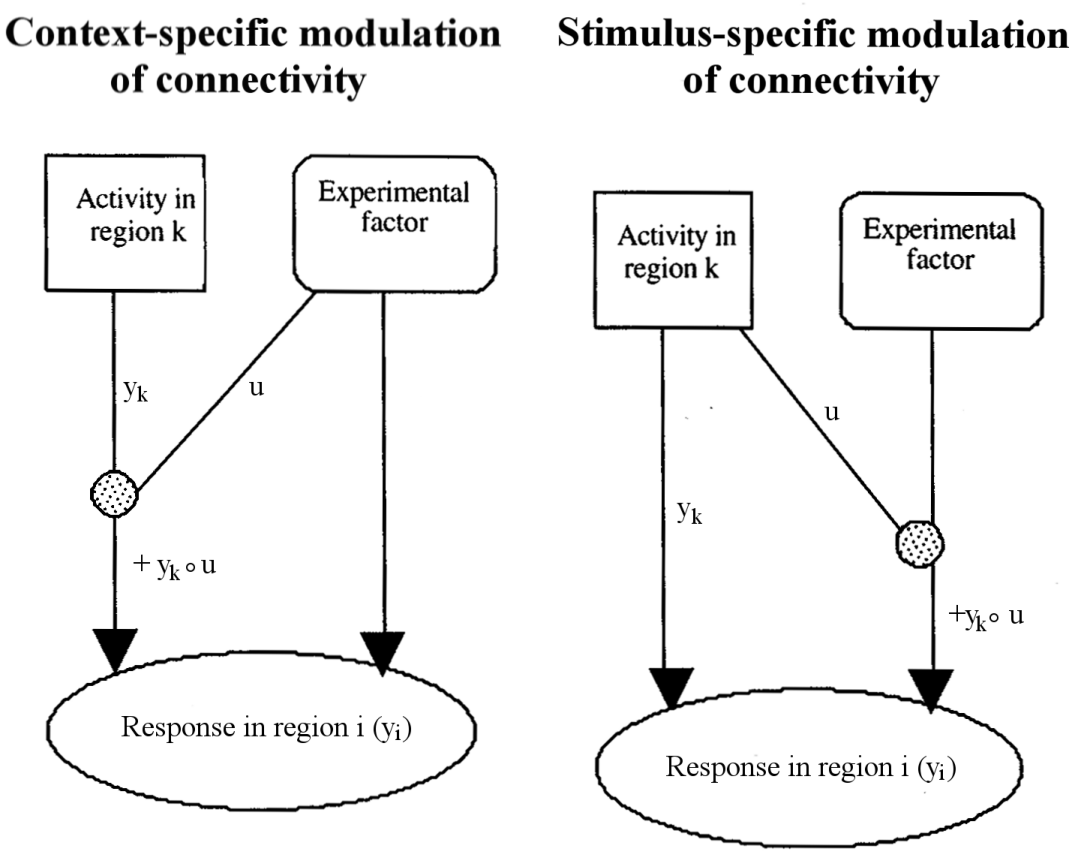

Figure 4.2: Schematic illustration on the two possible interpretations of PPI. On the left side, 'Context-specific modulation of connectivity' refers to the functional specific change of region i due to the contribution of region k under the manipulation of the psychological factor. On the right side, conversely, 'Stimulus-specific modulation of connectivity' indicates that the variation of the responses in region i is a result of the modulation of the psychological factor promoted by contributions from region k. Adapted from (Friston et al., 1997), with permission from the publisher.

or, conversely, *(ii)* the influence of the experimental manipulation due to the seed region activity (see Figure 4.2 for schematic representation). Nevertheless, both views encompass an important aspect of PPI. The approach summarizes functional integration mechanisms using techniques which relate to functional specialization, under a particular psychological context (Friston et al., 1997). It was thus very useful in our studies, since it permits inferences about functional connectivity during musical creativity solely based on the previous analyses concerning functional specialization. The results describing effects in specific brain regions associated with musical improvisation gave us indications about possible networks of connectivity involved

during this process. By selecting seed regions that correspond to these results, we could easily explore and assess functional connectivity mechanisms that are sustained by the performance of musically original and novel creations.

The standard method to implement a PPI analysis in SPM8 is defined by the following steps: *(i)* define a mask which comprises the source (seed) region; *(ii)* extract the time course of activity from that mask (for more details about regional responses extraction, consult section 4.6); *(iii)* set a boxcar function regressor representing the psychological factor, by introducing the dummy variables that correspond to periods of the relevant psychological context within the experiment; *(iv)* form the interaction term (source signal $\circ$ experimental treatment); *(v)* perform a GLM analysis with the three aforementioned regressors (i.e. the interaction term, the source region's extracted signal and the experimental vector of the design); produce a contrast with the parameter estimate of the interaction regressor (according to 4.5) to look for effects of the presumed interaction; and, at last, *(vi)* perform a between-subject analyses with the contrast of interest to test whether the interaction is significant at the group level (consult section 4.8 for further details).

Because the BOLD signal, represented by the time series, reflects the neural activity changes shaped by the hemodynamic response (see section 3.5.4.2), the regressors introduced in the GLM analysis (which describe the neural signal predicted by the model) must be convoluted by the HRF (see section 4.3). Interactions in the brain are strictly modulated by neural activity. A true representation of neural interactions requires computing the interaction term directly from the neural response. Thus, a robust deconvolution of the HRF from the BOLD signal in the seed region is necessary to extract its neural signal. On the other hand, modelling interactions at the hemodynamic level is not mathematically equivalent than modelling the same interactions at the neural level. So, the HRF must be deconvolved from the time course activity referred to the seed region. The obtained neural signal can then be multiplied by the psychological factor and the resulting vector re-convolved with the HRF. In addition, noise has more effect on HRF interactions and, subsequently, deconvolution will reduce noise impact (Gitelman et al., 2003).

4.4 Detect and Correct for Artifacts: the robust Weighted Least Squares

While performing the preprocessing of the neuroimaging data, several sources of artifacts among all subjects were identified: *(i)* magnetic susceptibility, *(ii)* spike noise signal due

to transient motion (usually, related to intrascan motion), and *(iii)* CSF pulsation artifacts. Detect and correct for artifacts image-by-image can be very time-consuming and, therefore, it would not be a feasible approach to pursue. Interestingly, a novel technique aiming to solve confounds that often arise from head motion within a TR have been recently reported. The method consists on radio frequency markers that perform real-time tracking motion and it proves to increase statistical power when compared to conventional retrospective correction (Muraskin et al., 2013). Nevertheless, these new technical approaches are latter-day and thus further improvements might still be necessary to implement.

After acquainted these limitations, we found convenient to choose a method that could identify potential artifacts of any type source. The *robust Weighted Least Squares* (rWLS) is a statistical approach that simply 'deweights' images by using the corresponding inverse of their variance estimated from the signal intensity. Hence, the influence of a particular image on the results relies upon its relative amount of variance in the signal, i.e., images with higher variance will have less impact on the results. It is thus assumed that images, whose variance in signal intensity is greater, were more likely to contain noise or artifacts regardless their source.

Let's consider the signal intensity from K voxels at acquisition time $t = 1...T$, where each of these T measurements constitutes an image. The time series of voxel k is an arbitrary linear function, as described by equation 4.3. The noise can be assigned to the error term of this equation, which contains part of the signal in the time series that cannot be explained by the independent variables of the model. The expected variance of the noise ϵ_k in the voxel k can be defined as:

$$\mathrm{Var}(\boldsymbol{\epsilon}_k) = \begin{bmatrix} s_1 & 0 & \dots & 0 \\ 0 & s_2 & \dots & 0 \\ \vdots & \vdots & \ddots & 0 \\ 0 & 0 & \dots & s_T \end{bmatrix} \sigma_k^2 = \boldsymbol{V}\sigma_k^2 \tag{4.9}$$

where $\boldsymbol{V}$ is a diagonal $T \times T$ matrix and σ_k^2 is a scalar. $\boldsymbol{V}$ describes the relative amount of variance in the image s_t whereas σ_k^2 represents the overall noise observed in the voxel k. It shall be stressed that the variance scaling parameters s_t are equal for all voxels belonging to the same image. Therefore, if there's an increase of noise in some voxels due to artifacts, all other voxels will show an equal increase. Equation 4.9 assumes that artifacts, which lead to increased noise, are spatially extended, encompassing other regions in the brain. Besides, equation 4.9 describes a non-stationary noise process, albeit neglecting any temporal correlation phenomenon of the noise. In addition, the variance model follows the assumption that increases in noise variance

are multiplicative. Although there are specific sources of noise (e.g. noise in the receiver coils or amplifiers) that are likely to be additive in contrast to other sources that appear to be multiplicative, such as movement-by-susceptibility interactions, tests on representative data showed that overall noise artifacts impact images variance in a multiplicative fashion.

Because correlation between noise in the N voxels from the same image exists and the corresponding variances are unequal (σ_k^2 has different values in every voxel), the OLS approximation for the maximum likelihood estimate of the β-values, described in equation 4.4, has to be extended to the *generalized least squares* (GLS). Thus, the estimates for voxel k are calculated as it follows:

$$\hat{\boldsymbol{\beta}}_{k,GLS} = (\boldsymbol{X}^T\boldsymbol{V}^{-1}\boldsymbol{X})^{-1}\boldsymbol{X}^T\boldsymbol{V}^{-1}\boldsymbol{y}_k \tag{4.10}$$

Since $\boldsymbol{V}^{-1}$ is a diagonal matrix, equation 4.10 is usually named the *weighted least squares* (WLS) estimate of β_k.

To apply equation 4.10, an estimate of the noise level from each image must be obtained. The estimate of the variance of the error according to the GLM model (see equation 4.3) is $\boldsymbol{r}_k\boldsymbol{r}_k^T$, where $\boldsymbol{r}$ are the residuals from the WLS regression. The expected sum of squares of the residuals can be deduced from equation 4.3 and combining the final expression with equation 4.9, leading to:

$$E(\boldsymbol{r}_k\boldsymbol{r}_k^T) = \boldsymbol{R}\boldsymbol{V}\boldsymbol{R}\sigma_k^2 \tag{4.11}$$

where $\boldsymbol{R}$ is the residual-forming matrix for the WLS regression. Because the effect of the noise is spatially extended, the variance scaling estimates $\hat{\boldsymbol{s}} = [\hat{s}_1, ..., \hat{s}_T]$ can be obtained by averaging the estimates of the variance of the error and weighting them by σ_k^2 across the whole brain. Thus, the estimators are defined as follows:

$$\hat{\boldsymbol{s}} = \frac{1}{K}\sum_{i=1}^{K} \mathrm{diag}(\boldsymbol{r}_k\boldsymbol{r}_k^T/\hat{\sigma}_k^2) \tag{4.12}$$

$$\hat{\sigma}_k^2 = \boldsymbol{r}_k\boldsymbol{r}_k^T/(T - \mathrm{rank}(\boldsymbol{X})) \tag{4.13}$$

where the operator 'diag' transforms the diagonal of a square matrix into a column vector and 'rank' returns the size of the linearly independent columns of its argument.

The above analysis considered the noise temporally uncorrelated. However, fMRI time series typically display temporal autocorrelation due to continuous effect of noise from the source(s) during short periods of time. To address this issue within the framework of rWLS, a

term that compensates for temporal autocorrelation is added to equation 4.9. Therefore, the variance model becomes:

$$\mathrm{Var}(\boldsymbol{\epsilon}_k) = \left(\begin{bmatrix} s_1 & 0 & 0 & \dots \\ 0 & s_2 & 0 & \dots \\ \vdots & \vdots & \vdots & \vdots \\ 0 & 0 & \dots & s_T \end{bmatrix} + s_{T+1} \begin{bmatrix} 1 & a & a^2 & \dots \\ a & 1 & a & \dots \\ \vdots & \vdots & \vdots & \vdots \\ a^{T-1} & a^{T-2} & \dots & 1 \end{bmatrix} \right) \sigma_k^2 = \boldsymbol{V}\sigma_k^2 \quad (4.14)$$

The second term describes the autocorrelation as if it would have arisen from an autoregressive noise phenomena with a regression coefficient a. The autoregressive model assumes a continuous linear dependence of the noise at each voxel across time.

Lastly, *Monte Carlo* simulations showed that this method leads to consistently higher estimation efficiency of noise. Therefore, this approach demonstrated to be an effective technique that allows the detection and adjustment of artifacts regardless their origin and form (Diedrichsen and Shadmehr, 2005).

4.5 fMRI Model Specification and Contrasts

The experimental designs were built regarding subtraction strategy, where the difference of activity either between a 'task of interest' and baseline or between two tasks of interest were estimated. This technique relies upon the assumption that two (or more) conditions can be cognitively added, assuming no interaction among all components of each condition. Even though it is a simplified approach, it was proved to produce very useful information (Amaro and Barker, 2006). Most importantly, it was shown that allows for *efficient* design matrices in the context of block-design experiments, i.e., when regressors result from the convolution of a specific boxcar function (representing the behavioral conditions) and the HRF (Friston et al., 1999).

4.5.1 Study I

Two pipeline analyses were employed in the first study: *(i)* a standard GLM analysis to assess for effects in contrasts of interest and *(ii)* PPI analysis to investigate how connectivity might be influenced by improvisation practising. Next, it follows a brief description outlining general features of the implemented models.

4.5.1.1 fMRI Effect Analysis

In order to explore regional brain correlates of music improvisation due to training, Study I was designed with one regressor of interest, i.e. 'improvisation'. This regressor aggregated all four active conditions, representing the explicit musical performance. It had a duration of 15 seconds, comprising the time between 3.5 seconds and 18.5 seconds from the total period of the trial (35.5 seconds). The design matrix also included one regressor representing an instruction period for the next performance (i.e. the first 3.5 seconds of the total duration of the trial); one regressor including bad performances, where the instruction was not followed accordingly (this regressor has the same onset and duration as the regressors of interest; for more details, see sub-subsection 5.3.6.3); one regressor containing the fixation cross and initial phase of the distractor task, i.e. the image presentation of the aesthetical judgment task (these two conditions were gathered in the same regressor because they both represent visual stimuli; onset at 18.5 seconds of each trial with a duration of 8 seconds); and rating corresponding to the final phase of the distractor task, where the participant rated the aesthetical quality of the previously presented image (onset at 26.5 seconds of each trial with a duration of 3 seconds). Rest was not explicitly modelled in the design matrix, but it was taken as implicit baseline instead. It corresponded to the last 6 seconds of every trial.

The main effect of music improvisation was thus investigated by comparing *Improvisation* with *Rest* for all participants. The resulting contrasts were then correlated with hours of improvisation training (for more details, see sub-subsection 5.3.6.3).

4.5.1.2 PPI Analysis

In order to explore variations in functional connectivity due to improvisation practising, we extracted the neural responses referring to improvisation period (F-contrast used to adjust the data for the corresponding regressor; for more details, consult section 4.8.2) from six different seed regions previously reported to be implicated on the production of musically creative tasks (for further details, consult sub-subsection 5.3.6.3). It was also set the experimental boxcar function regressor containing dummy variables, whose attributed values were 1 and -1 for the improvisation period and rest, respectively. Hence, we could compare whether there would be changes in connectivity during improvisation relative to a baseline (i.e. rest) dependent on the number of hours of improvisation training. The time series of the seed regions were deconvolved and the resulting regressor, which described the neural process, was then multiplied (element-by-element) by the experimental regressor. Both interaction regressor

and experimental regressor were convoluted by the HRF.

The three regressors were introduced in a the design matrix for model estimation. The main effect of the interaction term was investigated for all participants. The mean of the resulting contrasts was estimated on a between-subject analyses and the significance of its correlation with hours of improvisation training was tested using the multiple linear regression approach (for more details, see sub-subsection 5.3.6.3).

4.5.2 Study II

Similarly to study I, three pipeline analyses were set in this study. First, a GLM analysis was implemented for exploring differences between conditions representing different types of constraints during improvisation. Second, PPI analysis was performed in order to investigate whether these conditions implicate differences in connectivity of the DLPFC. Third, time course activity profiles during different conditions of several brain regions were extracted and analyzed separately.

4.5.2.1 fMRI Effect Analysis

The fMRI data were modelled using the GLM, defined by four conditions of interest ('tonal', 'atonal', 'happy' and 'fearful'), corresponding to the periods at each trial during which the participant improvised in the piano (i.e. the period of time between 3.5 seconds and 18.5 seconds referring to the total duration of the trial). The design matrix was also composed by one regressor representing the instructions for the improvisation task (i.e. first 3.5 seconds of the 35.5 seconds); one regressor including bad performances, i.e. all performances that didn't meet the criteria of correctness regarding the constraints imposed (this regressor has the same onset and duration as the regressors of interest; for more details, see sub-subsection6.3.8.1); one regressor containing the fixation cross and initial phase of the distractor task (for extended explanation, see section 4.5.1.1); rating corresponding to the final phase of the distractor task (for extended explanation, see section 4.5.1.1); one regressor controlling number of keys played during musical performance, since analysis of behavioral data revealed that its mean was slightly higher for emotional conditions than for structural conditions; and another regressor controlling for Lempel-Ziv complexity, where higher mean values concerning this measure were also registered during emotional conditions when compared with structural conditions. Rest was modelled as part of the implicit baseline, corresponding to the last six seconds of every trial.

Differences in brain activity between structural and emotional conditions were assessed with the contrast *Structural - Emotional*, as well as *Emotional - Structural*. Contrasts between conditions within the same category were also investigated, i.e., *Tonal - Atonal*, *Atonal - Tonal*, *Happy - Fearful* and *Fearful - Happy*. Nuisance regressors (the two last ones aforementioned) were contrasted with *Rest* for checking purposes.

4.5.2.2 PPI Analysis

A PPI analysis was set in order to explore possible networks of functional connectivity associated with different musical improvisation scenarios. Therefore, the time series of right and left DLPFC corresponding to the improvisation period (F-contrast used to adjust the data for the four active conditions; for further details, consult sub-subsection 6.3.8.2) were extracted, since DLPFC was previously reported to be highly involved in multiple functions regarding musical creativity (for more details, see 1.1.4.1.1 and 1.2.1). The experimental boxcar function regressor of dummy variables referring to structural and emotional conditions were respectively set to 1 and -1. In this manner, we were able to investigate differences in connectivity between the two categories of conditions. The time series of both seed regions were deconvolved by the HRF implemented on SPM8. The obtained regressor, representing neural activity, was multiplied (element-by-element) by the experimental regressor. Both interaction regressor and experimental regressor were afterwards convoluted by the same HRF.

The three regressors were introduced in a the design matrix for GLM analysis. Similarly to what was done in study I, the main effect of the interaction term was estimated for all participants. This interaction term specifically contained information about higher functional connectivity during structural condition when compared to emotional conditions. The mean of the contrast was evaluated using a between-subject analyses. Afterwards, we tested whether this mean would be above or below zero at every voxel using a One-sample t-test (using $H_0 = 0$). We were thus able to look at significant results corresponding to the contrast *Structural - Emotional* as well as *Emotional - Structural* (for more details, see sub-subsection 6.3.8.2).

4.6 Time Course Analysis

To perform a time course analysis, where the pattern of activity from a particular region is analyzed, we first had to extract the regional responses from the region of interest. The regional responses represent the first *eigenvariates* of the original time series relative to the selected

voxels. In general, the eigenvariates describe the time-dependent profile of the time series from all voxels and they are obtained using the *singular value decomposition* (SVD) (Friston et al., 2007, pp. 493-494). The first eigenvariates, belonging to a region of interest, use the temporal covariance of voxels in order to get coherent spatial modes of activity (aka eigen-images) (Friston et al., 2006). It basically summarizes responses that are not homogeneously distributed. Thus, the first eigenvariate reflects the weighted mean across voxels within the region of interest that captures the maximum amount of variance featuring the time series (Saxe et al., 2010).

Afterwards, the time series were mean-corrected for the effects strictly related to improvisation, using the corresponding F-contrast.

The ultimate purpose was to depict the time-dependent pattern of activity within aparticular region. Since the subjects were instructed to prepare themselves before initiating their performance, the onset of the improvisations (within the preset block-period for improvisation) was variable between trials. Because we wanted to obtain a true representation of the cognitive pattern following the execution of the musical task, the time points were aligned with reference to the actual moment when the subject started to play and averaged across trials. The standard errors for each point were also estimated and depicted on the plots. They represent the profile of activity in a particular region during improvisation, either for structural or emotinal conditions.

4.7 Random Effects Analysis

The analysis of multiple-subject fMRI data requires to account for two sources of variance: *(i)* the variability of measurements concerning the estimated response within subject (in other words, the variability of the measurement error of an estimate for a single individual) and *(ii)* the variability of the true response between subjects (i.e. variability of the individual differences). *Fixed-effects* (FFX) analysis, usually employed on case studies, takes only into account the within-subject variability (Worsley et al., 2002; Beckmann et al., 2003)(Friston et al., 2007, pp. 156-165). So, only conclusions from the data sample can be drawn using FFX and, thus, statistical inferences about population effects are not possible in this context. *Random-effects* (RFX) analysis, in turn, takes into account both sources of variability and, therefore, permits formal inferences about the population from which the sample belongs (Friston et al., 2007, pp. 156).

Mixed-effects (MFX) models are statistical models that combine FFX with RFX. *Summary-*

statistic (SS) approach, implemented in SPM8, belongs to the class of MFX analysis and it employs a hierarchical structure. Strictly, RFX analysis is used in neuroimaging to address MFX analysis, whose term is applied in statistics instead (Friston et al., 2007, pp. 163). It will be thus adopted the terminology in agreement to the neuroimaging discipline henceforth.

RFX method implies a two-level model:

$$\begin{aligned} \bar{w}_i &= w_i + \epsilon_i \\ w_i &= w_{pop} + z_i \end{aligned} \tag{4.15}$$

where $\bar{w}_i$ is the sample mean effect for subject i, w_i is the true mean effect for subject i, ϵ_i is the within-subject Gaussian error for the subject i, w_{pop} is the true effect for the population and z_i is the between-subject error for the subject i. SS method deals with sample mean value instead of computing directly with the observed effects. This is particularly useful in the context of neuroimaging because a typical fMRI study handles with an enormous amount of images. In the first level, the variance of the sample mean for each subject around the true mean is $\mathrm{Var}(\epsilon_i) = \frac{\sigma_w^2}{n}$, where σ_w^2 is the within-subject variance and n is the number of replications of the effect per subject. At the second level, the corresponding between-subject variance is defined as $\mathrm{Var}(z_i) = \sigma_b^2$.

Merging the two levels into one:

$$\bar{w}_i = w_{pop} + z_i + \epsilon_i \tag{4.16}$$

According to equation 4.3, $\epsilon_i \overset{iid}{\sim} \mathcal{N}(0, \frac{\sigma_w^2}{n})$ and $z_i \overset{iid}{\sim} \mathcal{N}(0, \sigma_b^2)$. The estimate of the population mean is thus:

$$\hat{w}_{pop} = \frac{1}{N}\sum_{i=1}^{N} \bar{w}_i \tag{4.17}$$

So, the mean of the estimate is $E[\hat{w}_{pop}] = w_{pop}$, which is calculated according to WLS (see section 4.4). The corresponding variance is given by:

$$\begin{aligned} \mathrm{Var}(\hat{w}_{pop}) &= \mathrm{Var}\left(\frac{1}{N}\sum_{i=1}^{N} \hat{w}_i\right) \\ &= \mathrm{Var}\left(\frac{1}{N}\sum_{i=1}^{N} z_i\right) + \mathrm{Var}\left(\frac{1}{N}\sum_{i=1}^{N} \epsilon_i\right) \\ &= \frac{\sigma_b^2}{N} + \frac{\sigma_w^2}{Nn} \end{aligned} \tag{4.18}$$

Equation 4.18 contains contributions from both between-subject variance (first term) and within-subject variance (second term) (Friston et al., 2007, pp. 157-158). Usually, σ_b^2 is much larger than σ_w^2. In order to minimize the variance of the estimate response of the population mean, N shall also be larger than n. It is thus more important to include more participants in the experiment rather than collect many individual sessions (Friston et al., 2007, pp. 164) (Worsley et al., 2002).

SS requires balanced designs to be valid because it assumes within-subject variance homogeneity, becoming mathematically inexact otherwise. However, it was shown numerically that it also maintains a very robust performance for unbalanced designs (Friston et al., 2007, pp. 159). This is particularly important in the context of the Study II (see section 4.5.2). The design matrix had four regressors of interest. Each of them contained data at most from four different trials. The criteria for distinguishing 'good' from 'bad' performances in structural conditions enabled the possibility that two regressors could contain at least one trial, though. As a consequence, the model specification led up to some extent the creation of unbalanced designs within specific sessions for some participants. Nevertheless, this issue didn't raise any concerns due to the optimal implementation of RFX for unbalanced designs using SS approach in SPM8.

4.8 Statistical Hypothesis Tests

To generate statistical activation maps, the linear contrasts described above (see equation 4.5), i.e. the combinations of parameter estimates, are used to compute the *statistical hypothesis test*. A generic statistical test Q (e.g. t-test or F-test) is a function of data that summarizes evidence against the *null hypothesis* (H_0). H_0 is usually formulated according to the opposite of what one hopes to find. In SPM8, all null hypothesis are of the form $c^T\beta = 0$, i.e. null hypothesis within SPM8 framework always states that no effect in the specified volume exists (Friston et al., 2007, pp. 105).

The p-value can be estimated by comparing the results of the statistical test q with the *null distribution*, i.e. the probability density function of the distribution associated to the statistical test when H_0 is true. If q lies in the middle of the distribution, it is consistent with H_0 and, consequently, *not significant*. If q, in turn, assumes an extreme value in the distribution, then it is *significant*. For any type of Q, p-value thus expresses the evidence against H_0:

$$p = Pr(Q \geq q \mid H_0) \tag{4.19}$$

In other words, the p-value represents the probability of observing a statistical test Q as large or larger than the one obtained under the assumption that H_0 is true (Poldrack et al., 2011, pp. 110).

4.8.1 *t*-statistic

The contrasts *t*-statistics are calculated for each voxel using (Friston et al., 1995; Worsley and Friston, 1995):

$$t = \frac{\boldsymbol{c}^T\hat{\boldsymbol{\beta}}}{\mathrm{SD}(\boldsymbol{c}^T\hat{\boldsymbol{\beta}})} \sim t_{J-p} \tag{4.20}$$

where $\mathrm{SD}(\boldsymbol{c}^T\hat{\boldsymbol{\beta}})$ is the standard deviation of $\boldsymbol{c}^T\hat{\boldsymbol{\beta}}$ and it can be computed as the square root of the variance (Friston et al., 2007, pp. 132). This statistical test follows a Student's *t*-distribution with $J - p$ degrees of freedom. Regarding equation 4.10, the variance of the parameter estimates is:

$$\mathrm{Var}(\boldsymbol{c}^T\hat{\boldsymbol{\beta}}) = \hat{\sigma}^2\boldsymbol{c}^T\boldsymbol{X}^{-1}\boldsymbol{V}(\boldsymbol{X}^{-1})^T\boldsymbol{c} \tag{4.21}$$

where $\hat{\sigma}^2$ is determined according to 4.13 for every voxel. Introducing 4.21 into 4.20, the *t*-statistic function can then be formed as follows (Friston et al., 2007, pp. 122-123):

$$t = \frac{\boldsymbol{c}^T\hat{\boldsymbol{\beta}}}{\sqrt{\hat{\sigma}^2\boldsymbol{c}^T\boldsymbol{X}^{-1}\boldsymbol{V}(\boldsymbol{X}^{-1})^T\boldsymbol{c}}} \tag{4.22}$$

To summarize, the contrasts are linear combinations of the β-values that are used to compare differences in responses evoked by two or more conditions of interest. Linear increases of brain activity during specific conditions can also be checked by comparing the corresponding β-value with the implicit baseline. *t*-statistic ratios of these linear combinations are usually computed to determine whether these differences are significant or not.

In both studies, the effects of interest were assessed upon the aforementioned reasoning. The linear combinations for each subject, which represent differences in neural activity to be tested, are introduced at the between-subject analyses (aka second level analysis) to implement MFX models and, then, to perform RFX analysis (see section 4.7 for further details). In the context of the analyses developed for both studies, the models that led to the main results were *Multiple Regression* and *One-sample t-test*. Multiple Regression allows for testing the null hypothesis of zero correlation between the mean of the effect of interest across subjects and one or more covariates that usually represent individual differences. On the other hand,

One-sample t-test evaluates whether the estimated mean is above zero, considering $H_0 = 0$ (for reversed contrast, it tests if the mean is below zero) (Friston et al., 2007, pp. 117).

4.8.2 *F*-statistic

The *F*-contrast is used to test whether any of the specified linear combinations of the β-values is true. It consists of a set of one-dimensional contrasts, each of them testing against the null hypothesis. It can thus be considered as an 'OR' operation that handles with several *t*-contrasts. If any of them is true, then the *F*-contrast is also true. The *F*-contrast becomes particularly useful for detecting activation among conditions when no requisite about which condition triggered the response is pre-specified.

Another way of thinking about the *F*-contrast is considering a 'reduced model', where only the regressors of 'no-interest' are specified. The test then compares the variance of the residuals of the reduced model with the original model. The F-test basically computes the extra sum of squares accounting for the inclusion of the regressors of interest (Friston et al., 2007, pp. 135).

In the context of both studies featuring this thesis, *F*-contrasts were estimated for the four active conditions after within-subject analysis (aka first-level analysis). The *F*-contrasts were thus calculated for each participant, separately. The aim was to adjust (for the effects of interest) the time series extracted from specific volumes of interest (seed regions) for the subsequent PPI and time-series analyses. Adjusted data simply contains components of the time series that express the most variance only due to the effects of interest, whereas non-adjusted data represent components of the time series, whose variance is the greatest due to activation effects *relative to error* (Friston et al., 2007, pp. 504).

4.9 Corrections for Multiple Comparisons

As it was stated previously, standard functional imaging analysis implemented in SPM8 is based upon the mass-univariate approach (Friston et al., 2007, pp. 101-125). Hence, both *t*-statistic and *F*-statistic can be calculated for every single brain voxel that tests for the contrast of interest in that voxel. The result is a large amount of statistical tests. Multiple comparison problems arise when one considers a large number of statistical inferences simultaneously. A correction for multiple comparisons is thus necessary to avoid the incidence of false positives (type I errors) that would compromise the validity of the conclusions. Nevertheless, there is a trade-off between the appropriate treatment of false positives and false negatives. If the criteria

for assessment are too conservative, there will be no statistical power to detect meaningful results. On the other hand, if the threshold is too liberal, the results will become contaminated by an excess of false positives. Ideally, we aim to maximize the number of true positives while minimizing false reports (Bennett et al., 2009; Poldrack, 2012).

One possible statistical correction for multiple comparisons is the *family-wise error* (FWE) rate. Since there are typically many voxels, and therefore many statistical values, to consider in functional imaging data analysis, the hypothesis shall refer to the whole volume of statistics observed in the brain. Evidence against the null hypothesis is such that this volume of values is unlikely to have arisen by chance. Hence, FWE refers to the accepted risk of error concerning this volume of values, i.e. the *family* of voxel statistics. Typically, one useful method to test a family-wise null hypothesis is to look for any statistic value that are larger than expected under the premise that comes from the null statistical distribution. The method requires to find a threshold to apply to every statistical value, in order that any values above this threshold are unlikely to have arisen by chance. This is called *height thresholding* and its main advantage is that provides an estimate of the effect of interest at the voxel locations. Nevertheless, the values in the statistical volume must not be all considered as *independent* because spatial correlation of fMRI data is universally present. It is a consequence of the intrinsic nature of the data and spatial preprocessing, especially explicit smoothing. There is thus a correlation between neighbouring statistic values and, consequently, fewer independent values in the statistic volume than voxels. Because of this limitation, FWE corrections were implemented within the framework of *random field theory* (RFT). It considers the spatial smoothness of the data when computing the *resels*, which are defined as the volume of resolution elements with the same size of the effective FWHM of the smoothing kernel (Friston et al., 2007, pp. 223-231) (Gentile, 2013). In spite of being the most rigorous method to tackle the multiple comparisons problem, FWE voxel-level corrections can be very conservative, resulting in a test with poor statistical sensitivity (i.e. high type II error rate) and reduced statistical power. To compensate for this restriction, cluster-extent based thresholding of statistical maps is widely used as an alternative method for multiple comparisons correction in neuroimaging studies. Specifically, the cluster-level extent threshold that controls FWE (cFWE) accounts for statistically significant clusters formed by the contiguous voxels whose FWE values lie above the pre-established threshold. First, a 'primary' threshold is defined in order to determine suprathreshold voxels. Then, the cFWE can be obtained based on the estimated distribution of cluster sizes under the null-hypotheses of no activation in any voxel within the assessed

clusters at their largest size (Woo et al., 2014). The aforementioned distributions are estimated in SPM8 using RFT methods (Friston et al., 2007, pp. 232-236). In contrast with FWE voxel-level corrections, cluster-extent based thresholding has a relative high sensitivity (Friston et al., 2007, pp. 237-245).

References

Amaro, E. J. and Barker, G. J. (2006). Study design in fMRI: basic principles. *Brain and Cognition*, 60(3):220–232.

Ashburner, J., Barnes, G., Chen, C.-C., Daunizeau, J., Flandin, G., Friston, K., Gitelman, D., Kiebel, S., Kilner, J., Litvak, V., Moran, R., Penny, W., Stephan, K., Henson, R., Hutton, C., Glauche, V., Mattout, J., and Phillips, C. (2010). *SPM8 Manual: The FIL Methods Group (and honorary members)*. Functional Imaging Laboratory; Wellcome Trust Centre for Neuroimaging; Institute of Neurology, UCL, 12 Queen Square, London WC1N 3BG, UK. `http://www.fil.ion.ucl.ac.uk/spm/doc/manual.pdf`.

Ashburner, J. and Friston, K. J. (1997). Spatial transformation of images. In Frackowiak, R. S. J., Friston, K. J., Frith, C., Dolan, R., and Mazziotta, J. C., editors, *Human Brain Function*. Academic Press USA.

Ashburner, J. and Friston, K. J. (2005). Unified segmentation. *Neuroimage*, 26(3):839–851.

Beckmann, C. F., Jenkinson, M., and Smith, S. M. (2003). General multilevel linear modelling for group analysis in FMRI. *Neuroimage*, 20(2):1052–1063.

Bennett, C. M., Wolford, G. L., and Miller, M. B. (2009). The principled control of false positives in neuroimaging. *Social Cognitive and Affective Neuroscience*, 4(4):417–422.

Collignon, A., Maes, F., Delaere, D., Vandermeulen, D., Suetens, P., and Marchal, G. (1995). Automated Multi-Modality Image Registration Based On Information Theory. In Bizais, Y., Barillot, C., and Paola, R. D., editors, *Information Processing in Medical Imaging*, Computational Imaging and Vision, pages 263–274, Dordrecht, The Netherlands. Kluwer Academic Publishers.

Diedrichsen, J. and Shadmehr, R. (2005). Detecting and adjusting for artifacts in fMRI time series data. *Neuroimage*, 27(3):624–634.

Doğanaksoy, A. and Göloğlu, F. (2006). On Lempel-Ziv Complexity of Sequences. In Gong, G., Helleseth, T., Song, H.-Y., and Yang, K., editors, *Sequences and Their Applications - SETA 2006*, volume 4086 of *Lecture Notes in Computer Science*, pages 180–189. Springer Berlin Heidelberg.

Friston, K. J. (1994). Functional and Effective Connectivity in Neuroimaging: A Synthesis. *Human Brain Mapping*, 2(1-2):56–78.

Friston, K. J., Ashburner, J. T., Kiebel, S. J., Nichols, T. E., and Penny, W. E., editors (2007). *Statistical Parametric Mapping: The Analysis of Functional Brain Images*. Academic Press, 1st edition.

Friston, K. J., Buechel, C., Fink, G. R., Morris, J., Rolls, E., and Dolan, R. J. (1997). Psychophysiological and Modulatory Interactions in Neuroimaging. *Neuroimage*, 6(3):218–229.

Friston, K. J., Holmes, A. P., Worsley, K. J., Poline, J.-P., Frith, C. D., and Frackowiak, R. S. J. (1995). Statistical Parametrical Maps in Functional Imaging: A General Linear Approach. *Human Brain Mapping*, 2(4):189–210.

Friston, K. J., Rotshtein, P., Geng, J. J., Sterzer, P., and Henson, R. N. (2006). A critique of functional localisers. *Neuroimage*, 30(4):1077–1087. Comments and Controversies.

Friston, K. J., Zarahn, E., Josephs, O., Henson, R. N. A., and Dale, A. M. (1999). Stochastic Designs in Event-Related fMRI. *Neuroimage*, 10(5):607–619.

Gentile, G. (2013). *Investigating the Mutisensory Representation of the Hand and the Space Around it Using FMRI*. PhD thesis, Karolinska Institutet, Stockholm, Sweden.

Gitelman, D. R., Penny, W. D., Ashburner, J., and Friston, K. J. (2003). Modeling regional and psychophysiologic interactions in fmri: the importance of hemodynamic deconvolution. *Neuroimage*, 19(1):200–207. Technical Note.

McIntosh, A. R. and Gonzalez-Lima, F. (1994). Structural Equation Modelling and Its Application to Network Analysis in Functional Brain Imaging. *Human Brain Mapping*, 2(1-2):2–22.

Muraskin, J., Ooi, M. B., Goldman, R. I., Krueger, S., Thomas, W. J., Sajda, P., and Brown, T. R. (2013). Prospective active marker motion correction improves statistical power in BOLD fMRI. *Neuroimage*, 68:154–61.

Poldrack, R. A. (2012). The future of fMRI in cognitive neuroscience. *Neuroimage*, 62(2):1216–1220.

Poldrack, R. A., Mumford, J. A., and Nichols, T. E. (2011). *Handbook of Functional MRI Data Analysis*. Cambridge University Press, 1st edition.

Saxe, R., Brett, M., and Kanwisher, N. (2010). Divide and Conquer: A Defense of Functional Localizers. In Hanson, S. J. and Bunzl, M., editors, *Foundational Issues in Human Brain Mapping*, chapter Averaging Signal in the fROI and Other Summary Measures, pages 37–39. MIT Press.

Shannon, C. E. (1948). A Mathematical Theory of Communication. *The Bell System Technical Journal*, 27:379–423,623–656.

Smith, S. M. (2002). Fast Robust Automated Brain Extraction. *Human Brain Mapping*, 17(3):143–155.

Stephan, K. E., Riera, J. J., Deco, G., and Horwitz, B. (2008). The Brain Connectivity Workshops: Moving the frontiers of computational systems neuroscience. *Neuroimage*, 42(1):1–9. Comments.

Unser, M., Aldroubi, A., and Eden, M. (1993). B-Spline Signal Processing: Part II - Efficient Design and Applications. *IEEE Transactions on Signal Processing*, 41(2).

Weaver, W. (1949). Recent Contributions to the Mathematical Theory of Communication. In Shannon, C. E. and Weaver, W., editors, *The Mathematical Theory of Communication*, pages 93–117. University of Illinois Press, Urbana.

Woo, C.-W., Krishnan, A., and Wager, T. D. (2014). Cluster-extent based thresholding in fMRI analyses: Pitfalls and recommendations. *Neuroimage*, 91:412–419.

Worsley, K. J. and Friston, K. J. (1995). Analysis of fMRI Time-Series Revisited - Again. *Neuroimage*, 2(3):173–181.

Worsley, K. J., Liao, C. H., Aston, J., Petre, V., Duncan, G. H., Morales, F., and Evans, A. C. (2002). A General Statistical Analysis for fMRI Data. *Neuroimage*, 15(1):1–15.

Part III

Results

Chapter 5

Study I

Connecting to Create - Expertise in Musical Improvisation Is Associated with Increased Functional Connectivity between Premotor and Prefrontal Areas

This section refers to: Pinho, A. L., de Manzano, Ö., Fransson, P., Eriksson, H., and Ullén, F. (2014). Connecting to Create: Expertise in Musical Improvisation Is Associated with Increased Functional Connectivity between Premotor and Prefrontal Regions. *The Journal of Neuroscience*, 34(18):6156 - 6163.

http://dx.doi.org/10.1523/JNEUROSCI.4769-13.2014

5.1 Abstract

Musicians have been used extensively to study neural correlates of long-term practice, but no studies have investigated the specific effects of training musical creativity. Here, we used human functional MRI to measure brain activity during improvisation in a sample of thirty nine professional pianists with varying backgrounds in classical and jazz piano playing. We found total hours of improvisation experience to be negatively associated with activity in frontoparietal executive cortical areas. In contrast, improvisation training was positively associated with functional connectivity of the bilateral dorsolateral prefrontal cortices, dorsal premotor cortices, and presupplementary areas. The effects were significant when controlling for hours of classical piano practice and age. These results indicate that even neural mechanisms involved in creative behaviors, which require a flexible online generation of novel and meaningful output, can be automated by training. Second, improvisational musical training can influence functional brain properties at a network level. We show that the greater functional connectivity seen in experienced improvisers may reflect a more efficient exchange of information within associative networks of importance for musical creativity.

Key words: Creativity; expertise; fMRI; improvisation; music; plasticity

5.2 Introduction

Creative products are by definition both novel and meaningful. Correspondingly, creative cognition is commonly assumed to involve the free generation of possible solutions as well as selection among the produced alternatives (Campbell, 1960). The neuropsychology of creativity has been studied using tasks ranging from pseudorandom generation of simple responses to the production of musical or verbal materials (Frith, 2000; Nathaniel-James and Frith, 2002; Lau et al., 2004). Interestingly, pseudorandom and musical generation appear to rely on a common set of regions, which includes the DLPFC, the ACC, the PreSMA, and the IFG (de Manzano and Ullén, 2012b). These regions presumably fulfill several cognitive functions during creative thinking, including attention to action (Lau et al., 2004), response generation (Lau et al., 2004; Bengtsson et al., 2007), action planning and monitoring (Nathaniel-James and Frith, 2002), and inhibition of repetitive responses (Frith, 2000). Studies do not suggest a simple mapping in which different cognitive processes are subserved by distinct cortical subregions. Rather, most involved brain regions appear to interact in several such processes,

indicating that creative thinking relies on distributed networks (de Manzano and Ullén, 2012b).

Musical training can have dramatic effects on the brain (Schneider et al., 2002; Bengtsson et al., 2005; Kleber et al., 2010; Pantev and Herholz, 2011). Many correlates of training presumably reflect task automation and the acquisition of specific expertise-related skills. Although several studies have investigated the neural effects of musical training, there is, to our knowledge, no study on the specific consequences of training musical creativity (i.e., improvisation). A key difference between creative and reproductive performance is that the former to a higher degree appears to rely on the executive frontal circuits (Bengtsson et al., 2007; de Manzano and Ullén, 2012b). Therefore, an interesting question is to what extent, if at all, neural circuits involved in creativity can be optimized by systematic training.

Here, we investigated this issue in a sample of 39 pianists with a wide range of experience in both classical piano playing and improvisation. Brain activity was measured with fMRI while the pianists performed brief keyboard improvisations. Total hours of classical piano playing and improvisation were assessed using a self-report questionnaire. We addressed two questions. First, to test whether creative performance is subject to similar training effects as reproductive performance, we investigated whether frontoparietal brain activity during improvisation was negatively associated with experience in improvisation. Second, creativity requires an integration of different types of information, which can result in the discovery of new and interesting combinations of familiar elements (Campbell, 1960). Given this, it appears reasonable to hypothesize that experienced creators have more extensive task-specific functional connectivity between the distributed neural circuits that are involved in creative performance. To test this, we investigated whether experience in improvisation was correlated with functional connectivity during improvisation. This analysis was based on six seed brain regions known to be involved in free generation of behavior: the right and left PreSMA, PMD, and DLPFC.

5.3 Materials and Methods

5.3.1 Participants

Thirty-nine pianists (15 female) participated in the study, ranging in age between 19 and 67 years (mean = 32.4, SD = 11.0). Handedness was determined with the Swedish version of the Edinburgh Handedness Inventory (Oldfield, 1971). All participants, who were recruited by poster advertisements, were right-handed, healthy, and had no history of neurological or psychiatric illness. The participants had varied experience in classical and/or jazz piano playing;

all had piano as first instrument and, except for one (a self-taught jazz piano player), all pianists also had a university degree in piano performance or were students at the Royal College of Music in Stockholm, the Guildhall School of Music and Drama in London, or the Nordic Masters in Jazz program (Nomazz) at the Norwegian University of Science and Technology in Trondheim. All participants were active as performers. The experimental procedures were undertaken with the informed written consent of each participant according to Declaration of Helsinki and were approved by the Regional Ethical Review Board in Stockholm (Dnr 2011/637−32 and Dnr 2011/1682−32). Participants were reimbursed with 600 Swedish Krona.

5.3.2 Materials

5.3.2.1 Piano experience questionnaire

The participants were asked to fill out a brief questionnaire about how much they had played the piano throughout their lifetime. Experience was estimated as the mean intensity of playing (hours/week) in three age periods: *(1)* age<11 years, *(2)* age 12-17 years, and *(3)* age 18 years to present. Separate estimates were given for improvisation and total piano playing. From these data, estimates were calculated of the total number of hours spent improvising (*Imphours*), total experience (*Totalhours*), and experience in classical (nonimprovisatory) piano playing (*Classhours* = *Totalhours* − *Imphours*). Only *Imphours* and *Classhours*, that is, total training of improvisation and classical piano playing, were used in the data analysis. To evaluate the test-retest reliability of the practicing data, we performed a second administration of the questionnaire on total piano playing throughout lifetime as part of an independent Internet-based data collection. Thirty of our original 39 participants chose to participate in this second data collection, which took place 10-18 months (mean = 13.8, SD = 2.3) after the first data collection.

5.3.2.2 Piano keyboard, auditory feedback, and musical recordings

The participants performed on a custom designed MR-compatible fiber optic piano keyboard (LUMItouch) of about one octave (12 authentic keys ranging from F to E) during scanning. The keyboard was connected to an opticalelectrical converter placed in the control room. The converter was connected to a MIDI-keyboard (Midistart-2 Pro Keys; Miditech) generating a MIDI signal, which was subsequently sent to a MIDI patchbay/processor (MX-8; Digital Music) producing two different MIDI outputs. The first output was relayed to a sound module (SD-50; Roland), which synthesized the piano sound (GM2; European Pf). This device was

connected to the audio system of the MR scanner to provide audio feedback (keys F2-E3) to the participants. The second output was relayed to an external sound card, which was in turn connected to a PC recording the musical samples with a music production software (Cubase 5; Steinberg).

5.3.2.3 Visual stimuli

The visual stimuli consisted of a set of images providing instructions on which conditions to perform. They were presented at the beginning of each experimental trial. The display was controlled by a custom made E-Prime script (E-Prime 2.0 Professional; Psychological Software Tools). The instructions were presented on MR-compatible OLED display goggles (Nordic Neuro Lab's visual system) mounted on the head coil.

5.3.2.4 MRI scanner

The fMRI data were acquired using a 3T scanner (3T Discovery MR750; GE) with a 32-channel coil (MR Instruments) at the MR center of the Karolinska Hospital.

5.3.3 Experimental procedure

Upon arrival at theMRcenter, the participants were first rebriefed about the purpose of the study and safety procedures, after which they completed a screening form regarding general health and history of disease, as well as the piano experience questionnaire and the informed consent. Finally, they were given detailed instructions on how to perform the experimental conditions in a training session outside of the scanner room. During practice, the participants were seated in a chair with a laptop on the desk in front of them for the presentation of the stimuli and the piano keyboard was positioned on their right side on the desk. The participants were instructed that they should play simple musical improvisations, under different constraints, with the right hand on the keyboard. They were informed that they were allowed to improvise freely as long as they followed the constraints of the condition and that they should continue to play throughout the duration of the trial. In addition, they were instructed not look to the piano keys or their right hand while playing, as would be the case inside the scanner. They then completed one training session that was similar in procedure, visual stimuli, and audio feedback to the real experiment. In total, the training lasted for $\sim$30 min. No difficulties with executing the paradigm were observed by the experimenters nor reported by the participants. The participants were scanned in the supine position with the keyboard placed on their lap. The

right arm was supported by a sponge pad to avoid fatigue and to minimize arm movements. Ear plugs and headphones were used to reduce scanner noise and to allow auditory feedback from the piano and verbal communication with the experimenters. The volume of the auditory feedback and dioptric settings in the goggles were adjusted for each participant.

5.3.4 Experimental design

The experiment was performed in six sessions. Each session consisted of 16 trials arranged in a block design. Each trial was composed of four consecutive parts: *(1)* instruction (3.5 s), *(2)* performance (15 s), *(3)* a distractor task (11 s), and *(4)* rest (6 s). Therefore, one trial lasted for 35.5 s. During the instruction session, a visual instruction slide was presented. Four different improvisation conditions were used with different instruction slides. The four conditions differed in the type of constraints the participant should adhere to when improvising. In two conditions (tonal and atonal), a structural constraint was used. The participant was instructed to improvise using only six different pitches. These were displayed as six whole notes, notated on a single musical staff. In tonal, the pitches were all from the same Western musical scale (major, minor). The pitches thus naturally suggested a tonality for the improvisation. Pitch sets for atonal, in contrast, were randomly generated to fulfill two different criteria: *(1)* that the pitches were not all part of the same major or minor scale and *(2)* that there would be at least one interval equal to or larger than a minor third (to avoid chromatic sequences). Therefore, this pitch set did not suggest any particular tonality. The specific pitch sets were unique for each trial of tonal and atonal. For the two other conditions (happy and fearful), the participant was instructed to produce an improvisation with the corresponding emotional character. The instruction slide for these conditions showed a happy or fearful clip art face. The order of trials were randomized with the constraint that the same condition could never appear in more than two consecutive trials and that no more than three consecutive trials would consist of conditions in the same category (structural or emotional). Each condition (tonal, atonal, happy, and fearful) occurred four times in each session. Because correlations between brain activity and improvisation experience were similar in all four improvisation conditions (Fig. 5.1C), data were pooled across conditions in the present study. The participants had been instructed to commence the performance once the instruction phase was over; that is, when the instruction slide disappeared after 3.5 s.

The performance phase was interrupted by the distractor task. This task was included to interrupt musical cognitive processes from the previous trial and to minimize planning of

the next improvisation. The distractor task was constructed as a visual esthetical judgment task. The participant would view a fixation cross for 3 s and then watch a computer-generated image for 5 s. Then, during the final 3 s of the task, they were to provide a rating of the aesthetic quality of the image by pressing on the keys on the piano (higher note = higher rating). Results from the analyses of this task will be presented in a separate manuscript.

5.3.5 Data acquisition

All behavioral (musical) data were recorded in MIDI format and analyzed by a custom-made script in MATLAB 7 (The MathWorks). The fMRI data were collected using a gradient echo pulse, EPI T_2* - weighted sequence with BOLD contrasts using the following parameters: TR = 2.5 s; TE = 30 ms; flip angle = 90°;FOV = 28.8 cm; slice spacing = 0mm; voxel size = 3×3×3 mm^3; data acquisition matrix = 96×96, interpolated during reconstruction to 128×128; slice order = interleaved; number of slices = 48. A total of 228 functional image volumes were acquired per session, giving a total of 1368 image volumes per participant. At the beginning of each session, 10 "dummy" image volumes were scanned, but not saved, to allow for T_1-equilibration effects. Subsequently, a 3D fast-spoiled gradient echo T_1-weighted anatomical image volume covering the whole brain was acquired: voxel size = 1×1×1 mm^3; axial slice orientation; flip angle = 12°; inversion time = 450 ms; FOV = 24 cm.

5.3.6 Data analysis

5.3.6.1 Analysis of behavioral data

For the structural conditions, criteria for distinguishing "good" (i.e., when the participant adhered to the structural constraint with a reasonable degree of correctness) from "bad" performances were used. A good performance corresponded to a trial in which the participant used at least five of the presented pitches and used at maximum one wrong pitch. In this way, we removed performances in which the participant held an incorrect representation of the instructions but at the same time allowed for small involuntary slips. The excluded bad performances accounted for $\sim 9\%$ of the data in the analysis; 2% of the collected data were removed due to various technical problems, for example, with MIDI recordings.

Three different measures were used to characterize the complexity of the musical samples: 0 - order melodic entropy (considering the distribution of single notes), 1 - order melodic entropy (considering the distribution of bigrams of two consecutive pitches), and the Lempel-Ziv complexity measure. Entropy measures were calculated as Shannon entropies as follows:

0 - order entropy was calculated as follows:

$$H = -\sum_{i=1}^{n} p(x_i) \log_2 p(x_i) \tag{5.1}$$

1 - order entropy was calculated as follows:

$$H = -\sum_{i=1}^{n} p(x_i) \sum_{j=1}^{n} p(x_j \mid x_i) \log_2 p(x_j \mid x_i) \tag{5.2}$$

where H is the entropy, n is the number of different elements present in the sequence, and x_i is the i:th of these elements. The probabilities $p(x_i)$ and the conditional probabilities $p(x_j \mid x_i)$ were estimated from the frequencies of the corresponding elements and bigrams twice, respectively. The Lempel-Ziv complexity is a measure of the number of unique patterns present in a sequence (Doğanaksoy and Göloğlu, 2006).

5.3.6.2 Preprocessing of fMRI data

The MRI data were processed and analyzed using the SPM8 software package (Wellcome Department of Imaging Neuroscience, London). For each participant, all fMRI image volumes were realigned to the first image of the first session and resliced using a third-degree B-spline interpolation scheme (Friston et al., 1995). To remove residual variance caused by susceptibility by movement interaction, the fMRI images were afterward unwarped with a fourth-degree B-spline interpolation sampling transformation (Andersson et al., 2001). The T_1-weighted anatomical image was then coregistered onto the fMRI unwarped mean image (Ashburner and Friston, 1997). The Brain Extraction Tool was used to remove nonbrain tissue from the anatomical image (Smith, 2002). This image was then segmented to estimate the deformation field for the normalization of all functional and anatomical images (Ashburner and Friston, 2005).

5.3.6.3 fMRI analyses

The fMRI data were modeled using a GLM using the standard HRF as implemented in SPM8. At the first level, five regressors of interest were included: *(1)* instruction, corresponding to the initial instruction phase before the improvisation; *(2)* improvisation, corresponding to the performance phase of the good performances (see sub-subsection 5.3.6.1); *(3)* bad performances, corresponding to the performance phase of the bad performances; *(4)* distractor presentation, corresponding to the initial phase (fixation cross and image presentation) of the esthetical judgment task; and *(5)* distractor rating, corresponding to the final phase of the

distractor task in which the participant rated the esthetical quality of the presented image. Rest was modeled implicitly. The high-pass filter was set to 71 s, or 2× the condition duration. The design matrix weighted each preprocessed image according to its overall variability to reduce the impact of movement artifacts (Diedrichsen and Shadmehr, 2005). For a few participants, one or two sessions were excluded as a consequence of the inclusion criteria for good performances. For one participant, four sessions were thus used and, for three other participants, five sessions were used. For the remaining 35 participants, all six sessions were used. Contrasts were weighted with the number of included sessions. The contrast images were smoothed using a Gaussian kernel with a FWHM of 10 mm.

A multiple regression at the second level was then performed, regressing the first-level beta estimates of the *Improvisation* regressor on age, *Imphours*, and *Classhours*. A gray matter mask was estimated during the segmentation process for each participant. The mean of these images was used as an explicit mask in the second-level analysis. The significance of effects was assessed using t statistics to create statistical parametric maps. A PPI analysis was performed to analyze differences in functional connectivity between brain regions between the experimental conditions (Friston et al., 1997). Specifically, we tested the hypothesis that functional connectivity during *Improvisation*, compared with *Rest*, would be positively related to *Imphours*. We identified six regions that have been implied in improvisation in earlier studies (de Manzano and Ullén, 2012a,b) and that were confirmed to be active during improvisation in the present experiment, which we used as seed regions: the left and right DLPFC, the left and right PMD, and the left and right PreSMA. The extent of each seed region was determined as the intersection of the corresponding clusters of activity in the GLM contrast *Improvisation - Rest* (onesample t test) and the respective region as defined by the Human Motor Area Template (HMAT). The HMAT was created from a meta-analysis of 126 studies and describes the spatial extent of various regions in the motor system (Mayka et al., 2006). Because the HMAT does not include the DLPFC, this seed was defined using the corresponding cluster of activity from the contrast *Improvisation-Rest*.

For each PPI analysis, the BOLD signal of the seed region was deconvolved with the HRF. Second, the PPI was formed by multiplying this neural activity signal with a block regressor representing the conditions *Improvisation* and *Rest* as 1 and -1, respectively. Third, a GLM analysis was performed with all three regressors in the model: the neural activity, the block regressor representing the two conditions, and the PPI. The high-pass filter was set to 71 s. Each preprocessed image was weighted with its overall variability (more variable images

receiving a lower weighting) to reduce the impact of movement artifacts (Diedrichsen and Shadmehr, 2005). The resulting contrast images were smoothed with an isotropic Gaussian kernel of 10mm FWHM. Last, a second-level random effect analysis was performed using a multiple regression model in which the contrast images were regressed on participant age, *Imphours*, and *Classhours*. The mean of the gray matter masks from all participants was used as an explicit mask during this analysis.

5.4 Results

The participants displayed a wide range of both improvisational and classical piano experience: *Imphours* varied between 0 and 68,120 h (mean = 9100, SD = 13,014); *Classhours* varied between 0 and 56,212 h (mean = 14,685, SD = 13,062). *Imphours* correlated positively with age (r = 0.43, p = 0.006) and negatively with *Classhours* (r = -0.34, p = 0.04). Both age and *Classhours* were therefore included as covariates in all analyses. Test-retest data on the retrospective estimates of total piano experience (*Totalhours*) was available for 30 of the 39 participants. The retesting was administered 10-18 months after the original test and the test-retest correlation was r = 0.76 (p <0.0001).

We found a significant negative correlation between improvisation experience (*Imphours*) and brain activity during improvisation (*Improvisation - Rest*) in a number of cortical regions in the right hemisphere: the DLPFC, the IFG, the anterior insula, and angular gyrus (Fig. 5.1B, Table 5.1). The negative association between improvisation experience and brain activity was seen for all individual improvisation conditions, as illustrated for the angular gyrus in Figure 5.1C. In contrast, brain activity during improvisation did not show any significant relation to classical piano training (*Classhours*). Age was positively related to brain activity in the DLPFC, the right parietal lobe, and the inferior frontal cortex, partly overlapping with the clusters for *Imphours*.

Second, we found that more experienced improvisers showed higher functional connectivity between prefrontal, premotor, and motor regions of the frontal lobe during improvisation compared with rest. Significant effects were found for each of the six seed regions (Fig. 5.2, Table 5.2). Particularly, extensive effects were seen when using the right PMD as the seed region (Fig. 5.2). No negative correlations between *Imphours* and functional connectivity were found and there were no associations between *Classhours* and functional connectivity. The brain regions where functional connectivity correlated with *Imphours* were anatomically nonoverlapping with the regions that showed a lower activity (Fig. 5.3). Finally, we investigated

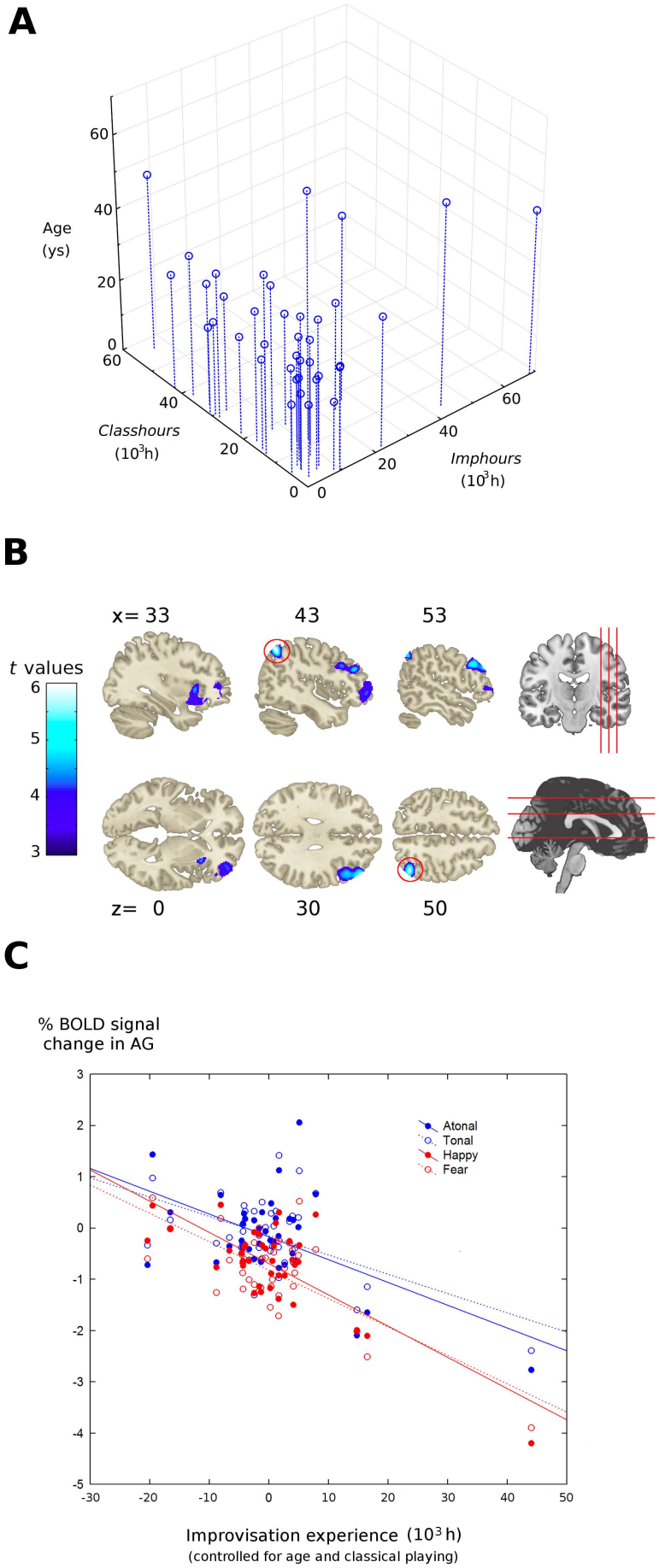

Figure 5.1: Piano experience and brain activity during improvisation. ***A***, 3D scatter plot showing the age, improvisational piano experience (*Imphours*), and classical piano experience (*Classhours*) of each participant. ***B***, Negative associations between brain activity and improvisational training. The clusters represent regions for which there was a significant between-participant negative association between brain activity during improvisation and number of hours of improvisation experience. ***C***, Brain activity and improvisation experience for individual conditions. The plot shows, for all four individual conditions (tonal, atonal, happy, and fearful), the semi-partial correlation between brain activity (BOLD percentage signal change in *Improvisation-Rest*) in the right angular gyrus (red circle in ***B***) and *Imphours* after partialling out the effects of age and *Classhours* on the latter variable.

Table 5.1: Associations between brain activity during improvisation, improvisation experience and age.

		Coordinates[a]			Voxel Level[b]		Cluster level[c]	
Region	Side	x	y	z	t	p	p	k_E
Improvisation (negative)								
AG	Right	44	-61	52	5.98	0.008	–	–
DLPFC	Right	48	38	30	–	–	0.035	1322
Insula	Right	33	18	1	–	–	0.039	1273
IFG	Right	39	50	-6	–	–	0.028	1419
Age (positive)								
AG	Right	48	-54	40	–	–	0.035	1325
DLPFC	Right	51	33	25	5.43	0.033	0.025	1459
IFG	Right	44	48	-17	5.38	0.037	0.004	2295

AG, angular gyrus; DLPFC, dorsolateral prefrontal cortex; IFG, inferior frontal gyrus.

[a] Coordinates in milimeters in the MNI space.

[b] Voxel-level familywise error rate, corrected p=0.05,

[c] Cluster-level familywise error rate, corrected extent threshold k_E=1273 (improvisation) and k_E=1325 (age)

whether the observed effects of improvisation experience were confounded with the complexity of motor output during improvisations. We found no evidence for this, because *Imphours* was uncorrelated with all used measures of melodic complexity: Lempel-Ziv string complexity (r = 0.12, p = 0.48), 0 - order entropy (r = 0.13, p = 0.43), 1 - order entropy (r = 0.12, p = 0.47), and number of notes of the improvisation (r = 0.28, p = 0.09).

5.5 Discussion

During improvisation, more trained improvisers displayed an overall lower activity in frontoparietal association areas, as well as greater functional connectivity among prefrontal, premotor, and motor regions of the frontal lobe. The effects were specific to improvisation experience; that is, they were independent of classical piano experience and age, and appeared not to be confounded by differences in the complexity of the musical output between more and less experienced improvisers.

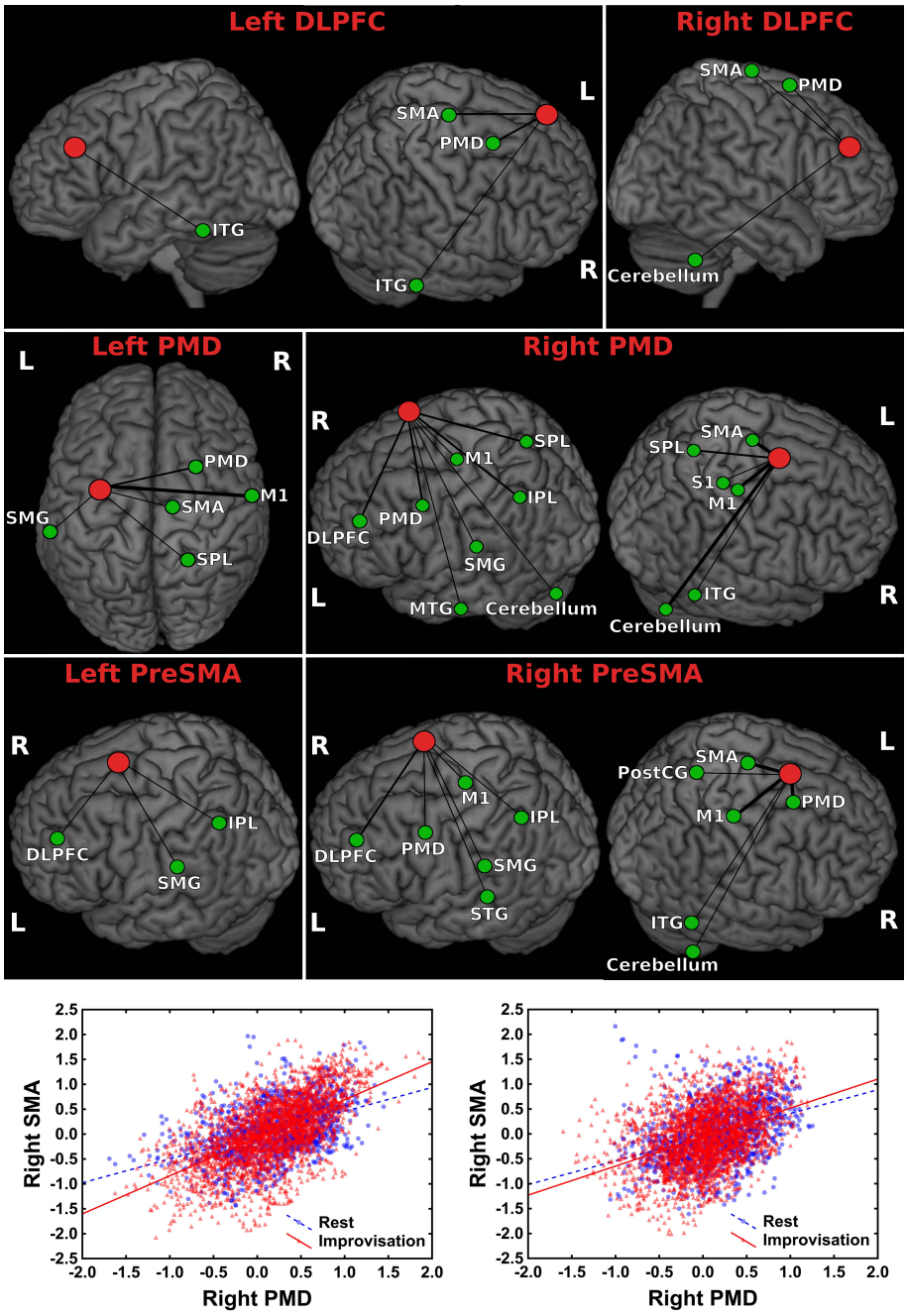

Figure 5.2: Positive correlations between improvisational training and functional connectivity. Associations between functional connectivity and improvisational training are illustrated schematically for all seed regions. The red circles indicate the location of the seeds. Green circles represent regions for which a significant between-subject correlation was found between improvisational training and the strength of the functional connectivity with the seed. For each involved region, only the cluster with the highest peak activation is illustrated. The thickness of the connecting lines represents the strength of the effect (thin: t value 5 - 6; middle: t value 6 - 7; thick: t value 7). The scatterplots show activity (% BOLD response) in the right supplementary motor area (SMA) as a function of activity in the right PMD during improvisation (red dots) and rest (blue dots) for the participant with the longest (left) and shortest (right) improvisation experience. The increase in functional connectivity during improvisation, compared with rest, is higher for the participant with longer experience, which is illustrated by a greater increase in slope of the ordinary least-squares fitted regression line for improvisation (red) compared with rest (blue).

Table 5.2: Brain regions for which there was a positive association between improvisation experience and the functional connectivity during improvisation

				Coordinates[a]			Voxel Level[b]	Cluster level[c]
Seed	Side	Region	Side	x	y	z	t	k_E
DLPFC	Right	PMD/SFG	Right	26	11	69	5.81	13
		Cerebellum	Right	6	-49	-36	5.49	33
		SMA/PreCG	Right	14	-15	78	5.25	7
	Left	PMD/SFG	Right	26	11	69	6.37	93
		SMA/FL	Right	12	-16	78	6.34	39
		ITG	Left	-48	-49	-21	5.68	90
		ITG	Right	46	-34	-24	5.38	23
		ITG	Right	48	-49	-23	5.26	70
PMD	Right	SMA/FL	Right	10	-13	78	9.55	186
		Cerebellum	Right	54	-67	-30	7.59	1569
		M1/CS[c]	Right	51	-18	62	7.07	301
		Cerebellum	Right	6	-52	-39	7.00	272
		M1/CS[d]	Right	63	-7	40	6.73	284
		DLPFC/MFG	Left	-36	45	36	6.54	113
		SPL	Right	15	-48	78	6.40	255
		IPL	Left	-50	-55	54	6.31	96
		PMD/PreCG	Left	-52	3	49	6.03	53
		Precuneus/SPL	Left	-6	-60	69	6.01	42
		M1/PreCG	Left	-34	-10	70	5.93	130
		MTG	Left	-69	-19	-20	5.75	14
		Cerebellum	Right	9	-90	-38	5.72	22
		Cerebellum	Right	18	-60	-18	5.65	45
		SMG	Left	-68	-28	31	5.63	32
		Cerebellum	Left	-16	-67	-21	5.52	38
		Cerebellum	Right	14	-78	-42	5.51	68
		M1/CS	Left	-24	-27	75	5.46	4
		M1/ParaCL	Left	-14	-24	78	5.42	5
		S1/PostCG	Right	30	-31	45	5.41	16
		ITG	Right	45	-25	-20	5.40	28
		M1/PreCG	Left	-45	-15	63	5.36	15
		ITG	Right	46	-19	-14	5.25	4
	Left	M1/CS[d]	Right	63	-7	40	7.35	127
		M1/CS[c]	Right	52	-15	58	7.17	112
		PMD/SFG	Right	30	12	66	6.85	88
		SMG	Left	-68	-30	31	5.75	50
		SMA/FL	Right	10	-13	78	5.57	13
		SPL	Right	21	-46	76	5.37	11
PreSMA	Right	SMA/PreCG	Right	14	-15	78	7.18	79
		PMD/SFG	Right	26	11	69	7.15	126
		M1/CS[c]	Right	51	-18	62	7.02	316
		M1/CS[d]	Right	63	-7	40	6.69	288
		DLPFC/MFG	Left	-36	45	36	6.07	71
		IPL	Left	-46	-57	55	5.95	53
		SMG	Left	-68	-30	31	5.80	89
		Cerebellum	Right	54	-67	-30	5.78	52
		STG	Left	-69	-37	12	5.69	21
		Cerebellum	Right	3	-49	-39	5.68	91
		ITG	Right	48	-28	-23	5.54	37
		PostCG	Right	20	-46	76	5.54	19
		M1/PreCG	Left	-28	-21	73	5.40	14
		ITG	Right	52	-51	-18	5.35	38
		PMD/PreCG	Left	-52	5	48	5.30	4
	Left	IPL	Left	-48	-57	54	5.75	66
		SMG	Left	-68	-28	31	5.72	40
		DLPDC/MFG	Left	-39	42	34	5.39	10

CS, central sulcus; FL, frontal lobe; IPL, inferior parietal lobe; ITG, inferior temporal gyrus; M1, primary motor cortex; MFG, middle frontal gyrus; MTG, middle temporal gyrus; ParaCL, paracentral lobule; PMD, dorsal premotor region; PMV, ventral premotor region; PostCG, postcentral gyrus; PrecG, precentral gyrus; S1, primary somatosensory cortex; SFG, superior frontal gyrus; SMA, supplementary motor area; SPL, superior parietal lobe; STG, superior temporal gyrus; SMG, supramarginal gyrus

[a] Coordinates in milimeters in the MNI space.

[b] Voxel-level familywise error rate, corrected $p = 0.05$.

[c] The cluster extended into de PreCG.

[d] The cluster extended into de PMV/PreCG.

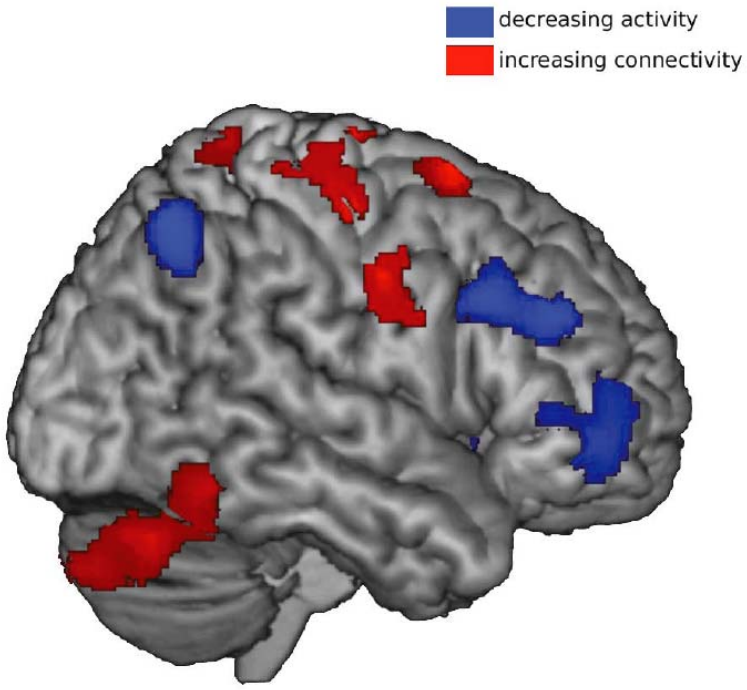

Figure 5.3: Anatomical relation between training effects on activity and training effects on connectivity. Regions where improvisation experience was related to lower activity (blue) were nonoverlapping with regions showing increased functional connectivity (red). Connectivity effects from all seed regions are displayed.

These findings are of general interest in several ways. First, they show that the neural effects of musical training may depend on the type of training in which a musician engages. Earlier studies have typically focused on the effects of conventional, classical musical training. Some of these studies have also provided evidence that neural correlates of musical training differ depending on the instrument trained, with subtle differences between singers and various instrumental players in both the anatomy and functional organization of motor and auditory regions. For example, the relative size of the left and right motor cortices differs between piano and string players (Bangert and Schlaug, 2006), the ultrastructure of the arcuate fasciculus differs between singers and instrumentalists (Halwani et al., 2011), and auditory cortical representations for tones are enhanced in a timbre-specific way for tones from the instrument that the musician has trained (Pantev et al., 2001). The present results provide an example of another type of "specialization of the specialized" (Bangert and Schlaug, 2006), in which the specific effects of improvisation experience presumably relate to cognitive aspects of the training rather than the sensorimotor demands of piano playing.

An important focus of improvisation training is to acquire extensive long-term stores of musical patterns and cognitive strategies that can be used during extemporization (Pressing, 1988). Creativity in improvisation is thus not a matter of free generation of individual notes or sounds, but rather comes into play in the skilled combination, development, and expressive rendering of prelearned musical structures in real time. In an extensive review of improvisation from a cognitive psychological perspective, Pressing (1988) also emphasized the importance of rapid accessibility of musical patterns through the buildup of a rich structure of associations and the integration of simpler structures into larger assemblies, which facilitates complex performances. Consistent with this, we suggest that the greater functional connectivity of the frontal brain regions seen in the most experienced participants may reflect a more efficient integration of representations of musical structures at different levels of abstraction. A higher functional connectivity of the seed regions was observed with premotor regions and parietal and prefrontal association cortex, as well as with primary sensorimotor cortex and the cerebellum, suggesting that the training-related functional reorganizations may affect both cognitive and sensorimotor aspects of improvisation.

The lower overall level of activity in prefrontal and parietal association cortices in highly trained improvisers raises the intriguing question of to what extent a creative behavior such as improvisation can be automated. Sustained attention has been suggested to be critical for creative thinking and for tasks involving the processing of novel information in general (Dietrich, 2004). Both neuroimaging data and experimental interventions with transcranial magnetic stimulation show that prefrontal executive areas are involved in tasks involving free generation (Jahanshahi and Dirnberger, 1999; de Manzano and Ullén, 2012b). Notably, however, de Manzano and Ullén (2012b) found a significantly higher activity in frontoparietal association cortex when contrasting an untrained free generation task (pseudorandom generation) with musical improvisation in musicians. It appears possible, therefore, that long-term training could lead to an automation of the task-specific cognitive processes that are used to generate new and meaningful recombinations of musical structures by expert improvisers. Limb and Braun (2008) reported extensive prefrontal deactivations during free improvisations in a study of six experienced jazz musicians (Limb and Braun, 2008). The regions showing training-related activity decreases were essentially nonoverlapping with the regions showing training-related increases in functional connectivity. The lowered frontoparietal activity, indicating automation and reduced top-down cognitive control, was thus accompanied by increased interactions among regions that maintained a higher activity level during performance. In addition, a

subjective feeling of automaticity and psychological flow during performance has often been discussed in accounts of performances by improvising musicians (Pressing, 1988). In contrast to the effects of improvisational experience, we found age to be positively associated with frontoparietal activity. This is consistent with many earlier studies finding higher activity in older than in younger subjects in frontoparietal systems during the performance of demanding cognitive (Emery et al., 2008; Salami et al., 2014) and motor (Heuninckx et al., 2008) tasks. Possibly, this tendency for higher activity in executive regions in older participants could represent a compensation for age-related decline in functional capacity (Heuninckx et al., 2008), even though most of the participants in the present study were relatively young adults. The importance of frontoparietal systems for creativity is supported by several studies using EEG to study brain activity during tasks involving creative thinking (Fink and Benedek, 2014). Higher alpha-band power in the EEG activity, in particular at prefrontal and right parietal sites, has been reported during creative (e.g., divergent) compared with less creative tasks (Fink et al., 2009a; Jauk et al., 2012; Fink and Benedek, 2014), and more creative individuals have been found to have higher alpha-band power during creative task performance than less creative individuals (Fink et al., 2009b; Fink and Benedek, 2014). However, one should note that alpha synchronization is not specifically linked to creative thinking, but is also seen in other cognitive tasks such as working memory, and that the EEG literature on creativity shows considerably heterogeneity (Arden et al., 2010).

The present results provide further support for the multifaceted nature of neural correlates of long-term training. Earlier studies have reported that musical training is associated with regional gray matter volume and cortical thickness (Hyde et al., 2009), white matter ultrastructure and connectivity (Bengtsson et al., 2005; Halwani et al., 2011; Steele et al., 2013), and regional differences in the functional organization of brain areas and their level of activity during the performance of musical tasks (Schneider et al., 2002; Kleber et al., 2010; Pantev and Herholz, 2011). The present findings show that musical training also influences functional brain activity at a network level; that is, the patterns of communication between brain regions involved in musical performance. Interestingly, the results indicate that task performance in highly trained individuals compared with novices may involve a lower overall level of regional brain activity that is concomitant with an increase in functional connectivity. Skilled improvisational performance may thus be characterized by both lower demands on executive control and a more efficient interaction within the network of involved brain areas.

The performed improvisations were, necessarily, limited in duration and complexity. How-

ever, earlier comparisons between even more reduced musical improvisations (brief isochronous melodies) and pseudorandom response generation on the same keyboard demonstrated significantly higher activity in frontoparietal executive systems during the untrained, pseudorandom task, supporting that even highly simplified forms of musical improvisation tap into musical expertise (de Manzano and Ullén, 2012b). The fact that brain activity during performance was associated with real-life improvisational experience is in itself further support for the ecological validity of the task. In addition, the effects of improvisational training were consistent across the improvisation conditions. This suggests that the training effects, although specific to improvisational training, were generic in the sense that they were not limited only to certain strategies for improvisation. It appears likely that experienced improvisers not only show a more efficient neural control of improvisation, but also have a higher capacity to perform complex improvisations with a high musical quality. To investigate such differences in improvisational capacity, a design in which participants are allowed to perform more complex and challenging improvisations at the top of their capacity would presumably be needed.

Training data were collected as retrospectively estimated typical training per week in different age periods, which is common practice in expertise studies. Cumulative estimates of total hours of training were for simplicity based on the assumption of 52 training weeks per year. This assumption is obviously somewhat arbitrary and the absolute values of total practicing hours should therefore be viewed with some caution. Musicians typically combine training with concert performances and teaching and a more realistic estimate is presumably lower. Importantly, however, the assumed number of active training weeks per year will of course not influence the associations between training and other variables.

5.6 Acknowledgments

This work was supported by the Foundation for Science and Technology
(Grant SFRH/BD/33895/2009), the Swedish Research Council (Grant 521-2010-3195), and the Sven and Dagmar Salén Foundation. We thank Jonathan Berrebi for technical support and comments on the manuscript, László Harmat and Diana Muessgens for assistance during experiments, and Miguel Castelo-Branco for valuable discussions.

References

Andersson, J. L. R., Hutton, C., Ashburner, J., Turner, R., and Friston, K. (2001). Modeling Geometric Deformations in EPI Time Series. *Neuroimage*, 13(5):903–919.

Arden, R., Chavez, R. S., Grazioplene, R., and Jung, R. E. (2010). Neuroimaging creativity: A psychometric view. *Behavioural Brain Research*, 214(2):143–156.

Ashburner, J. and Friston, K. (1997). Multimodal Image Coregistration and Partitioning - A Unified Framework. *Neuroimage*, 6(3):209–217.

Ashburner, J. and Friston, K. J. (2005). Unified segmentation. *Neuroimage*, 26(3):839–851.

Bangert, M. and Schlaug, G. (2006). Specialization of the specialized in features of external human brain morphology. *European Journal of Neuroscience*, 24(6):1832–1834.

Bengtsson, S. L., Csíkszentmihályi, M., and Ullén, F. (2007). Cortical Regions Involved in the Generation of Musical Structures during Improvisation in Pianists. *Journal of Cognitive Neuroscience*, 19(5):830–842.

Bengtsson, S. L., Nagy, Z., Skare, S., Forsman, L., Forssberg, H., and Ullén, F. (2005). Extensive piano practicing has regionally specific effects on white matter development. *Nature Neuroscience*, 8(9):1148–1150.

Campbell, D. T. (1960). Blind variation and selective retention in creative thought as in other knowledge processes. *Psychological Review*, 67(6):380–400.

de Manzano, Ö. and Ullén, F. (2012a). Activation and connectivity patterns of the presupplementary and dorsal premotor areas during free improvisation of melodies and rhythms. *Neuroimage*, 63(1):272–280.

de Manzano, Ö. and Ullén, F. (2012b). Goal-independent mechanisms for free response generation: Creative and pseudo-random performance share neural substrates. *Neuroimage*, 59(1):772–780.

Diedrichsen, J. and Shadmehr, R. (2005). Detecting and adjusting for artifacts in fMRI time series data. *Neuroimage*, 27(3):624–634.

Dietrich, A. (2004). The cognitive neuroscience of creativity. *Psychonomic Bulletin & Review*, 11(6):1011–1026.

Doğanaksoy, A. and Göloğlu, F. (2006). On Lempel-Ziv Complexity of Sequences. In Gong, G., Helleseth, T., Song, H.-Y., and Yang, K., editors, *Sequences and Their Applications - SETA 2006*, volume 4086 of *Lecture Notes in Computer Science*, pages 180–189. Springer Berlin Heidelberg.

Emery, L., Heaven, T. J., Paxton, J. L., and Braver, T. S. (2008). Age-related changes in neural activity during performance matched working memory manipulation. *Neuroimage*, 42(4):1577–1586.

Fink, A. and Benedek, M. (2014). EEG alpha power and creative ideation. *Neuroscience and Biobehavioral Reviews*, 44:111–123.

Fink, A., Grabner, R. H., Benedek, M., Reishofer, G., Hauswirth, V., Fally, M., Neuper, C., Ebner, F., and Neubauer, A. C. (2009a). The Creative Brain: Investigation of Brain Activity During Creative Problem Solving by Means of EEG and fMRI. *Human Brain Mapping*, 30(3):734–748.

Fink, A., Graif, B., and Neubauer, A. C. (2009b). Brain correlates underlying creative thinking: EEG alpha activity in professional vs. novice dancers. *Neuroimage*, 46(3):854–862.

Friston, K. J., Buechel, C., Fink, G. R., Morris, J., Rolls, E., and Dolan, R. J. (1997). Psychophysiological and Modulatory Interactions in Neuroimaging. *Neuroimage*, 6(3):218–229.

Friston, K. J., Frith, C. D., Frackowiak, R. S. J., and Turner, R. (1995). Characterizing Dynamic Brain Responses with fMRI: a Multivariate Approach. *Neuroimage*, 2(2):166–172.

Frith, C. (2000). The Role of Dorsolateral Prefrontal Cortex in the Selection of Action as Revealed by Functional Imaging. In Monsell, S. and Driver, J., editors, *Control of Cognitive Processes*, Attention and Performance XVIII, pages 549–566. MIT Press, Cambridge, MA.

Halwani, G. F., Loui, P., Rüber, T., and Schlaug, G. (2011). Effects of practice and experience on the arcuate fasciculus: comparing singers, instrumentalists, and non-musicians. *Frontiers in Psychology*, 2:156.

Heuninckx, S., Wenderoth, N., and Swinnen, S. P. (2008). Systems Neuroplasticity in the Aging Brain: Recruiting Additional Neural Resources for Successful Motor Performance in Elderly Persons. *The Journal of Neuroscience*, 28(1):91–99.

Hyde, K. L., Lerch, J., Norton, A., Forgeard, M., Winner, E., Evans, A. C., and Schlaug, G. (2009). Musical Training Shapes Structural Brain Development. *The Journal of Neuroscience*, 29(10):3019–3025.

Jahanshahi, M. and Dirnberger, G. (1999). The left dorsolateral prefrontal cortex and random generation of responses: studies with transcranial magnetic stimulation. *Neuropsychologia*, 37(2):181–190.

Jauk, E., Benedek, M., and Neubauer, A. C. (2012). Tackling creativity at its roots: Evidence for different patterns of EEG alpha activity related to convergent and divergent modes of task processing. *International Journal of Psychophysiology*, 84(2):219–225.

Kleber, B., Veit, R., Birbaumer, N., Gruzelier, J., and Lotze, M. (2010). The Brain of Opera Singers: Experience-Dependent Changes in Functional Activation. *Cerebral Cortex*, 20(5):1144–1152.

Lau, H. C., Rogers, R. D., Ramnani, N., and Passingham, R. E. (2004). Willed action and attention to the selection of action. *Neuroimage*, 21(4):1407–1415.

Limb, C. J. and Braun, A. R. (2008). Neural Substrates of Spontaneous Musical Performance: and fMRI Study of Jazz Improvisation. *PLoS One*, 3(2):e1679.

Mayka, M. A., Corcos, D. M., Leurgans, S. E., and Vaillancourt, D. E. (2006). Three-dimensional locations and boundaries of motor and premotor cortices as defined by functional brain imaging: A meta-analysis. *Neuroimage*, 31(4):1453–1474.

Nathaniel-James, D. A. and Frith, C. D. (2002). The Role of the Dorsolateral Prefrontal Cortex: Evidence from the Effects of Contextual Constraint in a Sentence Completion Task. *Neuroimage*, 16(4):1094–1102.

Oldfield, R. C. (1971). The assessment and analysis of handedness: the Edinburgh inventory. *Neuropsychologia*, 9(1):97–113.

Pantev, C. and Herholz, S. C. (2011). Plasticity of the human auditory cortex related to musical training. *Neuroscience and Biobehavioral Reviews*, 35(10):2140–2154.

Pantev, C., Roberts, L. E., Schulz, M., Engelien, A., and Ross, B. (2001). Timbre-specific enhancement of auditory cortical representations in musicians. *NeuroReport*, 12(1):169–174.

Pressing, J. (1988). Improvisation: methods and models. In Sloboda, J., editor, *Generative Processes in Music: The Psychology of Performance, Improvisation, and Composition*, pages 129–178. Oxford University Press, New York.

Salami, A., Rieckmann, A., Fischer, H., and Bäckman, L. (2014). A multivariate analysis of age-related differences in functional networks supporting conflict resolution. *Neuroimage*, 86:150–163.

Schneider, P., Scherg, M., Dosch, H. G., Specht, H. J., Gutschalk, A., and Rupp, A. (2002). Morphology of Heschl's gyrus reflects enhanced activation in the auditory cortex of musicians. *Nature Neuroscience*, 5(7):688–694.

Smith, S. M. (2002). Fast Robust Automated Brain Extraction. *Human Brain Mapping*, 17(3):143–155.

Steele, C. J., Bailey, J. A., Zatorre, R. J., and Penhune, V. B. (2013). Early Musical Training and White-Matter Plasticity in the Corpus Callosum: Evidence for a Sensitive Period. *The Journal of Neuroscience*, 33(3):1282–1290.

Chapter 6

Study II

Dual Neural Pathways to Creativity

This section refers to the preliminary version of the second article on the research project featuring this thesis. The peer-reviewed article reports, in detail, the findings of Study II - Pinho, A. L., Ullén, F., Castelo-Branco, M., Fransson, P., and de Manzano, Ö. Addressing a Paradox: Dual Strategies for Creative Performance in Introspective and Extrospective Networks. *Cerebral Cortex*, 2015 Jun 17. pii: bhv130. [Epub ahead of print] (`http://dx.doi.org/10.1093/cercor/bhv130`)

6.1 Abstract

Different neuroimaging studies of creative performance have shown seemingly paradoxical results regarding the DLPFC, which has been found to activate, not activate or even deactivate relative to control conditions. On one hand, the DLPFC has been argued to exert active top-down control over generative thought by inhibiting habitual responses; on the other, a deactivation and concomitant decrease in monitoring and focused attention has been suggested to facilitate more spontaneous associations and novel insights. Here, we demonstrate that prefrontal engagement in creative cognition depends dramatically on experimental conditions, i.e. the goal of the task. We instructed professional pianists to perform piano improvisations on a piano keyboard during fMRI and play, either with a certain emotional content (happy/fearful), or on certain keys (tonal/atonal sets). The results showed a deactivation of primarily the right DLPFC, dorsal premotor region and superior parietal cortex during emotional conditions and, conversely, an activation of the same regions during structural conditions. Furthermore, the DLPFC was functionally connected to the default-mode network during emotional conditions and to the premotor network during structural conditions. We discuss these novel findings in terms of explicit vs. implicit processing and invite more refined research and nuanced notion of creative thinking.

Key words: Creativity; dorsolateral prefrontal cortex; fMRI; functional connectivity; improvisation

6.2 Introduction

Neuroimaging studies on creativity typically set out to identify brain regions involved in the generation of novel and meaningful content, e.g. using musical improvisation or verbal fluency tasks as model behaviors. Findings typically include regions such as the DLPFC, IFG, parietal association areas, ACC, PMD and the PreSMA (Bengtsson et al., 2007; Berkowitz and Ansari, 2008; Limb and Braun, 2008; de Manzano and Ullén, 2012a,b; Donnay et al., 2014), which all appear to contribute to creative cognition in one way or another. Specific outcomes, however, tend to vary between studies and what functions these regions serve within the context of creativity per se, is a matter of debate. In the particular case of the DLPFC, some findings and interpretations even appear to be curiously contradictory, as this region has been found to activate, not activate and even deactivate during creative performance

relative to control conditions. On one hand, the DLPFC has been argued to exert active top-down control over generative thought by inhibiting habitual responses, thereby enabling wider associations and more original output (de Manzano and Ullén, 2012b); on the other hand, a deactivation and concomitant decrease in monitoring and focused attention has been suggested to facilitate more spontaneous associations and novel insights (Limb and Braun, 2008). While such puzzling discrepancies have been noted in reviews (Dietrich and Kanso, 2010), no attempts have been made to explain experimentally how this peculiar range of outcomes is possible. Here, we present a theoretical perspective which can account for the above findings and then go on to present novel experimental results, which indicate that creative cognition can involve different neural networks under different sets of circumstances.

First, we review a line of psychological research which supports the idea that creativity (defined as the generation of original and useful ideas) can be achieved through two qualitatively different processes or pathways: the flexibility pathway and the persistence pathway (Nijstad et al., 2010). According to this dual pathway model, creative performance can be a function of either free associative thinking - characterized by fluent and flexible switching between cognitive categories - or more systematic, effortful and focused exploration of fewer categories; or a combination of the two. This model builds on the concept of "blind variation and selective retention", originating from ideas by (Guilford, 1950), formulated by (Campbell, 1960) and later developed by e.g. Simonton (reviewed in (Simonton, 2013)), where selection, elaboration and refinement of novel ideas is preceded by a pseudorandom (re-)combination of cognitive representations. Within the dual pathway model, these two stages of processing are rather viewed as different cognitive strategies, either or both of which can be utilized during creative problem solving.

While being a fairly recent approach in creativity research, the consideration of different strategies in creative performance has been entertained in artistic fields for quite some time. In the context of musical improvisation (which is the model behavior in the later presented experiment) (Clarke, 1988) has e.g. described three possible strategies or principles: *(i)* Current behavior may be part of a hierarchical structure, to some extent worked out in advance, and to some extent constructed in the course of the improvisation; *(ii)* current behavior may be part of an associative chain of actions, each new action derived from the previous sequence by the forward transfer of information; *(iii)* current behavior may be selected from a number of actions contained within the performer's repertoire, the rest of the improvisation consisting of further selections from this same repertoire, with a varying degree of relatedness between selections.

Clarke also asserts that in practice, performance structures are never entirely associative, or perfectly hierarchical, and that the selection of patterns from a repertoire of possibilities will necessarily take place within an overall framework (associative or hierarchical) of some sort. Certainly, there are parallels between these observed principles and the ones described for the dual pathway model. In conclusion, we find both theoretical and empirical support for that creative thinking/creative performance can be approached using different cognitive strategies.

It appears reasonable to assume that these different strategies for cognitive thinking are also implemented differently on the neural level. In other words, we should probably reexamine the view of creativity as having one distinct neural correlate. As an outset, we can make two important observations with reference to the dual pathway model; first, the degree of executive control will differ greatly between the two pathways. The persistence pathway/strategy involves attentional monitoring and explicit organization of behavior, while the flexibility strategy rather draws on implicit, spontaneous recombinations of established representations and routines. Thus, one can expect the former to draw much more on prefrontal and frontoparietal networks involved in action planning and working memory than the latter, for which such explicit processing might even hinder fluent extemporaneous behavior in much the same way as attending to the components of a well-learned skill can impair concurrent performance (Beilock et al., 2002; Gray, 2004; Jackson et al., 2006). Second, both dispositional (between-person) and/or situational (within-person) variables could conceivable influence the cognitive strategy a person tends to adopt for creative problem solving.

Keeping these observations in mind, we recently found that pianists more trained in improvisation display an overall lower activity in frontoparietal association areas during improvisation, as well as greater functional connectivity among prefrontal, premotor, and motor regions of the frontal lobe (Pinho et al., 2014). In other words, skilled improvisational performance may be characterized by both lower demands on executive control and a more efficient interaction within the network of involved brain areas. The overall interpretation of those results, was that even neural mechanisms that require a (creative) flexible online generation of novel and meaningful output, can be automated by training. An additional interpretation, in light of the above theoretical background, would be that more experienced improvisers may tend to, or are more able to rely on the less cognitively demanding flexibility pathway, while novices with e.g. a less extensive storage of musical patterns (Pressing, 1988), may have to resort to more explicit organization of behavior. Hence, expertise could be one between-subjects variable that influences the choice (deliberate or not) of cognitive strategy during creative

performance. Returning to our initial conundrum, this line of reasoning could also be used to explain the apparent inconsistencies in DLPFC activation across studies: E.g. Limb and Brown (Limb and Braun, 2008) have found decreased activity in the DLPFC compared to baseline during improvisation in jazz pianists (who would be well trained in improvisation), while we have consistently found an increased activation of the DLPFC in classical pianists (who presumably improvise less, on average) (Bengtsson et al., 2007; de Manzano and Ullén, 2012a,b).

Consequently, we may formulate a hypothesis about the DLPFC being recruited during creative performance to allow for explicit top-down control and action selection, primarily in situations where knowledge structures and memory processes are not defined or refined enough to guarantee novel and useful output by means of spontaneous free association. However, when skills and knowledge are quite on par with challenge, this system may instead need to be inhibited not to undermine fluent and flexible performance.

Given the above theoretical perspective, we wanted to conduct an experiment to test whether we would be able to "manipulate" activity in the DLPFC during creative performance by creating conditions which would bias cognition towards either the persistence or flexibility pathway. To that end, we asked professional piano players to perform piano improvisations on a piano keyboard during fMRI and either play on certain keys (tonal/atonal sets) or, express a certain emotion (happy/fearful). We hypothesized that the Structural conditions (playing certain keys) would require maintenance of the response set in working memory and integration of sensory information with behavioral intentions and correspondingly more explicit organization of movement sequences, while the Emotional condition would favor a more spontaneous and flexible cognitive strategy, particularly since it has been shown that explicit attention will interfere with selective emotion processing (Schupp et al., 2007). We accordingly hypothesized a greater activity (Structural-Emotional) in primarily the DLPFC, but also in regions which in combination with the DLPFC are involved in spatial working memory processes; more specifically, the PMD and superior parietal cortex, as ordinal/melodic structures are mainly represented and processed as spatial information (Bengtsson et al., 2004; Bengtsson and Ullén, 2006). Conversely, we expected less activity in the very same regions when reversing the contrast. For Emotional-Structural, we hypothesized an increased activity in the dorsomedial and ventromedial prefrontal cortex. These regions process/represent tonality (Janata et al., 2002), and enable associative processes between music, emotions and memories (Janata, 2009). We also expected activity in regions typically linked to emotion, such as insula,

amygdala and orbitofrontal cortex (Barbas, 2007; Hayes et al., 2014).

In addition to these activation patterns, we hypothesized that recruitment of the DLPFC during Structural would manifest in an increased functional connectivity between the PreSMA and DLPFC. We have previously suggested that the premotor network may extend to other regions during creative performance based on task specific demands (de Manzano and Ullén, 2012a). This idea was based on finding a higher functional connectivity between the PreSMA and cerebellum during rhythmic improvisation compared to melodic improvisation. Similar notions have later been forwarded also by Cole and colleagues (2013) (Cole et al., 2013), but instead with a frontoparietal brain network as the central hub. Interestingly, Lau and colleagues (2004) (Lau et al., 2004) found a task-dependent increase in functional connectivity between the PreSMA and the right DLPFC when participants went from attending a movement to attending their intention to move. Here, we expected a similar increase when sensory information needed to be maintained and used as a reference for subsequent improvisation.

Lastly, we wanted to explore the time course of activity in the DLPFC during Structural to investigate the temporal dynamics of response set maintenance during creative performance, i.e. whether activation would be transient or stable throughout performance.

6.3 Materials and Methods

6.3.1 Participants

Thirty-nine right-handed pianists (24 males, 15 females; age [mean $\pm$ SD] = 32 $\pm$ 11 years). All participants were healthy, with no history of psychotropic medication or neurological disease. All pianists were active performers with wide experience in classical or jazz piano playing. Apart from one subject (a self-taught professional jazz piano player), all pianists carried either a university degree in piano performance or were students at the Royal College of Music in Stockholm, the Guildhall School of Music and Drama in London or the Nordic Masters in Jazz programme (Nomazz) - Norwegian University of Science and Technology in Trondheim. The experiments were carried out with the understanding and formal consent of each participant, in accordance with The Code of Ethics of the World Medical Association (Declaration of Helsinki), and ethically approved by the Regional Ethical Review Board in Stockholm (Dnr 2011/637-32 and Dnr 2011/1682-32). Participants were reimbursed with 600 SEK.

6.3.2 Piano keyboard, auditory feedback and musical recordings

The participants improvised on a custom designed MR-compatible fiber optic piano keyboard (LUMItouch, Inc.) of about one octave (12 piano keys, ranging from F to E) during scanning. The keyboard was connected to an optical-electrical converter placed in the control room. The converter was connected to a MIDI-keyboard (Midistart-2 Pro Keys; Miditech) generating a MIDI signal, which was subsequently sent to a MIDI patchbay/processor (MX-8; Digital Music Corp.) producing two different MIDI outputs. The first output was relayed to a sound module (Roland SD-50) which synthesized the piano sound (General MIDI Level 2, European Pf). This device was connected to the audio system of the MR-scanner in order to provide audio feedback (keys F2-E3) to the participants. The second output was relayed to an external sound card which was in turn connected to a PC recording the musical samples with a music production software (Cubase 5; Steinberg).

6.3.3 Visual stimuli

Visual instructions were given at the start of each experimental trial. The display was controlled by a custom made E-Prime script (E-Prime 2.0 Professional; Psychological Software Tools, Inc.). The instructions were presented via MR-compatible OLED display goggles (Nordic Neuro Lab's visual system) mounted on the head coil. There were two main types of instructions (see Figure 3.3), introducing the Structural and Emotional constraints/conditions respectively. The Structural slides displayed a musical staff with a set of allowed notes, corresponding to either the Tonal or Atonal conditions. There were 24 trials of each condition in the experiment. Structural slides were randomized, with no repeats, to each trial for each participant from a pool of 32 slides/condition. The Emotional slides displayed a clip art face expressing the emotions/conditions Happy or Fearful (Figure 3.3). These were also displayed in a randomized order. The reason for using two conditions per constraint was to limit the otherwise confounding effect of a particular emotion or structure on the main contrast of interest (Structural vs. Emotional).

6.3.4 Training session and preparations

Upon arrival at the MR-center, the participants were firstly re-briefed about the purpose of the study and safety procedures, after which they completed a screening form regarding general health and history of disease. Finally, they were given detailed instructions on how to perform the specific experimental conditions in a training session outside the scanner room. During

practice, the participants were seated in a chair in front of a desk. On the desk there was a laptop which would present the visual stimuli and positioned to their right, the piano keyboard (the same as later used in the scanner). Thus, they could get familiarized with the piano keyboard and with the different experimental conditions (see Experimental procedure). The participants were informed that they were allowed to improvise freely and that they should play throughout the duration of the improvisation trial. In addition they were instructed to play only with the right hand and not look at the piano keys/right hand while playing, in order to match conditions inside the scanner. They then completed one training session (similar in procedure, visual stimuli and audio feedback to the real experiment). The training sessions lasted about half an hour. All participants were able to testify that they had understood the instructions before going into the scanner. No major difficulties executing the paradigm were observed by the experimenters nor reported by the participants. The participants were scanned in supine position with the piano keyboard placed on their lap. The right arm was supported by a sponge pad in order to avoid fatigue and to minimize arm movements. Ear plugs and headphones were used to reduce scanner noise and to allow auditory feedback from the piano and verbal communication with the experimenters located in the control room. The volume of the auditory feedback and dioptric settings in the goggles were adjusted for each participant.

6.3.5 Experimental procedure

The experiment was carried out in 6 sessions. Each session consisted of 16 trials, i.e. every condition was presented four times in each session. The trials were composed of four consecutive blocks: Instruction (3.5 s), Performance (15 s), a Distractor task (11 s) and Rest (6 s). Thus, one trial lasted for 35.5 s.

During Instruction, a visual instruction slide was presented (see subsection 6.3.3), introducing conditions with either a Structural (Tonal or Atonal) constraint or Emotional (Happy or Fearful) constraint. In the Structural conditions, the participants were to improvise using only the displayed notes. In Tonal, the notes/pitches were a subset taken from a specific western musical scale (major, minor). The pitches thus naturally suggested a tonality for the improvisation. Pitch sets for Atonal, in contrast, were randomly generated to fulfill two different criteria: *(i)* that the pitches were not all part of the same major or minor scale, and *(ii)* that there would be at least one interval equal to or larger than a minor third (in order to avoid chromatic sequences). Thus, this pitch set did not suggest any particular tonality. The specific pitch sets were unique for each trial of Tonal and Atonal. For the Emotional

conditions, the participants were to express or convey a particular emotion (Happy or Fearful). The order of trials were randomized with the limitations that a certain condition could only appear maximum two times in a row and that no more than three consecutive trials would consist of conditions with the same constraint (Structural or Emotional). There were four trials of conditions in each category (Structural or Emotional) in each session.

The performance phase was interrupted by the distractor task. This task was included to interrupt musical cognitive processes from the previous trial and to minimize planning of the next improvisation. The distractor task was constructed as a visual aesthetical judgment task. The participant would view a fixation cross for 3 s, then watch a computer generated image for 5 s and then, during the final 3 s of the task, provide a rating according to own aesthetical judgment of the image by pressing on the keys on the piano (higher note $->$ higher rating). Results from analyses of this task will be presented in a separate manuscript.

6.3.6 Data acquisition

All behavioral (musical) data were recorded in MIDI format and analysed using a custom-made script in MATLAB 7 (The MathWorks). The fMRI data were acquired using a 3T scanner (GE 3T Discovery MR750) with a 32-channel coil (MR Instruments Inc.) at the MR-center of the Karolinska Hospital. Imaging was performed using a gradient echo pulse, EPI T_2* - weighted sequence with blood oxygenation level-dependent (BOLD) contrasts, using the following parameters: repetition time (TR) = 2.5 s; echo time (TE) = 30 ms; flip angle = 90°; field of view (FOV) = 28.8 cm; slice spacing = 0 mm; voxel size = 3×3×3 mm^3; data acquisition matrix = 96×96, interpolated during reconstruction to 128×128; slice order = interleaved; number of slices = 48. 228 functional images volumes were acquired per session, giving a total of 1368 image volumes per participant. At the beginning of each session, 10 "dummy" image volumes were scanned, but not saved, to allow for T_1 - equilibration effects. Subsequently, a three-dimensional fast spoiled gradient echo T_1 - weighted anatomical image volume covering the whole brain was acquired: voxel size = 1×1×1 mm^3; axial slice orientation; flip angle = 12°; inversion time = 450 ms; FOV = 24 cm.

6.3.7 Analysis of behavioral data

A set of criteria were employed in order to distinguish valid performances: First, trials where the participant started the performance during instruction phase were excluded. Second, trials where the participant had not initiated performance within 6.25 s from the start of

the performance phase were excluded. Third, performances from the Structural conditions were evaluated to make sure instructions were followed to a reasonable degree. Thus, a valid Structural performance would correspond to a trial where the participant used at maximum one wrong pitch. By this filtering, we should have removed performances during which the participant held an incorrect representation of the instructions, but at the same time, allowed for small involuntary slips. Lastly, sessions in which there were no correct trials for at least one condition were excluded in the analysis. Consequently, 4 sessions were used for 2 participants and 5 sessions were used for 6 participants. For the remaining 31 participants, all 6 sessions were used. Another 5 sessions (2% of the data) had to be removed due to various technical problems, e.g. with MIDI-recordings.

The Lz was used in order to characterize the complexity of the musical samples. This index is a measure of the number of unique patterns present in a sequence (Doğanaksoy and Göloğlu, 2006). For the present analyses, the melodic structure of each improvisation was represented as a sequence of numbers. Single notes were represented as integers (0-11) corresponding to their pitch. If the inter-onset interval between two consecutive notes was less than 75 ms, those notes were considered to be part of the same single event (i.e. a musical chord). These musical chords were represented as larger integers that uniquely identified the component pitches of the chord. In addition to the Lz, we also measured the number of keys played (Nkeys) in each condition. These measures were created in order to be able to control for motor output in the imaging analysis.

6.3.8 Image processing and statistical analysis

The MRI data were processed and analysed using the SPM8 software package (Wellcome Department of Imaging Neuroscience, London, UK) in Matlab R2010a. For each participant, all fMRI image volumes were realigned to the first image of the first session and resliced using a 3rd degree B-Spline interpolation scheme (Friston et al., 1995). In order to remove residual variance caused by "susceptibility by movement interaction", the fMRI images were afterwards unwarped with a 4th degree B-Spline interpolation sampling transformation (Andersson et al., 2001). The T_1 - weighted (anatomical) image was then coregistered onto the fMRI unwarped mean image (Ashburner and Friston, 1997). The Brain Extraction Tool was used in order to remove non-brain tissue from the anatomical image (Jenkinson et al., 2005; Smith, 2002). This image was then segmented in order to estimate the deformation field for the normalization of all functional and anatomical images (Ashburner and Friston, 2005).

6.3.8.1 Comparing experimental conditions

The fMRI data were modeled using a GLM and the standard HRF. The model included ten regressors: *(i)* Instruction corresponding to the initial instruction phase before the improvisation; *(ii)* Tonal, *(iii)* Atonal, *(iv)* Happy, *(v)* Fearful, *(vi)* Bad performances, i.e. the performance phases of excluded performances, *(vii)* Distractor presentation corresponding to the initial phase (fixation cross and image presentation) of the aesthetical judgment task, and *(viii)* Distractor rating corresponding to the final phase of the distractor task, where the participant rated the aesthetical quality of the presented image. To control for motor output, two nuisance regressors were included: *(ix)* Nkeys, the mean of the number of keys played per trial, and *(x)* the Lz complexity measure estimated from the musical sample at each trial. These regressors were first centered to the mean and then Lz was orthogonalized with the respect to Nkeys. Thus, also the shared variance between these regressors was captured by the model (in this case, by the first nuisance regressor). Both nuisance regressors were also convolved with the HRF and entered into the model. Rest was not modeled but part of the implicit baseline. The high-pass filter was set to 497 s, i.e. 2 $\times$ the maximum period between an experimental condition and its repeat. The design matrix weighted each preprocessed image according to its overall variability to reduce the impact of movement artifacts (Diedrichsen and Shadmehr, 2005). The contrasts of interest were Structural-Emotional and Emotional-Structural. Contrasts were weighted by the number of included sessions. The resulting contrast images were smoothed using a Gaussian kernel with a FWHM of 10 mm.

A second level group analysis was performed on the contrast images using one sample t tests. A participant grey matter mask was created and used as an explicit mask. Regions where significant effects were found were manually labeled using the WFU PickAtlas - Human Atlas (Tzourio-Mazoyer et al., 2002; Maldjian et al., 2004), the SPM Anatomy Toolbox v1.8 (Eickhoff et al., 2005, 2006, 2007) and the HMAT (Mayka et al., 2006). Results are shown if they survive multiple comparisons correction using either a voxel-level family-wise error rate at $p = 0.05$ and extent threshold of 3 voxels, or cluster-level family-wise error rate based on voxels surviving $p = 0.001$ uncorrected.

6.3.8.2 Connectivity analysis

A PPI analysis (Friston et al., 1997) was performed to analyze differences in effective functional connectivity between the DLPFC and other brain regions when switching between Structural and Emotional. Two seed regions, representing the DLPFC in the right and left hemisphere

were created based on an additional GLM contrast Structural-Rest at a FWE adjusted threshold of p $\leq$ 0.05. The BOLD time series of the each seed region was deconvolved from the HRF in order to obtain the underlying neural time course of activity. The PPI was then estimated by multiplying the neural response with a block regressor representing the conditions Structural and Emotional. Afterwards, a GLM analysis was performed with all three regressors in the model: the PPI, the neural response and the experimental conditions. The high-pass filter was set to 497 s. Each preprocessed image was weighted with its overall variability (more variable images receiving a lower weighting) to reduce the impact of movement artifacts (Diedrichsen and Shadmehr, 2005). The resulting contrast images were smoothed with an isotropic Gaussian kernel of 10 mm FWHM. Lastly, a second-level analysis was performed using a one sample t-test on the contrast images from the first-level analysis. The same gray matter mask was used here as in the previous analysis.

6.3.8.3 Time series analysis

For exploratory reasons, we also plotted the BOLD time series for the DLPFC in both hemispheres. More specifically, we plotted the percent signal change of the average BOLD - response across the performance phase, for Structural and Emotional separately, first within and then across participants. Since the onset of actual performance would vary slightly across trials, the time courses of activation were aligned, before averaging, according to the onset of behavioral output for each trial. The same seed regions were used for the DLPFC here as in the previous PPI analysis. After the first analysis comparing brain activity between Structural and Emotional we decided to investigate the BOLD time series also for seed regions in the bilateral parietal cortex and bilateral PMD. Seed regions for the bilateral parietal cortex and PMD were defined as 10 mm spheres centered on the coordinates for the highest peak values in the GLM contrast Structural-Emotional.

6.4 Results

6.4.1 Analysis of behavioral data

The measures of motor output (Nkeys) and complexity (Lz) were compared between conditions. The mean Nkeys for Structural and Emotional was 30.17 $\pm$ 1.42 and 36.90 $\pm$ 1.77, respectively. A two sample t test showed that Nkeys was significantly higher during Emotional than Structural [t (2,76) = 2.96, p = .004]. The mean Lz was 6.54 $\pm$ 0.14 for Structural and

8.52 $\pm$ 0.33 for Emotional. A two sample t test showed that Lz was significantly higher during Emotional than Structural [t (2,76) = 5.46, p = .000]. In addition, Nkeys was correlated with Lz, r = .61 ($p < .001$). Because of these observed differences, both Nkeys and Lz were introduced as nuisance covariates in the analysis of the imaging data.

6.4.2 Functional MRI data

6.4.2.1 Comparing experimental conditions

Table 6.1 and Figure 6.1-A illustrate the results of the contrast Structural-Emotional. In line with the main hypothesis, the Structural conditions induced a comparably greater activation of

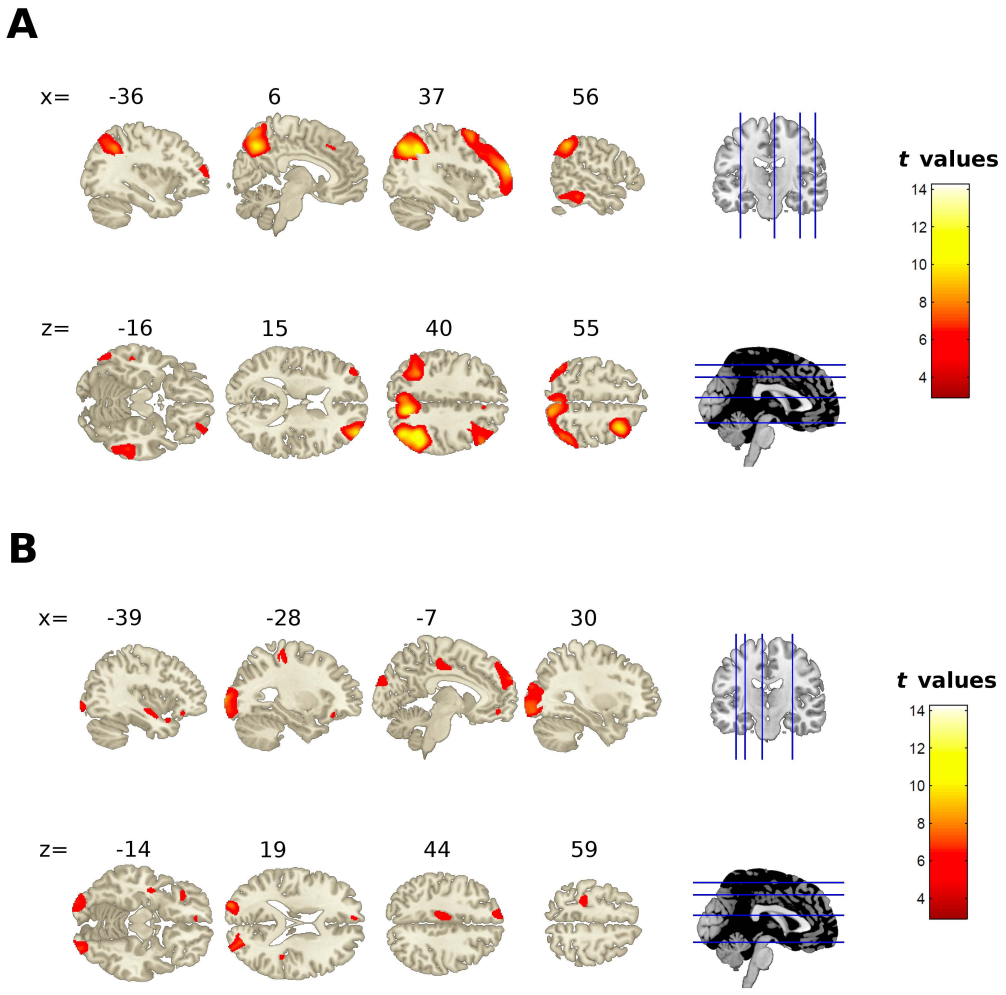

Figure 6.1: **(A)** Brain regions showing higher activity during Structural than Emotional conditions. Activations are significant at a cluster level FWE adjusted threshold of $p < 0.05$. **(B)** Brain regions showing higher activity Emotional than Structural than Emotional conditions. Activations are significant at a cluster level FWE adjusted threshold of $p < 0.05$.

the right DLPFC, PMD and bilateral parietal lobes extending into the associative visual cortex of the occipital lobe. In addition, there was also greater activation of inferior temporal gyri

Table 6.1: Imaging results for the contrast Structural-Emotional.

		Coordinates[3]			Voxel Level[4]		Cluster level[5]	
Region[1]	Side[2]	x	y	z	t	p	k_E	p
MFG	Right	38	58	15	9.65	0.000	16346	0.000
MFG/DLPFC	Right	46	27	37	7.94	0.000		
MFG/PMD	Right	30	11	55	9.70	0.000		
SOrbG	Right	28	58	-6	7.12	0.000		
SOrbG	Right	16	68	-11	5.12	0.033		
MFG	Left	-39	54	15	5.64	0.008	–	–
MFG	Left	-34	60	9	5.47	0.014		
SMedG/DMPFC	Right	6	29	40	5.15	0.031	–	–
CCrusI	Left	-32	-66	-35	5.13	0.033	3772	0.002
IOG	Left	-57	-67	-17	5.57	0.010		
ITG	Left	-51	-31	-18	5.54	0.011		
ITG	Right	56	-36	-20	6.80	0.000	3677	0.007
AG	Right	39	-69	40	10.06	0.000	29805	0.000
IPL	Right	42	-51	40	11.99	0.000		
IPL	Left	-36	-54	40	7.96	0.000		
IPL	Left	-44	-57	48	7.83	0.000		
SPL/Precuneus	Right	10	-66	42	10.92	0.000		
SPL/Precuneus	Right	12	-72	58	9.11	0.000		
SPL/Precuneus	Left	-2	-64	58	7.35	0.000		

[1] Lines separate different clusters

[2] Left/right hemisphere

[3] MNI coordinates

[4] Voxel-level FWE-corrected statistics

[5] Cluster-level FWE-corrected statistics

AG = angular gyrus, CCrusI = cerebellum crus I, DLPFC = dorsolateral prefrontal cortex, DMPFC = dorsomedial prefrontal cortex, IOG = inferior occipital gyrus, IPL = inferior parietal lobe, ITG = inferior temporal gyrus, MFG = middle frontal gyrus, PMD = dorsal premotor cortex, SMedG= superior medial gyrus, SOrbG = superior orbital gyrus, SPL = superior parietal lobe

Table 6.2: Imaging results for the contrast Emotional-Structural.

		Coordinates[3]			Voxel Level[4]		Cluster level[5]	
Region[1]	Side[2]	x	y	z	t	p	k_E	p
MedOrbG	Left	-8	50	-12	5.57	0.010	4727	0.001
SFG	Left	-14	42	51	6.25	0.002		
SMedG/DMPFC	Left	-9	63	30	7.12	0.000		
IFG (*Orbitalis*)	Left	-33	33	-14	5.68	0.008	9842	0.000
IFG (*Triangularis*)	Left	-48	30	-2	5.13	0.033		
Insula	Left	-40	-10	-11	5.72	0.007		
Insula	Left	-39	-1	-17	5.19	0.028		
STG	Left	-42	14	-21	5.92	0.004		
PreCG	Right	54	-9	54	4.99	0.047	–	–
RO	Right	40	-31	18	5.24	0.024	5394	0.000
STG	Right	44	-15	-5	5.48	0.013		
STG	Right	69	-28	15	4.99	0.047		
MCC	Left	-10	-21	43	6.51	0.001	2609	0.008
PostCG	Left	-28	-30	54	6.27	0.002	3773	0.002
CalG	Right	21	-78	7	6.01	0.007	17819	0.000
CalG	Right	18	-82	4	5.88	0.008		
CalG	Right	18	-85	1	5.76	0.011		
CalG	Right	18	-79	10	5.47	0.014		
FFG	Right	26	-61	-12	4.99	0.047		
IOG	Right	27	-93	-2	7.57	0.000		
IOG	Right	30	-90	-9	7.41	0.000		
MOG	Left	-28	-100	4	8.44	0.000		
MOG	Left	-24	-91	15	7.44	0.000		
MOG	Left	-33	-97	-8	7.23	0.000		
MOG	Left	-36	-96	-3	7.21	0.000		
MOG	Right	36	-91	7	6.57	0.001		
SOG	Left	-21	-96	24	8.22	0.000		
SOG	Right	24	-85	22	7.14	0.000		
SOG	Right	20	-87	28	6.91	0.000		

[1] Lines separate different clusters

[2] Left/right hemisphere

[3] MNI coordinates

[4] Voxel-level FWE-corrected statistics

[5] Cluster-level FWE-corrected statistics

CalG = calcarine gyrus, DMPFC = dorsomedial prefrontal cortex, FFG = fusiform gyrus, IFG = inferior frontal gyrus, IOG = inferior occipital gyrus, MCC = middle cingulate cortex, MedOrdbG = medial orbital gyrus, MOG = middle occipital gyrus, PreCG = precentral gyrus, PostCG = postcentral gyrus, RO = rolandic operculum, SFG = superor frontal gyrus, SMedG= superior medial gyrus, SOG = superior occipital gyrus, STG = superior temporal gyrus

(ITG), right superior orbital gyrus, right superior medial gyrus (SMedG), left inferior occipital gyrus and left cerebellum. Also in line with predictions, the reverse contrast (Emotional-Structural; Table 6.2, Figure 6.1-B) revealed comparably greater activation of the left DMPFC, IFG, Insula (extending to Amygdala) and bilateral STG. There was also higher activity in the left middle cingulate cortex and primary sensorimotor cortex.

6.4.2.2 Connectivity analysis

The whole-brain PPI-analysis showed that the left and right DLPFC (the seed regions) had constraint-dependent patterns of connectivity to other brain regions. During Structural conditions, there was a greater effective functional connectivity between the right DLPFC and the bilateral PMD and STG as well as the left *ventral premotor cortex* (PMV), SMA, primary sensorimotor cortices, left parietal lobe and right cerebellum (Figure 6.2, Table 6.3).

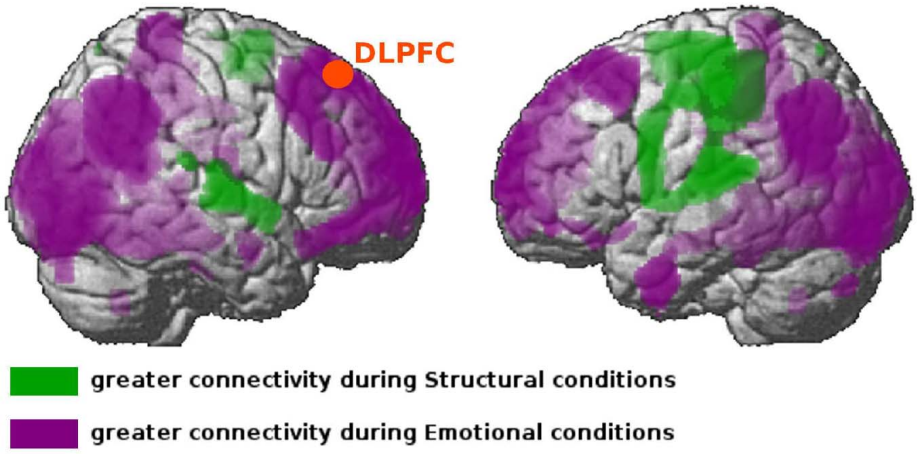

Figure 6.2: Rendered image of increased effective functional connectivity between right DLPFC and other regions during Structural (green) and Emotional (lilac).

During Emotional there was instead an increase in correlation between the right DLPFC and several regions of the default mode network (Buckner et al., 2008), including frontopolar, medial prefrontal and medial parietal regions (Figure 6.2; Table 6.4). For Emotional-Structural there was also greater functional connectivity between left DLPFC which largely resembled the pattern for the right DLPFC (Table 6.5). There were no significant results for the left DLPFC in the reverse contrast.

Table 6.3: Imaging results from the PPI-analysis during Structural compared with Emotional, based on the right DLPFC as seed region.

		Coordinates[3]			Voxel Level[4]		Cluster level[5]	
Region[1]	Side[2]	x	y	z	t	p	k_E	p
IPL	Left	-40	-36	39	6.77	0.000	30091	0.000
PostCG	Left	-57	-27	51	7.08	0.000		
PostCG	Left	-48	-28	40	6.40	0.001		
PostCG	Left	-36	-27	51	6.09	0.003		
PostCG	Left	-52	-12	43	5.99	0.004		
PostCG	Left	-46	-40	60	5.60	0.011		
PreCG	Left	-34	-18	60	6.52	0.001		
PreCG/PMV	Left	-50	3	16	6.22	0.002		
PreCG/PMV	Left	-58	5	30	6.16	0.002		
SFG/PMD	Left	-22	-13	58	6.61	0.001		
SFG/PMD	Right	26	-7	57	5.40	0.019		
SFG/SMA	Left	-12	-9	61	6.82	0.000		
SMG	Left	-54	-21	18	6.88	0.000		
SPL	Left	-16	-69	64	5.45	0.017		
STG	Left	-51	-19	10	6.89	0.000		
STG	Left	-45	-30	13	6.35	0.001		
STG	Right	54	-18	0	6.41	0.001	6528	0.000
STG	Right	50	-1	-6	5.55	0.013		
STG	Right	69	-31	18	5.42	0.018		
Cerebellum	Right	–	–	–	–	–	1665	0.017

[1] Lines separate different clusters

[2] Left/right hemisphere

[3] MNI coordinates

[4] Voxel-level FWE-corrected statistics

[5] Cluster-level FWE-corrected statistics

IPL = inferior parietal lobe, PMD = dorsal premotor cortex, PMV = ventral premotor cortex, PostCG = postcentral gyrus, PreCG = precentral gyrus, SFG = superior frontal gyrus, SMA = supplementary motor area, SMG = supramarginal gyrus, SPL = superior parietal lobe, STG = superior temporal gyrus

Table 6.4: Imaging results from the PPI-analysis during Emotional compared with Structural, based on the right DLPFC as seed region.

		Coordinates[2]			Voxel Level[3]		Cluster level[4]	
Region	Side[1]	x	y	z	t	p	k_E	p
IPL	Left	-54	-55	37	6.98	0.000	197981	0.000
AG	Left	-50	-67	27	7.28	0.000		
SFG	Left	-18	68	18	7.45	0.000		
ACC	Left	-2	39	22	7.05	0.000		
ACC/DMPFC	Right	5	39	24	7.32	0.000		
SPL/Precuneus	Right	6	-49	52	7.55	0.000		
SMG	Right	11	69	6	7.30	0.000		
SPL/Precuneus	Right	14	-63	30	7.13	0.000		
MCC	Right	15	-36	45	6.94	0.000		
MCC	Right	17	-48	33	7.20	0.000		
Precuneus	Right	18	-54	25	6.96	0.000		
SFG	Right	20	57	36	6.94	0.000		
SFG	Right	24	68	12	7.53	0.000		
IPL	Right	51	-55	44	7.01	0.000		

[1] Left/right hemisphere

[2] MNI coordinates

[3] Voxel-level FWE-corrected statistics

[4] Cluster-level FWE-corrected statistics

ACC = anterior cingulate cortex, AG = angular gyrus, DMPFC = dorsomedial prefrontal cortex IPL = inferior parietal lobe, MCC = middle cingulate cortex, PostCG = postcentral gyrus, PreCG = precentral gyrus, SFG = superior frontal gyrus, SMG = supramarginal gyrus, SPL = superior parietal lobe, STG = superior temporal gyrus

Table 6.5: Imaging results from the PPI-analysis during Emotional compared with Structural, based on the left DLPFC as seed region.

		Coordinates[3]			Voxel Level[4]		Cluster level[5]	
Region[1]	Side[2]	x	y	z	t	p	k_E	p
SMedG	Left	-6	30	61	5.81	0.006	113620	0.000
MedOrbG	Left	-5	53	-11	5.09	0.043		
SMedG	Left	-3	41	55	5.48	0.015		
SMedG	Right	5	41	55	5.20	0.032		
SMedG	Right	5	45	52	5.06	0.046		
IFG (*Orbitalis*)	Left	-35	35	-11	5.20	0.032	–	–
IFG (*Triangularis*)	Right	56	26	22	6.70	0.001	2846	0.009
MTG	Right	56	-6	-23	5.05	0.048	–	–
CCrusII	Left	-29	-82	-39	5.80	0.006	476540	0.000
CCrusI	Left	-29	-90	-32	5.35	0.022		
CCrusII	Left	-17	-78	-41	5.25	0.028		
CCrusII	Left	-14	-87	-30	5.37	0.021		
CCrusII	Right	15	-82	-32	5.32	0.024		
CCrusII	Right	36	-78	-44	5.27	0.027		

[1] Lines separate different clusters

[2] Left/right hemisphere

[3] MNI coordinates

[4] Voxel-level FWE-corrected statistics

[5] Cluster-level FWE-corrected statistics

CCrusI = cerebellum crus I, CCrusII = cerebellum crus II, IFG = inferior frontal gyrus, DMPFC = dorsomedial prefrontal cortex, MedOrbG = medial orbital gyrus, MTG = middle temporal gyrus, SMedG= superior medial gyrus

6.4.2.3 Time Series Analysis

Figure 6.3 illustrates the time-activity curve for the left and right DLPFC during Structural and Emotional conditions. The right DLPFC showed a constant intensity above baseline during Structural and a decreasing deactivation over time during Emotional conditions. The left DLPFC was activated with no differences in intensity across time for both Structural and Emotional conditions. The activity was higher than baseline during Structural and around baseline during Emotional conditions. Given the similar patterns of activation between constraints for the DLPFC, PMD and parietal regions, we also analyzed activity across time for the PMD and parietal regions. The parietal regions bilaterally and the right PMD showed similar time-dependent activity profiles to the right DLPFC (Figure 6.4 and 6.5). The left PMD displayed a slight increase of activation over time during Structural conditions and a decrease of deactivation during Emotional, which by the end of performance had crossed baseline (Figure 6.5).

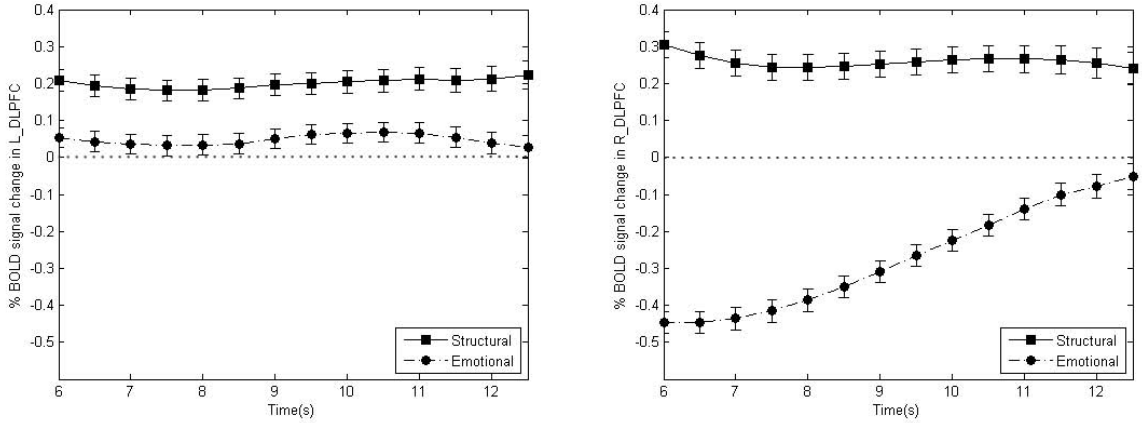

Figure 6.3: Brain activity (% BOLD signal change) in the DLPFC during improvisation. The plots show the progress of brain activity during Structural conditions (solid line) and Emotional conditions (dashed line) in the left DLPFC (left) and right DLPFC (right). The regions were selected based on significant clusters in the contrast Structural-Rest at FWE adjusted p - value threshold < 0.05. The origin is placed at Time = 6 s because of the hemodynamic lag. For illustration purposes we also removed the last four time points where data was more variable due to that participants sometimes cut improvisations short.

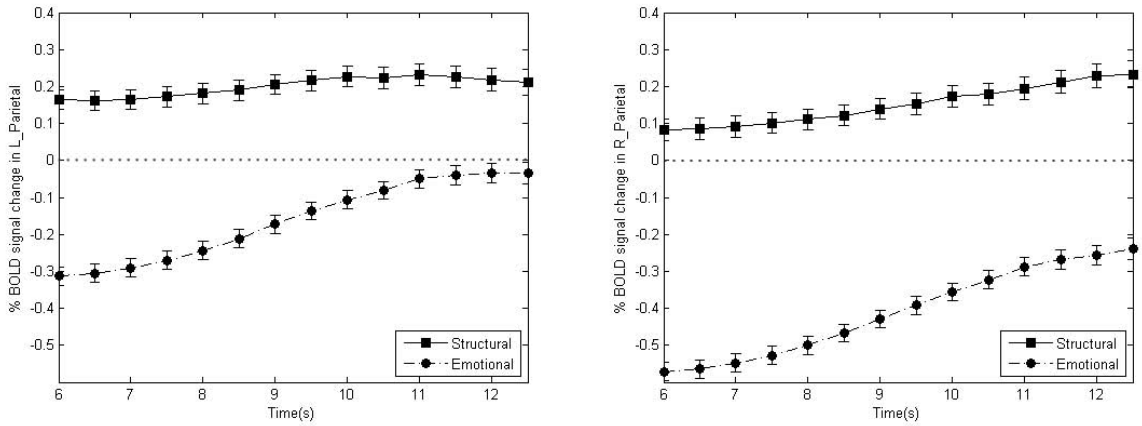

Figure 6.4: Brain activity (% BOLD signal change) in the parietal cortex during improvisation. The plots show the progress of brain activity during Structural conditions (solid line) and Emotional conditions (dashed line) in the left parietal cortex (left) and right parietal cortex (right). The regions were selected based on significant clusters in the contrast Structural-Rest at FWE adjusted p - value threshold < 0.05. The origin is placed at Time = 6 s because of the hemodynamic lag. For illustration purposes we also removed the last four time points where data was more variable due to that participants sometimes cut improvisations short.

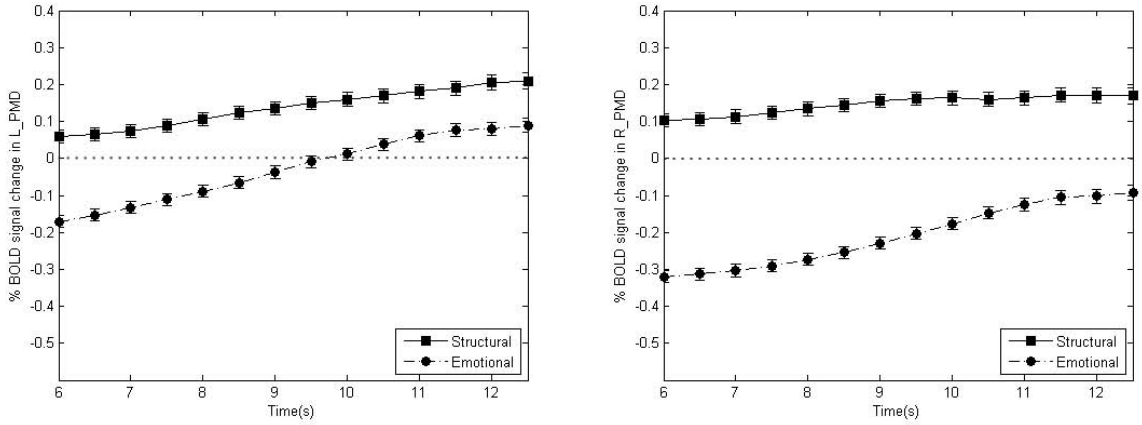

Figure 6.5: Brain activity (% BOLD signal change) in the PMD during improvisation. The plots show the progress of brain activity during Structural conditions (solid line) and Emotional conditions (dashed line) in the left PMD (left) and right PMD (right). The regions were selected based on significant clusters in the contrast Structural-Rest at FWE adjusted p - value threshold < 0.05. The origin is placed at Time = 6 s because of the hemodynamic lag. For illustration purposes we also removed the last four time points where data was more variable due to that participants sometimes cut improvisations short.

6.5 Discussion

In the present study, we sought to solve a paradox in current creativity research, i.e. how both an activation and deactivation of the prefrontal cortex can facilitate creative performance. Based our results, we argue that the level of prefrontal contribution to creative thinking critically depends on the required level of explicit control during extemporization.

During the Structural conditions, when improvisation was constrained by a certain response set, there was an increase of activity in primarily the PMD and frontoparietal networks with a concomitant increase in functional connectivity between the DLPFC and the PMD, *supplementary motor area* SMA, primary sensorimotor cortex and cerebellum. In other words, whenever external sensory information needed to be attended, maintained and integrated with creative processes, the visuospatial working memory system would activate and connect to the motor system. Conversely, when improvisation was constrained to express a certain emotion, activity in the DLPFC, PMD and parietal regions would decrease, even below baseline, and correlate with default mode regions; increased activity was instead found primarily in the orbital and dorsomedial prefrontal cortices, insula, IFG, and the primary auditory and motor cortices. Thus, we suggest that during Emotional, particularly in the beginning of the improvisation, explicit information processing was inhibited in order not to interfere with associative memory retrieval, sequence processing/fluency of performance and the representation of affective information. A certain disinhibition of such generative processes is also conceivable.

Given the nature of the task constraints (flexibility vs. persistence), it was not surprising to find that more keys were played during Emotional than Structural. In addition, given that the response set for Emotional was twice the size of that during Structural and that melodic structure is a key feature mediating emotional expression in music (Gabrielsson and Lindström, 2001), it was equally unsurprising to find greater melodic complexity during Emotional than Structural.

We did control for motor output in the imaging analysis, but it is also important to note the direction of effects. The Emotional conditions with higher motor output brought about a deactivation of the DLPFC and other working memory regions. If anything, the behavioral data thus support the interpretation that activity in those regions was reduced in order to facilitate and/or not interfere with behavioral fluency in more structurally complex improvisations.

6.5.1 Dual pathways to creativity

In conclusion, the results appear to largely support to our initial hypotheses derived from the dual pathway model where we postulated that creative performance can be a function of either systematic effortful cognition, or more spontaneous free associative thinking. We would not argue however, that processing along these pathways are necessarily mutually exclusive. Instead we imagine creative thinking to range on a continuum between extremes of implicit and explicit cognition; and that along this dimension there is a point beyond which, prefrontal regions are recruited to ensure novel and original content, i.e. when tasks introduce prerequisites that go beyond existing knowledge, skills and abilities. Here during Structural, cognition was pushed beyond that point when new information had to be perceived and used as a reference during subsequent improvisation.

Expertise is also likely an important factor. In one of our previous studies, we compared pseudo-random free generation to musical improvisation in order to elucidate music-specific creative processes (de Manzano and Ullén, 2012b). Professional classical pianists performed improvisation of melodies and pseudo-random key presses on a piano keyboard during fMRI. Improvisation did not induce more activity than pseudo-random generation in any region. Pseudo-random generation however, was accompanied by higher activity than improvisation in several frontal and parietal regions. We suggested then that musical expertise versus novel task performance could be one of the main reasons for the somewhat unexpected outcome. It is conceivable that we to some extent see a similar effect here when comparing our two types of improvisation constraints.

Extending on that notion and as mentioned in the introduction, we recently presented a study based on the same sample and improvisational tasks, where we found that participants with more experience in improvisation display less activity in the frontoparietal working memory network and greater functional connectivity between prefrontal, premotor and motor regions during improvisation (Pinho et al., 2014). In other words, results were just about identical to the outcomes in the present study. Thus, it appears likely that similar principles with regard to implicit and explicit processing applies both within-participants, as shown here for different task prerequisites, and between participants for different levels of expertise. Reexamining the previous findings in detail, we can even predict how much improvisation training was required for a participant's DLPFC activity to go from above to below baseline in each task. It appears that the Emotional tasks could be performed without top down control from the start, while the Structural tasks required considerable practice - around 5000 hours of improvisation

training (controlling for classical training) - to make frontoparietal functionality redundant. We suggest, that once this level of task specific expertise has been reached, a deactivation of the DLPFC and/or a disinhibition of generative processes during continuous creative performance becomes a viable and cognitively efficient approach, because long-term memory structures and retrieval strategies enable spreading activation and free association to yield spontaneous yet relevant responses at high fluency. If less experienced improvisers tried something similar, they would presumably produce less adequate responses that are either too simplistic or bizarre. Only with deliberate top down control supported by prefrontal functionality might they reach similar aesthetic criteria. In support of that argument, our less expert performers, who on average displayed higher activity in frontoparietal working memory systems, did not produce less complex improvisations. Thus, there might even in neural terms be dual pathways to creativity.

In light of the present findings and the above discussion, we return to the initial research question and the improvisation studies between which results differ with regard to prefrontal involvement and try to explain the apparent inconsistencies. As it turns out, the explanation might be a fairly simple. All of the studies that show a deactivation of the DLPFC have used jazz pianists making jazz improvisations, and all the studies that show an activation have used classical pianists. Thus, the apparent discrepancies could possibly be accounted by differences in expertise/improvisational skills between two experimental groups, in combination with the added effects of differences in task complexity between experimental paradigms. Firstly, improvisation is a much more central feature of jazz than classical music and jazz pianists should on average be more accustomed to, and well-trained in performing spontaneous improvisations than classical pianists. Secondly, genre and style of improvisation could play a role. Returning to Clarke (1988) (Clarke, 1988): "(...) free jazz is principally characterized by associative structure, since it eschews the constraints of a pre-planned structure, and attempts to avoid the use of recognizable 'riffs'. More traditional improvisation tends towards the hierarchical principle, in its adherence to a fairly strict harmonic outline". Thus, when we ask jazz and classical musicians to perform spontaneous improvisations, they might tend towards different styles of improvisation and different pathways of creative thinking. Thirdly, one could also point to specific methodological differences, where jazz and classical piano players have been exposed to different levels of complexity during experimentation. As an example, free improvisation on a well-learned scale or chord structure, as in Limb et. al. (2008) (Limb and Braun, 2008), is conceivably a less intricate task than ornamentation of

a melody presented a prima vista, as in Bengtsson et. al (2007) (Bengtsson et al., 2007). Moreover, in the studies on classical pianists that find DLPFC activity, free improvisation conditions were generally intermingled with conditions that loaded on executive functions and working memory, such as pseudorandom generation or generating melodies and/or rhythms based on visual templates. Since switching creative strategy could also be related to a certain cost, participants in those experiments might have been even more inclined to maintain explicit control across all conditions. Consequently, it does not seem paradoxical that classical pianists have been shown to activate a network including the PreSMA and DLPFC, typically associated with explicit processing of novel motor sequences, while jazz pianists have tended to rely on regions for implicit routine and automated behavior, showing a more caudal distribution of activity in the SMA and PMD in conjunction with activity in limbic regions and the basal ganglia (Doyon and Benali, 2005). Overall, it would seem that the prerequisites for prefrontal involvement in learning and performance of creative tasks is similar to other volitional behaviors (Halsband and Lange, 2006).

6.5.2 Conclusion

We demonstrate that creative performance can be associated with both an activation and deactivation of the DLPFC (and other working memory regions) depending on task prerequisites. The findings clearly indicate that creativity is the result of a dynamic interplay between several brain regions, networks and systems, and that the patterns of brain activity during creative problem solving depend strongly on the employed problem solving strategies. Thus, creative thinking is far more multifaceted in its nature and neural underpinnings than what has been commonly assumed. We suggest that a theoretical framework, which builds on the idea that some of the observed dynamics of creative thinking can be discussed in terms of an interaction between explicit and implicit cognition may be fruitful, and propose a number of factors which may influence processing in these two pathways.

6.6 Acknowledgements

We thank Jonathan Berrebi for technical support, as well as Diana Muessgens and László Harmat for assistance during experiments. This research was supported by Foundation for Science and Technology (FCT, Portugal; SFRH/BD/33895/2009), the Swedish Research Council (521-2010-3195) and the Sven and Dagmar Salén Foundation.

References

Andersson, J. L. R., Hutton, C., Ashburner, J., Turner, R., and Friston, K. (2001). Modeling Geometric Deformations in EPI Time Series. *Neuroimage*, 13(5):903–919.

Ashburner, J. and Friston, K. (1997). Multimodal Image Coregistration and Partitioning - A Unified Framework. *Neuroimage*, 6(3):209–217.

Ashburner, J. and Friston, K. J. (2005). Unified segmentation. *Neuroimage*, 26(3):839–851.

Barbas, H. (2007). Specialized Elements of Orbitofrontal Cortex in Primates. *Annals of the New York Academy of Sciences*, 1121:10–32.

Beilock, S. L., Carr, T. H., MacMahon, C., and Starkes, J. L. (2002). When Paying Attention Becomes Counterproductive: Impact of Divided Versus Skill-Focused Attention on Novice and Experienced Performance of Sensorimotor Skills. *Journal of Experimental Psychology: Applied*, 8(1):6–16.

Bengtsson, S. L., Csíkszentmihályi, M., and Ullén, F. (2007). Cortical Regions Involved in the Generation of Musical Structures during Improvisation in Pianists. *Journal of Cognitive Neuroscience*, 19(5):830–842.

Bengtsson, S. L., Ehrsson, H. H., Forssberg, H., and Ullén, F. (2004). Dissociating brain regions controlling the temporal and ordinal structure of learned movement sequences. *European Journal of Neuroscience*, 19(9):2591–2602.

Bengtsson, S. L. and Ullén, F. (2006). Dissociation between melodic and rhythmic processing during piano performance from musical scores. *Neuroimage*, 30(1):272–284.

Berkowitz, A. L. and Ansari, D. (2008). Generation of novel motor sequences: The neural correlates of musical improvisation. *Neuroimage*, 41(2):535–543.

Buckner, R. L., Andrews-Hanna, J. R., and Schacter, D. L. (2008). The Brain's Default Network: Anatomy, Function, and Relevance to Disease. *Annals of the New York Academy of Sciences*, 1124:1–38.

Campbell, D. T. (1960). Blind variation and selective retention in creative thought as in other knowledge processes. *Psychological Review*, 67(6):380–400.

Clarke, E. F. (1988). Generative principles in music performance. In Sloboda, J., editor, *Generative Processes in Music*, pages 1–26. Clarendon Press, Oxford.

Cole, M. W., Reynolds, J. R., Power, J. D., Repovs, G., Anticevic, A., and Braver, T. S. (2013). Multi-task connectivity reveals flexible hubs for adaptive task control. *Nature Neuroscience*, 16(9):1348–1355.

de Manzano, Ö. and Ullén, F. (2012a). Activation and connectivity patterns of the presupplementary and dorsal premotor areas during free improvisation of melodies and rhythms. *Neuroimage*, 63(1):272–280.

de Manzano, Ö. and Ullén, F. (2012b). Goal-independent mechanisms for free response generation: Creative and pseudo-random performance share neural substrates. *Neuroimage*, 59(1):772–780.

Diedrichsen, J. and Shadmehr, R. (2005). Detecting and adjusting for artifacts in fMRI time series data. *Neuroimage*, 27(3):624–634.

Dietrich, A. and Kanso, R. (2010). A Review of EEG, ERP, and Neuroimaging Studies of Creativity and Insight. *Psychological Bulletin*, 136(5):822–848.

Donnay, G. F., Rankin, S. K., Lopez-Gonzalez, M., Jiradejvong, P., and Limb, C. J. (2014). Neural Substrates of Interactive Musical Improvisation: an fMRI Study of 'Trading Fours' in Jazz. *PLoS One*, 9(2):e88665.

Doğanaksoy, A. and Göloğlu, F. (2006). On Lempel-Ziv Complexity of Sequences. In Gong, G., Helleseth, T., Song, H.-Y., and Yang, K., editors, *Sequences and Their Applications - SETA 2006*, volume 4086 of *Lecture Notes in Computer Science*, pages 180–189. Springer Berlin Heidelberg.

Doyon, J. and Benali, H. (2005). Reorganization and plasticity in the adult brain during learning of motor skills. *Current Opinion in Neurobiology*, 15(2):161–167.

Eickhoff, S. B., Heim, S., and Amunts, K. (2006). Testing anatomically specified hypotheses in functional imaging using cytoarchitectonic maps. *Neuroimage*, 32(2):570–582. Technical Note.

Eickhoff, S. B., Paus, T., Caspers, S., Grosbras, M.-H., Evans, A. C., Zilles, K., and Amunts, K. (2007). Assignment of functional activations to probabilistic cytoarchitectonic areas revisited. *Neuroimage*, 36(3):511–521.

Eickhoff, S. B., Stephan, K. E., Mohlberg, H., Grefkes, C., Fink, G. R., Amunts, K., and Zilles, K. (2005). A new SPM toolbox for combining probabilistic cytoarchitectonic maps and functional imaging data. *Neuroimage*, 25(4):1325–1335. Technical Note.

Friston, K. J., Buechel, C., Fink, G. R., Morris, J., Rolls, E., and Dolan, R. J. (1997). Psychophysiological and Modulatory Interactions in Neuroimaging. *Neuroimage*, 6(3):218–229.

Friston, K. J., Frith, C. D., Frackowiak, R. S. J., and Turner, R. (1995). Characterizing Dynamic Brain Responses with fMRI: a Multivariate Approach. *Neuroimage*, 2(2):166–172.

Gabrielsson, A. and Lindström, E. (2001). The influence of musical structure on emotional expression. In Juslin, P. N. and Sloboda, J. A., editors, *Music and emotion - theory and research*, pages 223–248. Oxford University Press, Oxford, UK.

Gray, R. (2004). Attending to the Execution of a Complex Sensorimotor Skill: Expertise Differences, Choking, and Slumps. *Journal of Experimental Psychology: Applied*, 10(1):42–54.

Guilford, J. P. (1950). Creativity. *American Psychologist*, 5(9):444–454.

Halsband, U. and Lange, R. K. (2006). Motor learning in man: A review of functional and clinical studies. *Journal of Physiology - Paris*, 99(4-6):414–424.

Hayes, D. J., Duncan, N. W., Xu, J., and Northoff, G. (2014). A comparison of neural responses to appetitive and aversive stimuli in humans and other mammals. *Neuroscience and Biobehavioral Reviews*, 45:350–368.

Jackson, R. C., Ashford, K., and Norsworthy, G. (2006). Attentional focus, dispositional reinvestment, and skilled motor performance under pressure. *Journal of Sport and Exercise Psychology*, 28(1):49–68.

Janata, P. (2009). The Neural Architecture of Music-Evoked Autobiographical Memories. *Cerebral Cortex*, 19(11):2579–2594.

Janata, P., Birk, J. L., Horn, J. D. V., Leman, M., Tillmann, B., and Bharucha, J. J. (2002). The Cortical Topography of Tonal Structures Underlying Western Music. *Science*, 298(5601):2167–2170.

Jenkinson, M., Pechaud, M., and Smith, S. (2005). BET2: MR-based estimation of brain, skull and scalp surfaces. In *Eleventh Annual Meeting of the Organization for Human Brain Mapping*.

Lau, H. C., Rogers, R. D., Ramnani, N., and Passingham, R. E. (2004). Willed action and attention to the selection of action. *Neuroimage*, 21(4):1407–1415.

Limb, C. J. and Braun, A. R. (2008). Neural Substrates of Spontaneous Musical Performance: and fMRI Study of Jazz Improvisation. *PLoS One*, 3(2):e1679.

Maldjian, J. A., Laurienti, P. J., and Burdette, J. H. (2004). Precentral gyrus discrepancy in electronic versions of the Talairach atlas. *Neuroimage*, 21(1):450–455. Technical report.

Mayka, M. A., Corcos, D. M., Leurgans, S. E., and Vaillancourt, D. E. (2006). Three-dimensional locations and boundaries of motor and premotor cortices as defined by functional brain imaging: A meta-analysis. *Neuroimage*, 31(4):1453–1474.

Nijstad, B. A., Breau, C. K. W. D., Rietzchel, E. F., and Baas, M. (2010). The dual pathway to creativity model: Creative ideation as a function of flexibility and persistence. *European Review of Social Psychology*, 21(1):34–77.

Pinho, A. L., de Manzano, Ö., Fransson, P., Eriksson, H., and Ullén, F. (2014). Connecting to Create: Expertise in Musical Improvisation Is Associated with Increased Functional Connectivity between Premotor and Prefrontal Regions. *The Journal of Neuroscience*, 34(18):6156–6163.

Pressing, J. (1988). Improvisation: methods and models. In Sloboda, J., editor, *Generative Processes in Music: The Psychology of Performance, Improvisation, and Composition*, pages 129–178. Oxford University Press, New York.

Schupp, H. T., Stockburger, J., Bublatzky, F., Junghöfer, M., Weike, A. I., and Hamm, A. O. (2007). Explicit attention interferes with selective emotion processing in human extrastriate cortex. *BMC Neuroscience*, 22:8–16.

Simonton, D. K. (2013). Blind-variation and selective-retention theory of creativity. *Physics of Life*, 10(2):158–159. Comments.

Smith, S. M. (2002). Fast Robust Automated Brain Extraction. *Human Brain Mapping*, 17(3):143–155.

Tzourio-Mazoyer, N., Landeau, B., Papathanassiou, D., Crivello, F., Etard, O., Delcroix, N., Mazoyer, B., and Joliot, M. (2002). Automated Anatomical Labeling of Activations in SPM Using a Macroscopic Anatomical Parcellation of the MNI MRI Single-Subject Brain. *Neuroimage*, 15(1):273–289. Technical Note.

Part IV

Concluding Remarks

Chapter 7

Final Discussion

The primary goal of both studies was to further explore the neurocognitive mechanisms underlying musical creativity. To accomplish such an endeavor, experiments were conducted on a group of thirty nine professional pianist, using human fMRI for brain activity measurement. Musical improvisation was herein used as the model behavior, which stands for creative musical performance.

7.1 Study I: Expertise in Musical Creativity

Study I firstly demonstrated that brain activity during improvisation was specifically associated with improvisational training, controlling for age and conventional piano practice. The results revealed a significant negative association between improvisational training and activity in a number of cortical regions in the right hemisphere. In other words, improvisation expertise is associated with lower activity in the frontoparietal network primarily dedicated to higher cognitive functions. Secondly, improvisational training was shown to be specifically associated with functional connectivity during improvisation, using the premotor and prefrontal regions involved in improvisation as seed regions, and controlling for age and conventional piano practice. Thus, more experienced improvisers displayed higher functional connectivity during improvisation between prefrontal, premotor, and motor regions of the frontal lobe. In addition, the results were not confounded by more experienced improvisers producing more complex improvisations (see chapter 5) (Pinho et al., 2014).

Given the negative association between improvisation training and frontoparietal network, typically implicated on subserving attentional control as well as high-order executive functions, one may ask whether creative behavior such as improvisation can be automated. Indeed, de Manzano and Ullén (2012) had already reported higher activity in the prefrontal and parietal

associative areas in professional musicians, when contrasting untrained pseudorandom generation tasks, included in the category of free generation tasks, and improvisational musical tasks (de Manzano and Ullén, 2012). This evidence presumably reflects the expertise associated with music improvisation, whereas attaining for pseudorandom generation sequences may rather requisite an overall load of working memory and executive control in order to sustain attention and further real-time performance. Additionally, Limb and Braun (2008) reported a widespread of prefrontal deactivations during free improvisation in a study of six experienced jazz musicians (Limb and Braun, 2008), which provides extra support for this interpretation. As mentioned previously by Donnay et al. (2014) (Donnay et al., 2014), one can also speculate that activity decreases might be related to a subjective feeling of automaticity and subjective "flow" during performance, often discussed on accounts of performances by improvising musicians.

Musicians have been used extensively to study brain adaptations in response to long-term practice. Many studies have provided evidence that musical training can have dramatic effects in the brain not only at the functional level but also at the anatomical level (Pantev and Herholz, 2011). For example, Pantev et al. (2001) demonstrated that auditory cortical representations of tones are enhanced in a timbre-specific way for tones from the instrument for which the subject has trained (Pantev et al., 2001). Anatomical differences due to neuroplasticity effects related to musical training have also been identified. Interestingly, it was found hemispherical differences in Omega Sign, highly associated with hand movement representation, between keyboard players and string players. The keyboard players showed enhanced grey matter volume on the left hemisphere of this region, whereas the string players displayed the same feature on the right hemisphere. These results thus indicate a brain adaptation depending on the instrument played, i.e. a "specialization of the specialized" (Bangert and Schlaug, 2006). Similarly, the present results also elicited the specific effects of improvisation experience that might be related to high-order cognitive aspects of the training rather than merely sensorimotor demands of piano playing.

An important focus of improvisational training is to acquire extensive long-term stores of musical patterns and cognitive strategies that can be used during extemporization (Pressing, 1988). Thus, musical improvisation is not a merely collection of free selected individual notes and sounds, but rather it comes into play in a skilled combination, development and expressive rendering of musical structures in real time. Consistent with this, the results indicate that task performance in highly trained individuals as compared to novices may involve a lower overall

level of regional brain activity that is concomitant with an increase in functional connectivity. Skilled improvisational performance may thus be characterized by both lower demands on executive control and a more efficient interaction within the network of involved brain areas. In line with this, we suggest that the extensive functional connectivity between premotor and prefrontal regions seen in the highly trained participants may reflect a more efficient integration of musical structures' representations.

7.2 Study II: Dual Neural Pathways to Creativity

As it was previously hypothesized, Study II confirmed higher activity in frontoparietal executive regions, namely the right DLPFC, and right premotor regions, such as PMD, when contrasting structural conditions with emotional conditions. These results suggest higher attentional effort and cognitive control when the participant had to conform to the structural constraint. On the other hand, higher activity during emotional conditions when compared with structural conditions was identified in regions contributing to emotion processing (Koelsch, 2010), such like middle occipital gyrus, insula as well as amygdala. Interestingly, the results displayed deactivations in the right DLPFC, PMD and superior parietal cortex during emotional conditions. Further, the results also demonstrated task-dependent patterns of connectivity. Specifically, greater connectivity, during structural conditions when compared with emotional conditions, was found between right DLPFC and parietal lobe, cerebellum, motor and premotor regions, thus enhancing a load of attention, working memory and control/planning on movement sequencing. Conversely, a widespread functional connectivity between right DLPFC and many regions in frontal, temporal, parietal and occipital lobes was evident when contrasting emotional conditions with structural conditions, highlighting a functional association with the default network. In addition, left DLPFC also showed higher connectivity during emotional conditions (compared with structural conditions) between right IFG, bilateral superior medial gyrus, medial orbital gyrus, as well as cerebellum (Pinho et al., 2015).

Most importantly, the overall contribution of the DLPFC for creative cognition was examined in the context of the present results. By comparing the profile of activity of this region during musical improvisation under different prerequisites, the findings sustain the idea that creative cognition is a contextual-dependent system, thus depending on the circumstances in which it occurs. In particular, the discrepancy of the results regarding the DLPFC reflect either explicit or implicit processing according to real-time task-related specificities. Nathaniel and Frith (2002) claimed that the most likely single cognitive function of the DLPFC is to specify a

set of responses suitable during a free selection task, i.e., the 'sculpting of the response space' (Nathaniel-James and Frith, 2002). The present findings thus reinforce this idea (Pinho et al., 2015).

References

Bangert, M. and Schlaug, G. (2006). Specialization of the specialized in features of external human brain morphology. *European Journal of Neuroscience*, 24(6):1832–1834.

de Manzano, Ö. and Ullén, F. (2012). Goal-independent mechanisms for free response generation: Creative and pseudo-random performance share neural substrates. *Neuroimage*, 59(1):772–780.

Donnay, G. F., Rankin, S. K., Lopez-Gonzalez, M., Jiradejvong, P., and Limb, C. J. (2014). Neural Substrates of Interactive Musical Improvisation: an fMRI Study of 'Trading Fours' in Jazz. *PLoS One*, 9(2):e88665.

Koelsch, S. (2010). Towards a neural basis of music-evoked emotions. *Trends in Cognitive Sciences*, 14(3):131–137.

Limb, C. J. and Braun, A. R. (2008). Neural Substrates of Spontaneous Musical Performance: and fMRI Study of Jazz Improvisation. *PLoS One*, 3(2):e1679.

Nathaniel-James, D. A. and Frith, C. D. (2002). The Role of the Dorsolateral Prefrontal Cortex: Evidence from the Effects of Contextual Constraint in a Sentence Completion Task. *Neuroimage*, 16(4):1094–1102.

Pantev, C. and Herholz, S. C. (2011). Plasticity of the human auditory cortex related to musical training. *Neuroscience and Biobehavioral Reviews*, 35(10):2140–2154.

Pantev, C., Roberts, L. E., Schulz, M., Engelien, A., and Ross, B. (2001). Timbre-specific enhancement of auditory cortical representations in musicians. *NeuroReport*, 12(1):169–174.

Pinho, A. L., de Manzano, Ö., Fransson, P., Eriksson, H., and Ullén, F. (2014). Connecting to Create: Expertise in Musical Improvisation Is Associated with Increased Functional Connectivity between Premotor and Prefrontal Regions. *The Journal of Neuroscience*, 34(18):6156–6163.

Pinho, A. L., Ullén, F., Castelo-Branco, M., Fransson, P., and de Manzano, Ö. (2015). Addressing a Paradox: Dual Strategies for Creative Performance in Introspective and Extrospective Networks. *Cerebral Cortex*. doi: 10.1093/cercor/bhv130 [Epub ahead of print].

Pressing, J. (1988). Improvisation: methods and models. In Sloboda, J., editor, *Generative Processes in Music: The Psychology of Performance, Improvisation, and Composition*, pages 129–178. Oxford University Press, New York.

Chapter 8

Future Directions

Both studies featuring this thesis are no more but a small step towards the understanding of the intricate phenomena involved in creativity. Future research will be described next.

In Study I, effects of improvisational training were consistent across the improvisation conditions (i.e. improvisational performances under different types of constraint, investigated in detail in Study II). This suggests that the training effects, although related to improvisational training, were not limited only to certain strategies for improvisation. Nevertheless, it seems likely that more experienced improvisers not only exhibit a more efficient neural control of improvisation, but also have a greater capacity to perform complex improvisations. To investigate such differences in improvisational capacity, a experimental paradigm allowing for more complex and challenging improvisations would presumably be needed. Such investigation could be complemented by introducing different groups of musicians specialized in different musical genres.

Study I also opened an intriguing question concerning to what extent anatomical differences might occur due to extensive improvisational training. Gaser and Schlaug (2003) found gray matter volume differences in motor, auditory and visual-spatial brain regions when comparing professional keyboard players with amateur musicians and non-musicians (Gaser and Schlaug, 2003). More recently, Groussard (2014) studied the dynamic structural brain changes related to musical experience in a group of non-musicians and amateur musicians with different levels and types of training experience. Results revealed that changes gradually appear in the left hippocampus and right middle and superior frontal regions, and later in the right insula, supplementary motor area, left superior temporal as well as in the posterior cingulate areas. Groussard et al. (2014) Nonetheless, no study has explored so far to what extent different levels of improvisational musical training may bring about structural changes in the brain.

Voxel-based morphometry analysis or cortical thickness are the most appropriate techniques to tackle this question. In order to ensure complete causality, a more challenging enterprise would be to perform a longitudinal study under this framework.

Study II examined the effects exerted by the DLPFC in creative thinking under the context of musical improvisation. Particularly, the exact cognitive function of the DLPFC was discussed in terms of explicit vs. implicit process. A meta-analysis by Cielisk (2013) identified functional heterogeneity in the right DLPFC and demonstrated that this region is subdivided into two distinct subregions: an anterior-ventral and a posterior-dorsal one. Each of them were reported to display different functional connectivity between distinct neural networks. These results thus provided evidence regarding different specificities of cognitive action control at different locations within right DLPFC. The anterior network was shown to be involved in attention and action inhibition processes, whereas the posterior one was assigned to action execution and working memory. Cieslik et al. (2013) One may also ask whether implicit and explicit processing during musical improvisation might not be associated with such subregions. To investigate that, a new experimental paradigm matching the aforementioned cognitive functions with behavioral conditions, during musical improvisation, would presumably be needed. For instance, a possible design could be implemented by defining a preparation block-period before musical improvisation. Consequently, attention and action inhibition would be firstly tested, followed by the improvisational musical performance that would test for execution and working memory.

Musicians in general, improvising musicians in particular, have often reported, while performing, a subjective feeling of full control, total commitment and complete neglect of time passing. Mihaly Csikszentmihalyi has dedicated part of his studies to investigate *Flow*. In his seminal work about the topic, he defines the concept of flow as: *"the state in which people are so involved in an activity that nothing else seems to matter; the experience itself is so enjoyable that people will do it even at great cost, for the sheer sake of doing it"* (Csikszentmihályi, 1990). The physiological processes associated with the flow experience during musical performance were already tackled by de Manzano (2010) (de Manzano et al., 2010). Since flow has been linked to optimal performance and creative achievement (Csikszentmihályi, 1997), a further step is to study the neural correlates of flow under musical improvisation framework. State of flow can be assessed by using questionnaires, that are administrated immediately after task performance (Jackson and Eklund, 2004). Combining this information with brain activity measured during musical improvisation, using functional neuroimaging techniques like

fMRI or *Magnetoencephalography* (MEG)[1], would provide valuable contributions for a better comprehension of the biological substrates underlying the mechanisms that might link flow with creativity. Further, *flow proneness* can be defined as a trait that refers to the tendency of a person to experience flow (Ullén et al., 2010). It can also be assessed by administrating questionnaires where the participants state how often they have experiences matching to specific characteristics assigned to flow state. Given this, associations between brain anatomy and flow proneness could also be explored using MRI.

So, the enterprise of research must proceed. Bit by bit and piece by piece, the conundrum will eventually be unveiled...

[1]MEG is a functional neuroimaging technique with high temporal resolution (Hämäläinen et al., 1993). Combined with MRI, it can provide both high temporal and spatial resolution, which is fundamental for a complete evaluation of the dynamic aspects underlying the cognitive mechanisms of musical performance across the whole brain.

References

Cieslik, E. C., Zilles, K., Caspers, S., Roski, C., Kellerman, T. S., Jakobs, O., Langner, R., Laird, A. R., Fox, P. T., and Eickhoff, S. B. (2013). Is There "One" DLPFC in Cognitive Action Control? Evidence for Heterogeneity From Co-Activation-Based Parcellation. *Cerebral Cortex*, 23(11):2677–2689.

Csikszentmihályi, M. (1990). *Flow: The psychology of optimal experience*. Harper & Row, New York.

Csikszentmihályi, M. (1997). *Creativity: flow and the psychology of discovery and invention*. HarperPerennial, New York.

de Manzano, Ö., Theorell, T., Harmat, L., and Ullén, F. (2010). The Psychophysiology of Flow During Piano Playing. *Emotion*, 10(3):301–311.

Gaser, C. and Schlaug, G. (2003). Brain Structures Differ between Musicians and Non-Musicians. *The Journal of Neuroscience*, 23(27):9240–9245.

Groussard, M., Viader, F., Landeau, B., Desgranges, B., Eustache, F., and Platel, H. (2014). The effects of musical practice on structural plasticity: The dynamics of grey matter changes. *Brain and Cognition*, 90:174–180.

Hämäläinen, M., Hari, R., Ilmoniemi, R. J., Knuutila, J., and Lounasmaa, O. V. (1993). Magnetoencephalography—theory, instrumentation, and applications to noninvasive studies of the working human brain. *Rev. Mod. Phys.*, 65:413–497.

Jackson, S. A. and Eklund, R. C. (2004). *The Flow Scales Manual*. Publisher Graphics, Morgantown.

Ullén, F., de Manzano, Ö., Theorell, T., and Harmat, L. (2010). The Physiology of Effortless Attention: Correlates of State Flow and Flow Proneness. In Bruya, B., editor, *Effortless Attention: A new perspective in the cognitive science of attention and action*, pages 205–217. MIT Press, Cambridge, MA.

List of Publications

Pinho, A. L., de Manzano, Ö., Fransson, P., Eriksson, H., and Ullén, F. (2014). Connecting to Create: Expertise in Musical Improvisation Is Associated with Increased Functional Connectivity between Premotor and Prefrontal Regions. *The Journal of Neuroscience*, 34(18):6156–6163.

Pinho, A. L., Ullén, F., Castelo-Branco, M., Fransson, P., and de Manzano, Ö. (2015). Addressing a Paradox: Dual Strategies for Creative Performance in Introspective and Extrospective Networks. *Cerebral Cortex*. doi: 10.1093/cercor/bhv130 [Epub ahead of print].

Acknowledgments

Firstly and foremost, I want to express my deepest and sincere gratitude to my supervisors Fredrik Ullén and Örjan de Manzano for making this whole project possible, believing in me as well as for the constant support, mentorship, patience, enthusiasm, inspiration and opportunity to meet so many talented people. Particularly, I am very thankful to Örjan for assisting me with the experiments and analyses throughout the entire project and with whom I learnt so much about neuroimaging. I am also very grateful to Peter Fransson for the valuable discussions concerning the technical approach to the project. Further, I wish to thank Prof. Miguel Castelo-Branco for the national supervision and for having assured my link to University of Coimbra.

Special thanks go to all musicians who kindly participated in the experiments.

I am also very happy for having gotten the chance to meet quite nice, interesting and warm people at *Retzius* building, MR-center and SBI. I kindly regard Jonathan Berrebi for the huge help he provided by setting the equipment at the MR-center, running some experiments with me as well as the SPM support during analyses and patience plus unique humor towards my multiple and infinite set of questions. I want also to thank to the remaining members of Fredrik's research group - Diana Müssgens, László Harmat, Miriam Mosing, Helene Eriksson and, former colleague, Luca Iemi - for the companionship and interesting discussions. Many thanks to Rita Almeida, my portuguese fellow, for the valuable support in the statistics and convivial times at lunch. I dedicate a special thank you note to Rouslan Sitnikov for being always available to help and answer thoughtfully to our questions. Thanks for the coffee breaks (awesome "fika"!), discussions, nice dinners, pub evenings, concerts, retreats and so on, to: Şermin Tükel (thank you for hosting me when I most needed and the super-awesome trip to Gotland), Mominul Islam, Benjamin Garzon, Katell Mevel, Valeria Petkova, Tanja Dadakova, Anaïs Louzolo, Catherine Preston, Alva Appelgren, Pär Flodin, Fahimeh Darki, Giovanni Gentile, Linda Holmström, Mikael Lindahl, Martin Schain, Eleni Kopsida, Sofia Martinsen, Louise von Essen (thank you for organizing my complicated travels and paper work) and Mimmi

Wernman (I love your laugh!). I acknowledge all staff from the MR-center for the technical support on the MRI experiments. Also, I greatly appreciate the scientific contributions of Hugo Zeberg, Peter Århem and Arvid Guterstam in the development of side projects. Further, I want to thank Guy Madison, Umeå University, for his contributions regarding the experiment's settings as well as for his fellowship. In addition, I am thankful to Lars Flemström for his technical support.

I acknowledge and honour *Fundação para a Ciência e a Tecnologia* (Foundation for Science and Technology of Portugal), the *Vetenskapsrådet* (Swedish Research Council), the *Sven och Dagmar Saléns Stiftelse* (Sven and Dagmar Saléns Foundation) and the *Stiftelsen Riksbankens Jubileumsfond* (Bank of Sweden Tercentenary Foundation) for the financial support of my research.

I am also particularly very grateful to the wonderful "tuga family" I built in Stockholm and with whom I shared so many nice and joyful moments: Gisa Cunha (no space here for a full description of how awesome was to meet you); Pedro Petro (my Södermalm fellow!); Ana Catarina Araújo Silva (thanks for your amazing friendship, vivid and bright personality) as well as Oscar Norberg plus sweet Gabriel (many thanks to the three of you for always welcoming me at your place, the delicious and cheerful dinners and the super-cool thematic parties); Cátia Rocha and André Teixeira, who were able to convince me to go many times to the swimming pool early in the morning at the weekends (thanks for the sushi, the walks, your friendship); Ana Borges and Ivo Silva, my photographer friends (thanks a lot for all nice pics and your amiability): Catarina Pinho and Diogo Silva, for their cheerful spirit (thanks for bringing so many portuguese delights to the table and the unforgettable parties at Lappis); Nuno Leal, the best ever version of Angela M.; and Carlos Dias (hope to see you often in Portugal).

I am extremely grateful to my landlady, but above all, amazing friend Pia Van Hogerlinden for her warming spirit and good heart (loads of thanks for letting me feel at home in Sweden). My best wishes go to Tim and Alma, the youngest fellows of my journey. I am equally thankful to my flatmate and dear friend Paolo Frumento for his friendly spirit and challenging discussions (every time I was about to arrive home late in the evening and the kitchen's light was still switched on, I knew there would be a "messy flatmate" available for a nice chat.). Thanks also to Luca Biancofiore to be always super-cool.

Tons of thanks to my hiking/KI friends for having energized my life in Stockholm and filled it with loads of optimism through their lively spirits and open-minded personalities: Ilais Moreno, Nasren M. Jaff, Kristoffer Sahlholm, Giulia Meneghello, Silvia ("Aiv Lis"), Paola

Andrea Martinez Murillo, Max Vikström, Germán Darío Carrasquilla López, Heleen Feenstra, Maral Adel and Davide Bossoli.

I want to dedicate a very special note of immense gratitude to my dearest friend Celia García Pareja, who I lately met in Stockholm, for her soul's strength and contagious enthusiasm. My last months in Sweden would have never been so plenty of inspiring moments, full of joy and sharing, without her presence, who was always coming to me as a "train of thought". (Thanks for the constant support during my very last period in Stockholm, for the patience of waiting for me so many times, for helping me to surpass the stress and for the comprehension that I could have only asked to a longtime friend.)

Similarly, I want to thank Irina Pinheiro for her "extravaganza", trust and pleasant company, always spreading loads of fun, during my early days in Stockholm and with whom I discovered the city.

I want also to thank my KTH friends Camilla Terenzi, Ricardo Ferreira, Farhan Ansari, Ivón Hassel, Lars Ragnarsson and Michaela Salajkova for the cheerful dinners, interesting conversations, great jokes and the funniest boat trips. Additionally, I thank to Eduardo Oliveira (thanks for the cultural programs, walks and conversations), Jairo Ramírez Ante (my SFI friend), Carlos Silva Pereira (good times in Edinburgh, Porto, Stockholm and Helsinki), César Lima (nice to see you again in San Diego), Christina Pesonen, Anton Zidén, Pol Del Aguila Pla, Cyrille Laroche, Adeline Rachalski, Natasja Almhagen, Jesper Svarén, Marc Broh and Andréas Öbrink.

I spent the first year of my Ph.D. in Coimbra where I took the opportunity to meet extraordinary people showing great enthusiasm on research. I am thus very thankful to my BEB colleagues, Professors and administrative staff of the Doctoral Programme for the support during the first steps of this unforgettable and unequalled chapter of my life. I kindly regard my colleagues Paula Banca (thanks for the huge help on handling with the bureaucracy at UC, the endless discussions about our research topics and great friendship) as well as Ângela Crespo and Marília Cordeiro (girls, thanks a lot for teaching me so much about Biology nearly ten years later of my studies on the subject at the high school.). Many thanks to Inês Almeida from IBILI and my landlady Evelise Ramos, as well.

Living four years abroad implies leaving many friends from old times. Nevertheless, I am very grateful for their timeless friendship and the warm welcome every time I was back to Portugal. Many thanks to the "Técnico team" and related friends, whose friendship goes beyond the borders of the University: Ana Neves Vieira da Silva (thanks for being always so

supportive, cool, helpful, kind, loving and insightful), João Vasco Gama (thanks for all *tertúlias* about so many intricate subjects; thanks for furthering my criticism, skepticism and, at the same time, my willingness to think beyond), Cristina Carias (always sweet and caring; thanks for boosting my perseverance), Ana Mourão (thanks for always being careful and attentive as well as for your mighty power of analysis), Nuno Ribeiro (thanks for your relaxed but, at the same time, critical spirit), Vasco Henriques (thanks for the support during my early days in Stockholm), Susana Brandão, Luís Guimarãis, David Batista, Paulo Ferreira, Guillaume Riflet, ...(guys, you know who are the remaining ones!). I also want to thank to all my "IO" friends for having been always such good companions and with whom I grew up and literally lived for eight years. Many thanks to Catarina Leonardo, my "flamenco friend", for all moments spent together and for visiting me in Stockholm. Thanks to Sheina de Castro Ferrão, my chorus buddy, for her sensibility and inspiring conversations about music. Also, a special regard is sent to my eldest friend ever, Lúcia Costa; we know each other since we were four years old and I am very happy to have kept the contact and friendship up to the present time.

I dedicate a very special thank you note to my dear friends João Gato and André Janeirinho for the long friendship and their unique plus out-of-the-standard characters, with whom I inwardly grew and engendered the most awesome "theories of everything". Further, my interest in music and its various aspects flourished and it was nourished by their influence. This thesis thus represents a testimony of their presence in my life.

I also want to express an enormous gratitude to my good and old friend, Ana Francisca Ribeiro, for having always believed in me, for her positive energy and indubitable support. I utterly want to thank and honour her for the authorship of the cover image featuring the thesis. Many thanks also to Jens Selin and my best wishes go to Luna.

I kindly regard Arlete and Lúcio Correia for their remarkable contribution to my education.

Last but most, I wish to thank to all members of my close family: Tia Zézinha, Fábio, André, Andreia and Rafaela. A very deep gratitude goes to my sweet grandpa and grandmas: Francisco Pareto de Pinho, Ana Rosa da Conceição Carreiro and Maria Luísa Marques Trindade. And finally, there are no words that can express the unconditional love and uttermost support I have received since the very beginning of this enterprise from my beloved parents - João Manuel Carreiro Pinho and Maria da Conceição Trindade Grilo (a minha "Férica" querida) - to whom I dedicate this thesis. Thank you for keeping me stand up for my beliefs.

Muito Obrigada!

Ana Luísa Grilo Pinho, September 2014

Curriculum Vitæ

Ana Luísa Grilo Pinho was born on 14th of July, 1981 in Lisbon, Portugal. In 1999, she completed her high school education in Instituto de Odivelas (Infante D. Afonso) in Odivelas, Portugal. She obtained, in 2008, her master degree in Physics Engineering at Instituto Superior Técnico, Technical University of Lisbon, Portugal, with a thesis entitled *Probabilistic non-linear earthquake location in a 3-D velocity model*. In 2009, she enrolled in the PhD Programme in Experimental Biology and Biomedicine organized by the Center for Neuroscience and Cell Biology, University of Coimbra, Portugal. From September 2010 till June 2014, she developed her Ph.D. project as a guest doctoral student at Karolinska Institutet, Stockholm, Sweden, under the main supervision of Professor Fredrik Ullén and co-supervision of Doctor Örjan de Manzano and Professor Peter Fransson. The national co-supervision was assured by Professor Miguel Castelo-Branco, University of Coimbra.